DISSERTATION

ECOSYSTEM MODELING TO UNDERSTAND GLOBAL CHANGE EFFECTS TO TERRESTRIAL AND FRESH WATER SYSTEMS

Submitted by

Melannie Diane Hartman

Graduate Degree Program in Ecology

In partial fulfillment of the requirements

For the Degree of Doctor of Philosophy

Colorado State University

Fort Collins, Colorado

Spring 2013

Doctoral Committee:

Advisor: William J. Parton
Co-Advisor: Jill S. Baron

Dennis S. Ojima
John D. Stednick
Geof H. Givens

ABSTRACT

ECOSYSTEM MODELING TO UNDERSTAND GLOBAL CHANGE EFFECTS TO TERRESTRIAL AND FRESH WATER SYSTEMS

Concurrent changes in climate, atmospheric nitrogen (N) and sulfur (S) deposition, and increasing levels of atmospheric carbon dioxide (CO_2) affect ecosystems in complex ways. Atmospheric deposition of S and N species have the potential to acidify terrestrial and aquatic ecosystems, but nitrate and ammonium are also critical nutrients for plant and microbial productivity and are a potential cause of eutrophication. Climate change and CO_2 fertilization, with or without changes in N deposition, may affect rates of plant growth, water availability, soil organic matter decomposition rates, and net greenhouse gas flux. I developed a non-spatial biogeochemical model to simulate soil and surface water chemistry by linking the daily version of the CENTURY ecosystem model (DayCent) with a low temperature aqueous geochemical model, PHREEQC. The coupled model, DayCent-Chem, simulates the daily dynamics of plant production, soil organic matter, cation exchange, mineral weathering, elution, stream discharge, and solute concentrations in soil water and stream flow. The model was first validated against a rich data set for an alpine watershed in Rocky Mountain National Park, then for seven other forested montane and alpine watersheds in the United States. I modeled how much nitrogen deposition it takes to acidify an alpine watershed, and whether the rate at which deposition increases matters. I also used the model to investigate the combined effects of N deposition, warming, and increasing CO_2 over the period 1980-2075 at seven forested montane and two alpine watersheds by looking at changes to net ecosystem production, soil organic C, soil nitrous

oxide (N_2O) emissions, and stream nitrate. I found that N was the main driver of change to net ecosystem greenhouse gas flux with warming and CO_2 fertilization playing lesser roles. Overall, simulations with DayCent-Chem suggest individual site characteristics and historical patterns of N deposition are important determinants of forest or alpine ecosystem responses to global change. Both the ecological response and the hydrochemical response to these human-caused drivers of global change are of interest to scientists as well as regulatory and land management agencies. This model is appropriate for accurately describing the ecosystem and surface water chemical response of small watersheds to atmospheric deposition and climate change.

ACKNOWLEDGEMENTS

I would like to express my gratitude to the five members of my committee for their support, encouragement, and guidance – each of them demonstrates the importance of collaboration to science. I thank my advisor Bill Parton for all that he has taught me about ecosystem processes over the past 20 years and for all the opportunities he has given me to contribute to the advancement of ecosystem modeling. This research would not have been possible without my co-advisor Jill Baron who envisioned DayCent-Chem and who secured the funding necessary to build and successfully apply the model; she supported me every step of the way through my PhD, from the day I first applied to the Graduate Degree Program in Ecology to the time I was making final edits to this dissertation. I thank Dennis Ojima for helping me understand how ecosystem modeling fits into the much the broader research of climate change effects to ecosystems around the world. I thank John Stednick for fueling my interest in land use and water quality and for providing an expanded perspective on watershed science in mountainous regions. I thank Geof Givens for helping me expand my knowledge of statistical methods.

I would also like to thank all my coauthors who participated in DayCent-Chem research and development including Jill S. Baron, David W. Clow, Irena F. Creed, Charles T. Driscoll, Holly A. Ewing, Bruce D. Haines, Jennifer Knoepp, Kate Lajtha, Dennis S. Ojima, William J. Parton, Jim Renfro, R. Bruce Robinson, Helga Van Miegroet, Kathleen C. Weathers, and Mark W. Williams. I thank David Parkhurst for his consultation with the PHREEQC model. Additional thanks go to Don Campbell, David Clow, D. Manthorne, and D. Hultstrand of the U.S. Geological Survey, Loch Vale Water Energy and Biogeochemical Budgets (WEBB)

and Todd Ackerman, Howard Bruner, and John Campbell who provided data or assisted with the data collection. Programming, database, graphics, and statistical support were provided by Cindy Keough, Lee Casuto, Guoming Wang, and Amanda Elliot Lindsey. Lois St. Brice—an undergraduate at Bates College who was mentored by Holly Ewing, Kathleen Weathers, and myself in exploring DayCent-Chem's performance and sensitivity for an Honor's thesis during 2006–2007—expanded our understanding of the model and of ecosystem dynamics at Acadia National Park. Funding was provided by the U.S. Environmental Protection Agency Clean Air Markets Division, National Park Service Air Resources Division, and by the U.S. Geological Survey Western Mountain Initiative.

DEDICATION

First I would like to dedicate this work to family who helped me develop from a young age the intellectual curiosity and discipline required to achieve this PhD: my parents John Henry and Mary Ann Hartman who supported my educational and personal goals throughout my life; my grandfather, the late John Svoboda, a farmer, gardener, and shop mechanic who shared his fascination in nature, science, and technology with me from the time I started walking. Secondly, this work is dedicated to my husband Mike Tuffly who shares my love for science and who recently completed his PhD also. Mike made my graduate days more fun and interesting and encouraged me to make that final push to finish my PhD.

TABLE OF CONTENTS

1 INTRODUCTION

1.1 Global Environmental Change

Across the globe, human population expansion and the industrial revolution have been drivers of environmental change, particularly in the past century. Human ingenuity has brought about many benefits to human-kind including widespread energy availability, increased food production, transportation and communication networks, and many useful industrial and technological products. However, the associated land use change, air and stream water pollution, and increased greenhouse gas emissions threaten ecosystems and the services they provide to all life.

Humans, through fertilizer production and use, N-fixing crops, fossil fuel burning, biomass burning, industrial processes, and livestock management create more fixed-N than all natural sources combined. The creation of this reactive N (Nr) is projected to increase in the future (Galloway et al. 2008). Forms of Nr include ammonia (NH_3) and N-oxide gases that lead to increased atmospheric N deposition. Nr cascades through the environment and its prevalence enhances fluxes of NO_x (nitric oxide (NO) and nitrogen dioxide (NO_2)) and nitrous oxide (N_2O) to the atmosphere plus N leaching to groundwater and streams. N_2O is a greenhouse gas with ~300 times the 100-year warming potential of CO_2 per molecule (Ramaswamy 2001). NO_x leads to the formation of tropospheric ozone (O_3), another GHG that also damages plants and has harmful respiratory effects on humans. In the stratosphere NOx can catalyze the destruction of O_3.

Fossil fuel burning has increased S as well as N emissions. Both S and N species are returned to terrestrial and aquatic environments as atmospheric deposition where they have the

potential to cause acidification, aluminum toxicity, and base cation depletion, all of which can limit plant production. On the other hand, N deposition may lead to unwanted fertilization effects on terrestrial systems and eutrophication of surface waters. While U. S. sulfur dioxide emissions have sharply decreased in response to the U.S. Clean Air Act Amendments, N emissions, particularly ammonia (NH_3) emissions, are largely unregulated. Atmospheric N deposition from NO_x and NH_3 emissions is elevated above background throughout the U.S. (NADP/NTN).

Global temperatures have been rising for decades. Most of the observed increase in global average temperatures since the mid-20th century is very likely due to the observed increase in anthropogenic greenhouse gas concentrations including CO_2, N_2O, and CH_4 (IPCC 2007). In their State of the Climate Global Analysis, the National Oceanic and Atmospheric Administration (NOAA) reports that all 12 years of the 21st century (2001-2012) rank among the 14 warmest in the 133-year period of record (NOAA 2012a). Year 2012 also marked the 36th consecutive year with a global temperature above the 20th century average; the last below-average annual temperature was 1976. NOAA's National Overview reports that 2012 was warmest and second most extreme year on record for the contiguous U.S. (NOAA 2012b). The average temperature for 2012 was 55.3°F, 3.2°F above the 20th century average, and 1.0°F above 1998, the previous warmest year.

In addition to increasing radiative forcing, elevated CO_2 may have a fertilization effect that increases plant growth and net ecosystem C sequestration; however, vegetation growth and soil organic matter turnover are interdependent and are governed by temperature and moisture conditions and nutrient availability. The availability of N may influence plant and soil C sequestration potential, since N is often limiting to plant growth (Vitousek and Howarth 1991). Nitrogen from deposition may alleviate some nutrient limitations that restrict C sequestration,

particularly in forests (Magnani et al. 2007), however, as mentioned above, N deposition can cause a number of harmful effects counteract the benefits of C sequestration.

Emissions of greenhouse gases are increasing at a faster rate than was projected by the Intergovernmental Panel on Climate Change (IPCC) (Nakicenovic 2000), and Canadell et al. (2007) suggest this implies a decline in the efficiency of terrestrial sinks, including forests and soils, to absorb C. The rate at which C is stored in plant biomass and soils is dependent on many complex interactions between drivers of change (climate, greenhouse gases, atmospheric deposition, and land use) and ecological processes. There will be positive and negative feedbacks, not only among ecological processes, but also between land-based and atmospheric processes (Bonan 2008, Chapin et al. 2008). The effects of environmental change can be expected to vary among ecosystems both in magnitude and direction depending on the initial states of their C and N pools, climate, plant type, soil type, and soil depth.

Science plays a critical role in the protection of all types of managed and natural ecosystems as well and informing pollution and climate mitigation policies. Agricultural areas can be managed to maximize food supply while reducing N leaching and GHG production. Forests and grasslands and be managed to maximize C sequestration. Mountain ecosystems which are hydrologically very important to the quality and quantity of our water supply, and ecologically very important for the plant and wildlife they support, are also vulnerable to pollution and climate change. The ecological response, hydrologic response, and the hydrochemical response to atmospheric deposition and climate change are topics of great interest to federal land managers who have a responsibility to protect Class I areas, national parks and wilderness areas granted special air quality protections under Section 162(a) of the federal Clean Air Act, from ecosystem degradation due to atmospheric deposition of pollutants.

1.2 Models in Ecosystem Science

Quantitative simulation models are necessary and important to understanding ecosystem science in both pristine and managed lands (Canham et al. 2003b). We develop models to provide answers that laboratory experiments, field experiments, and monitoring alone can not provide. Yet models could not exist without such measurements. From experiments and observations scientists form and test hypotheses to learn about ecosystem processes. We take this knowledge and describe it in the algorithms of computer models, representing the functions we think are most important to address the scientific questions of interest. We use measured data to parameterize and drive models, and to verify that the model can replicate observations. Models can be excellent heuristic tools which can reveal what we do, and do not, understand about how ecosystems function. They are also useful for solving the inverse problem – determining the processes and parameters that account for empirical evidence.

Ecosystems inherently have complex interactions between plants, soils, and organisms that make cause and effect difficult to decipher. Models are useful for linking together a number of processes that interact in complex ways. As models grow in complexity we need more data to drive them, to individually test all the important processes represented in the models, and again, to verify that the model represents ecological reality. Using these mechanistic models we can test sensitivity of a cascade of processes to changing inputs and to other processes.

Once we are assured that the model can replicate observations, we can use it as a predictive tool to perform experiments that are not feasible in the real world. For example, we simulate high N depositions loading to evaluate potential changes to stream chemistry. Such model experiments help scientists to understand how resilient or sensitive an ecosystem is to change: to quantify the critical loads to the ecosystem. We can use models to project response

of ecosystems to environmental change when the responses go beyond the time frame and spatial extent of experimental manipulation and observation. Reliable ecological models that correctly represent the C-N interactions and greenhouse gas emissions are important to coupled climate-carbon cycling models that depend on biosphere/atmosphere feedbacks to predict future climate change. We can also use models to help us understand processes that occurred in the past.

As a management tool models can help answer "what-if" scenarios. What if N deposition increases by 1% each year? What if the climate warms by 2 ºC over the next few decades? What if fertilizer inputs to corn crops are reduced? What if trees killed by bark beetle are removed rather than being left to decompose? For models to be useful to land managers their predictions must be something that people care about, such as water quality, forest health, and greenhouse gas emissions. If the drivers of potential harmful ecological change can be controlled, then model prediction may lead to policy changes or altered land management practices. If the drivers of change cannot be well controlled, then models can inform adaptive management practices necessary to protect ecosystems.

Much of my 20 years as a research associate at the Natural Resource Ecology Laboratory has been developing, testing, and applying ecosystems models. One model in particular has been central to my work, DayCent (Parton et al. 1998, Del Grosso et al. 2001). DayCent is the daily time step version of the CENTURY ecosystem model (Parton et al. 1987, Parton et al. 1988). CENTURY specializes in C and N cycling by incorporating detailed mechanistic representations of plant nutrient and water uptake, soil microbial activities, and soil organic matter evolution. In 1994, using the monthly CENTURY model as a basis, William J. Parton and I developed DayCent with the goal of simulating daily N trace gas fluxes due to nitrification

and denitrification (Parton et al. 1996). DayCent development has continued since this time with contributions from many other scientists and computer programmers (Del Grosso et al. 2000b, Eitzinger et al. 2000, Parton et al. 2001). It has been widely-applied to grasslands, forests, and agro-ecosystems around world (Parton et al. 1993, Lu et al. 2001, Parton et al. 2005, Del Grosso et al. 2006, Del Grosso et al. 2009, Hartman et al. 2011).

In 2005, at the beginning of my Ph.D. career, I expanded the capabilities of DayCent by linking it to another widely tested and accepted model that simulates low temperature soil and water geochemical equilibrium reactions, PHREEQC (Parkhurst and Appelo 1999). The purposes of creating the linked DayCent/PHREEQC model, which I named DayCent-Chem, were to capture the biogeochemical responses to atmospheric deposition and to explicitly consider those biogeochemical influences on soil and surface water chemistry (Hartman et al. 2007). The PHREEQC calculations utilized in DayCent-Chem are based on equilibrium chemistry of aqueous solutions interacting with minerals, gases, exchangers, and sorption surfaces. The linked model expands on DayCent's ability to simulate N, P, S, and C ecosystem dynamics and streamflow by incorporating the reactions of many other chemical species and processes of cation exchange, mineral weathering, and elution to predict solute concentrations in soil water and stream flow. The model can simulate short-term events such as episodic acidification, runoff, and soil freeze/thaw, as well as long-term ecosystem dynamics.

Models like DayCent-Chem that quantify many interactive processes, or in other words are "mechanistically rich", face scrutiny because of their complexity (DeAngelis et al. 2003). They are seen by some as being data-hungry, non-transparent, prone to error multiplication, and not amenable to vigorous testing. Sometimes empirical models are valuable and quite sufficient for determining the relationship between a dependent variable and one or more predictor

variables. However, these simpler models may not be suitable for predicting ecosystem response outside the range of the measurements that were used to derive them. It is true that mechanistic ecosystem models may require lots of data for input and parameterization, but they can also be derived by available data. We can increase model transparency and reduce error multiplication by comparing model outputs to multiple lines of validation data (e.g. Bonan et al. 2013). We gain confidence in models by validating them against data sets that were not used to determine parameterization (Janssen and Heuberger 1995) and testing them across a wide variety of sites and conditions. DayCent-Chem was developed using data from the well-studied data rich Loch Vale Watershed in Rocky Mountain National Park, Colorado (Hartman et al. 2007). The model has since been applied to eight diverse mountain and alpine watersheds across the United States (Hartman et al. 2009).

Hartman et al. (2009) describes the parameterization for the eight sites and validates model results against observations of ecosystem variables (above- and below-ground biomass and production, soil C, N_2O emissions), stream discharge, and stream chemistry. The contents of this report summarize a huge portion of my Ph.D. research but are not included in this dissertation because of the enormous size of the document.

1.3 The Science Underlying the Coupled Model

The DayCent-Chem model is a mechanistic representation of a complex interaction of biotic and abiotic processes that are dynamically affected by climate, atmospheric deposition, disturbance, and land management. Plants take up CO_2 from the atmosphere while also taking up N, P, and S from the soil to build and maintain biomass; in the process water is transpired from leaves. The C fixed in the leaves is allocated to different plant parts (leaves, wood, fine

roots) in ratios that depend not only on the type of plant, but also on the season and resource availability; some C may also be stored for later use. When plant litter falls to the ground or roots die, the dead biomass begins a decomposition process that is controlled by litter composition, and soil conditions (moisture, temperature, pH, and texture). Plant litter contains both labile and recalcitrant organic matter that gets partitioned into soil organic matter pools with varying decomposition rates (active, slow, and passive). Clay in soil can bind with organic matter, forming soil aggregates that make it more resistant to decomposition. Heterotrophic organisms consume the organic matter for energy, respiring CO_2. In the process they may immobilize mineral N if the C:N ratio of the plant material is too high to meet their nutrient requirements, or they may mineralize N if the N provided in organic matter exceeds their demand. Nitrifying bacteria oxidize ammonium (NH_4^+) to nitrate (NO_3^-) under aerobic conditions, whereby N_2O and NO are produced. Under anaerobic conditions, denitrifying bacteria reduce NO_3^- to gaseous N oxides and molecular N_2. Free living microbes and plants with symbiotic associations fix N_2 so that it becomes biologically available. Atmospheric deposition contributes cations and anions that alter soil chemistry and may enhance amounts of plant essential nutrients or alter soil microbial activity. The chemical and physical weathering of parent rock provides base cations, silica, S, P, and Al to the soils, and creates secondary minerals that also weather. Soil water moves up or down through the soil profile according to differences in soil water potential. Some water escapes the soil through evaporation. Water moving downward through the soil leaches organic C, N, and inorganic cations and anions, and some of this soil solution ends up in stream flow. Cations and acid ions in solution exchange on permanently negatively charged sites on clay particles. Soil organic matter and mineral particles

provide pH dependent exchange sites for soil anions and cations. The concentrations of H^+ and ANC in soil and stream water depend on concentrations of all chemical species.

Land use, land management, and disturbance are tightly integrated with ecosystem C and nutrient cycling (Robinson et al. 2013) and can be represented by the model. Humans and grazing animals harvest live and dead biomass, removing at least some C and nutrients from the system. Fire removes live and dead biomass, while releasing CO_2 and N-oxides into the atmosphere and returning some nutrients to the soil. Other natural and anthropogenic disturbances transfer live biomass to dead biomass pools. Agriculture cropland management alters soil decomposition rates and litter and nutrient inputs to the soil, all which affect net GHG fluxes (Hartman et al. 2011).

1.4 Assumptions and Limitations of DayCent-Chem

DayCent-Chem is a point model, not a spatial model, and will perform best in small watersheds that are relatively homogenous in terms of soil and vegetation properties. When there is spatial heterogeneity, model parameters can be adjusted to give a watershed average response, or results from multiple simulations can be combined. However there is a limit to how much heterogeneity can be lumped into a single simulation because watershed processes are not always additive.

If looking at the full chemistry represented by the model, DayCent-Chem will do best in non-arid environments because the PHREEQC model is based on aqueous calculations. Additionally, DayCent-Chem's cycling of base cations is limited primarily to abiotic reactions defined in the PHREEQC database, and storage and fluxes of base cations are confined to the mineral soil and streams. The model does not simulate the biotic cycling of base cations and

assumes base cation uptake by plants equals the base cation release through decomposition; therefore, the model may not be able to predict stream base cation and ANC concentrations in disturbed or aggrading ecosystems.

Because DayCent-Chem simulates so many processes, it requires many different types of data inputs, parameter estimates, and data to evaluate model performance. Uncertainty about the validity of input parameters increases the uncertainty of model results. I have the most confidence in the model when there are sufficient local data available. The minimum meteorological requirements are daily minimum and maximum air temperatures and precipitation. Daily solar radiation inputs, relative humidity, and wind speed are also utilized when available. Daily wet and dry atmospheric deposition amounts are required. Often daily deposition amounts aren't known, and must be estimated from weekly, monthly, or annual inputs. Dry deposition is not widely measured and may be poorly estimated, yet it can be an important source of base cations to a watershed. Meteorological stations and atmospheric deposition collectors may be miles away from the sites being simulated, and spatial variability in weather and deposition patterns can result in inaccurate model inputs.

Often site-specific soil properties and mineralogy are not known and are estimated from data for similar sites. The model requires inputs of soil texture, hydraulic properties, soil water holding capacity, cation exchange capacity, and mineral denudation reactions and rates. Decomposition and soil leaching rates are very sensitive to soil texture. Hydraulic conductivity, soil depth, and soil water holding capacity are important to accurately predict stream flow, moisture availability to plants, and aqueous reactions. The soil and stream pH and ANC calculations are very sensitive to mineral denudation and cation exchange processes. Furthermore, the chemical reaction database used by PHREEQC does not describe all the

mineral weathering reactions that commonly occur in watersheds, and care must be taken to add the appropriate site-specific reactions to the database.

My confidence in DayCent-Chem, as with any ecosystem model, increases when it can be validated against multiple lines of data. It is desirable to have all of the following: plant production, C and N in live biomass, soil organic matter C and N, daily stream flow, frequent stream chemistry measurements, and frequent soil chemistry measurements. However it is rare that this much monitoring data is available at any one site. The model has been used to calculate the inputs that account for empirical evidence such as inputs from mineral denudation or total S deposition amounts at Acadia National Park (Hartman et al. 2009).

I am most confident in the DayCent-Chem's ability to represent biological cycling of C and N, stream discharge, and stream NO_3^- estimates. DayCent-Chem's predictions of stream discharge match quite well to observations when local meteorological drivers are available and other water inputs are known. The model does well predicting stream NO_3^- concentrations when total atmospheric N deposition is known and streamflow is well represented. However, predicting stream concentrations of chemical species other than C and N is a greater challenge and requires the modeler to simultaneously predict base cation, silica, chloride, and sulfate concentrations. ANC and pH can only be predicted accurately if the concentrations of all other aqueous species are well represented. I would like to see more rigorous testing of the model's soil chemistry predictions against empirical data, similar to the analysis I performed for Loch Vale watershed (Chapter 2). Additionally, the model's sulfate absorption algorithm needs more development and testing. I implemented a simple Michaelis–Menten saturation function to describe sulfate sorption/desorption with changing soil sulfate concentrations. Sulfate absorption may not be important in many western U.S. watersheds that have low sulfate inputs (except

perhaps where pyrite is an important mineral in parent material), but many eastern U.S. watersheds have a history of sulfate deposition and may be absorbing sulfate or releasing it as they recover from decades acid deposition.

There are a few more caveats related to the PHREEQC model. The models's ion association and Debye Huckel expressions are only appropriate for low ionic strength solutions. Therefore, DayCent-Chem may not do well predicting stream chemistry from highly polluted waters or acid mine drainage. Care must be taken to select a good reaction database: Parkhurst and Appelo (1999) noted that there have been internal inconsistencies in the databases that have been distributed with PHREEQC, with no systematic attempt to determine whether the reactions remain consistent with experimental data.

1.5 Summary

This dissertation describes the DayCent-Chem model, its application to eight mountainous ecosystems in the U.S., and how I used the model to evaluate the effects of N deposition, climate change, and elevated atmospheric CO_2 concentrations on C- and N-cycles and stream chemistry.

- Chapter 2. *Application of a coupled ecosystem-chemical equilibrium model, DayCent-Chem, to stream and soil chemistry in a Rocky Mountain watershed (Hartman et al. 2007)*. This chapter contains the original DayCent-Chem model description paper and its inaugural application at Andrews Creek watershed in Rocky Mountain National Park.
- Chapter 3. *Modeling stream acidification from excess nitrogen deposition in an alpine watershed*. Using scenarios of N deposition for Andrews Creek watershed in Rocky Mountain National Park, DayCent-Chem was used to determine the amount of N deposition that leads to episodic acidification and chronic acidification.

- Chapter 4. *Combined effects of warming and atmospheric nitrogen deposition on net ecosystem production, greenhouse gas flux and water quality in nine United States mountain ecosystems.* DayCent-Chem was used to address the combined effects of warming, N deposition, and elevated atmospheric CO_2 concentrations on six mountain forest and two alpine tundra ecosystems of the United States.
- Chapter 5. *Conclusion*. Ecosystem response to global environmental change, unexpected results, and the future of DayCent-Chem.

2 APPLICATION OF A COUPLED ECOSYSTEM-CHEMICAL EQUILIBRIUM MODEL, DAYCENT-CHEM, TO STREAM AND SOIL CHEMISTY IN A ROCKY MOUNTAIN WATERSHED[1]

2.1 Chapter Overview

Atmospheric deposition of sulfur and nitrogen species have the potential to acidify terrestrial and aquatic ecosystems, but nitrate and ammonium are also critical nutrients for plant and microbial productivity. Both the ecological response and the hydrochemical response to atmospheric deposition are of interest to regulatory and land management agencies. We developed a non-spatial biogeochemical model to simulate soil and surface water chemistry by linking the daily version of the CENTURY ecosystem model (DayCent) with a low temperature aqueous geochemical model, PHREEQC. The coupled model, DayCent-Chem, simulates the daily dynamics of plant production, soil organic matter, cation exchange, mineral weathering, elution, stream discharge, and solute concentrations in soil water and stream flow. By aerially weighting the contributions of separate bedrock/talus and tundra simulations, the model was able to replicate the measured seasonal and annual stream chemistry for most solutes for Andrews Creek in Loch Vale watershed, Rocky Mountain National Park. Simulated soil chemistry, net primary production, live biomass, and soil organic matter for forest and tundra matched well with measurements. This model is appropriate for accurately describing ecosystem and surface water chemical response to atmospheric deposition and climate change.

[1] Reprinted from Ecological Modelling, Vol. 200, Melannie D. Hartman, Jill S. Baron, and Dennis S. Ojima, Application of a Coupled Ecosystem-Chemical Equilibrium Model, DayCent-Chem, to Stream and Soil Chemistry in a Rocky Mountain Watershed, Pages 493-510 Copyright (2007), with permission from Elsevier.

2.2 Introduction

Watershed response models to atmospheric deposition have long focused on geochemical processes that lead to surface water acidification. As U.S. sulfur dioxide emissions have sharply decreased in response to the U.S. Clean air Act Amendments, the importance of atmospheric nitrogen species in wet and dry deposition has become apparent. Nitrogen deposition, from both nitrogen oxide and ammonia emissions, is elevated above background throughout the U.S. (NADP/NTN 2004). Excess N deposition will cause lake and stream acidification in a process similar to that caused by sulfate deposition, with an important difference. Because nitrogen is a critical nutrient for plants and microbes, any realistic projection of nitrogen-caused acidification must include understanding of ecosystem nutrient cycling. Nitrogen export is a function of deposition, climate, and internal nitrogen-cycling processes, including plant uptake and nitrogen immobilization in soil organic matter (Matson et al. 2002). Further, the addition of nitrogen to nearly all ecosystems stimulates biological activity, leading to increases in plant productivity, microbial activity, trace gas emissions, and alteration of species assemblages (Matson et al. 2002). Models that ignore the ecological aspects of atmospheric nitrogen deposition are missing processes that are important in their own right, and can inform decision makers of environmental changes well in advance of acidification.

We coupled two widely accepted and tested models, one of daily biogeochemistry for forest, grassland, cropland, and savanna systems, DayCent (Parton et al. 1998), and the other of soil and water geochemical equilibrium, PHREEQC (Parkhurst and Appelo 1999). The purposes of creating the linked DayCent/PHREEQC model, hereafter referred to as DayCent-Chem, were to capture the biogeochemical responses to atmospheric deposition and to explicitly consider those biogeochemical influences on soil and surface water chemistry. The linked model

expands on DayCent's ability to simulate N, P, S, and C ecosystem dynamics by incorporating the reactions of many other chemical species in surface water. We use DayCent-Chem to investigate how wet and dry deposition affect biological assimilation, soil organic matter composition, acid neutralization capacity (ANC) and pH of surface waters, aluminum mobilization, soil base cation depletion, and base cation flux. Because DayCent-Chem operates on a daily timestep, it has the potential to simulate episodic acidification.

Many computer models have be used to evaluate and predict the effects of atmospheric deposition and global change on ecosystems (Tiktak and van Grinsven 1995, Kickert et al. 1999). DayCent-Chem, a model of intermediate complexity, differs from several other non-spatial, non-empirical hydrochemical models in its process detail, types of processes simulated, and timestep. Some models, like MAGIC (Model of Acidification in Catchments) and AHM (Alpine Hydrochemical Model), are useful tools for forecasting and hindcasting acidification trends (Cosby et al. 1985, Wolford et al. 1996, Meixner et al. 2000, Cosby et al. 2001). PnET-BGC and NuCM represent ecosystem processes, but the former operates on a monthly time step and the latter requires extensive parameterization (Johnson et al. 1993, Gbondo-Tugbawa et al. 2001). SOILVEG and the combined FORGRO/NUCSAM models, with detailed descriptions of biogeochemical and canopy processes that include direct effects of pollution, have been used to evaluate the short- and long-term effects of multiple stressors on forest stands, but do not simulate stream discharge and chemistry (Mohren and van de Veen 1995, van Heerden et al. 1995). There is no one model to fit all applications, and the diversity of hydrochemical models gives researchers many comparative tools for investigating such problems as episodic or chronic acidification and metal toxicity in surface waters, ecosystem responses to deposition, and determining critical loads on ecosystems.

We tested DayCent-Chem against a long-term data set available from Andrews Creek in Loch Vale Watershed (LVWS), Rocky Mountain National Park, Colorado. The long-term data set has attracted other modelers: AHM and MAGIC have been applied to Andrews Creek, and two ecosystem models, RHESSys and CENTURY have been applied to the larger Loch Vale Watershed (Baron et al. 1994, Hartman et al. 1999, Baron et al. 2000, Meixner et al. 2000, Sullivan et al. 2005). We addressed the following questions. 1) How well can the model simulate ecosystem processes and chemistry of alpine tundra and subalpine forest? 2) Can the separate site-level runs be combined successfully to describe stream chemistry in spatially heterogeneous watersheds ? 3) Do the biological processes within DayCent-Chem contribute to the model's ability to simulate stream chemistry?

2.3 Model descriptions

2.3.1 DayCent 5 model

CENTURY is a non-spatial, lumped parameter model that simulates C, N, P, S, and water dynamics in the soil-plant system at a monthly timestep over time scales of centuries and millennia (Parton et al. 1987, Parton et al. 1994). CENTURY can represent a grassland, crop, forest, or savanna system with parameters that describe the site-specific plant community and soil properties. DayCent, the daily timestep version of CENTURY, adds layered soil temperature, a trace gas submodel, a more detailed soil hydrology submodel, and explicitly represents inorganic N as either NO_3^- or NH_4^+ (Parton et al. 1998, Kelly et al. 2000, Del Grosso et al. 2001). DayCent 5 is an object oriented model written in the C++ programming language, that implements a layered soil structure and algorithms to manage soil layers (CENTURY5 2006). The model is initialized with an organic soil depth and up to ten soil layers where each

layer has a specified thickness, texture, bulk density, field capacity, wilting point, and saturated hydraulic conductivity. Climate drivers required for DayCent 5 are daily precipitation, and minimum and maximum air temperatures. DayCent5 output includes daily evapotranspiration; soil water content; outflow; inorganic and organic C, N, P, and S stream fluxes; C, N, P, and S contents in soil and plant pools; net primary production (NPP); nutrient uptake; trace gas flux; and heterotrophic respiration (CENTURY5 2006).

2.3.2 PHREEQC model

PHREEQC (Parkhurst and Appelo 1999) is a model based on equilibrium chemistry of aqueous solutions interacting with minerals, gases, exchangers, and sorption surfaces. The model is written in the C programming language and has an extensible chemical data base. We used version 2.7 of PHREEQC in the linked model to compute aqueous speciation, ion-exchange equilibria, fixed-pressure gas-phase equilibria, dissolution and precipitation of mineral phases to achieve equilibrium, and irreversible aqueous mineral phase reactions. The aqueous model uses ion-association and Debye Hückel expressions. Ion-exchange reactions are modeled with the Gaines-Thomas convention and equilibrium constants derived from Appelo and Postma (1993) . Except for changing PHREEQC's main program to a subroutine, we did not alter the PHREEQC model.

2.3.3 Data flow in the linked model

In addition to DayCent 5's required inputs (described in section 2.1), the user must provide: (1) Daily atmospheric wet deposition concentrations for precipitation species Ca^{2+}, Cl^{-}, K^{+}, Mg^{2+}, Na^{+}, NH_4^{+}, NO_3^{-}, SO_4^{2-}, and H^{+}; (2) Daily dry deposition amounts or dry:wet ratios

for all precipitation species; (3) Initial snow pack water content and chemical composition; (4) Initial soil solution concentrations; (5) Exchangeable cations in each soil layer; (6) Potential annual denudation rates for each mineral phase that could be dissolved in the soil, groundwater, or stream solutions.

DayCent-Chem implements a geochemical submodel of layered pools and properties that provides information exchange, such as of water fluxes and solute concentrations, between the coupled models, and performs daily geochemical output (Figure 2.1). The geochemical submodel defines soil layers and a groundwater pool that correspond to those in DayCent 5's original soil class. DayCent-Chem calculates daily wet deposition amounts from precipitation concentrations and dry deposition amounts from dry:wet ratios if dry amounts are not input explicitly. Surface water concentrations are computed in a two step process where solutes are first transported, then PHREEQC undertakes solution reactions. At each timestep the model updates exchangeable cation pools (CaX_2, MgX_2, NaX, KX, NH_4X, HX, FeX_2, MnX_2, AlX_3, $AlOHX_2$, where X^- is a permanent negatively charged exchange site) and soil solutions in each soil layer, along with groundwater and stream solutions. In addition to standard DayCent 5 output files (section 2.1), at each daily timestep the model writes the solution chemistry for soil layers, groundwater, and stream.

DayCent-Chem invokes the PHREEQC model through a subroutine call, but the transfer of information to and from PHREEQC occurs through its standard ASCII input and output files. For each daily timestep, the model writes the initial compositions of the soil layers, groundwater, and stream solutions to the PHREEQC input file, soln.pqi (Figure 2.1). When there are ***n*** soil layers, there are ***n***+2 solutions defined in soln.pqi, plus a SELECTED_OUTPUT block that tells PHREEQC what information to put out. PHREEQC performs its calculations on each initial

solution in soln.pqi, it writes its reacted solution results to a "selected output file", soln.sel. The model parses soln.sel, and updates its soil, groundwater, and stream pools with these values.

2.3.4 DayCent-Chem model processes

DayCent-Chem (Figure 2.2) simulates atmospheric deposition, plus snowpack, plant, soil, and stream dynamics (left side of figure) while utilizing PHREEQC's soil and stream water reactions (right side of figure).

2.3.4.1 Atmospheric deposition and fertilization

Atmospheric deposition occurs in wet and dry forms. If the air temperature is cold enough, deposition will be routed to the snowpack, otherwise it will be routed to the soil surface where it can infiltrate the soil, seep into groundwater, or run off directly to stream flow. Additional N, P, and S may be incorporated into the top soil layer through inorganic fertilizer or organic matter additions.

2.3.4.2 Plant dynamics

Carbon is dynamically allocated to above and below ground plant parts according to nutrient availability, water stress, and vegetation type. Plants take up nutrients (NO_3^-, NH_4^+, P, and S) from soil as needed to maintain carbon:nutrient ratios in the range specified for the plant. Nutrients from scenescing leaves are translocated to plant storage at the end of the growing season. Dead plant material remains standing or is dropped onto the soil surface. Some plant types are able to reduce their mineral N demand by symbiotically fixing nitrogen.

Because the DayCent model simulates only C, N, P, and S dynamics, there is no assimilation of base cations (Ca^{2+}, Mg^{2+}, K^{+}) by plants in the linked model; we assume that annual plant uptake of these three nutrients equals the amount released through decomposition of plant material. This assumption may hold for undisturbed ecosystems, but not for recently disturbed areas or relatively young forests. Net cation assimilation is small (25 meq m^{-2} yr^{-1}) in the old-growth forest of LVWS, but there may be spatial variation within the soil profile between the uptake of base cations and their release through decomposition of fine roots and litter (Arthur 1990).

2.3.4.3 Soil and weathering dynamics

Organic matter is incorporated into the soil through litter fall and death of roots. Decomposing organic matter is redistributed among active, passive, and slow pools while N, P, and S is either mineralized or immobilized. CO_2 produced by heterotrophic respiration is dissolved in soil solutions. Rainfall and snowmelt infiltrating the litter leach dissolved organic C, N, P, and S (DOC, DON, DOP, and DOS, respectively). Both inorganic and organic species are transported downward with water that further leaches organic and mineral soil. Nitrification and denitrification produce N_2, N_2O, and NO_x through oxidation and reduction of NH_4^+ and NO_3^-, respectively. Cations in solution are adsorbed and desorbed from permanent negatively-charged exchange sites (X^-). Dissolution of primary and secondary minerals releases base cations, aluminum hydroxides, bicarbonate, metallic cations, hydrogen ions, silica, sulfate, and other inorganic species into soil layer, groundwater, and stream solutions. A portion of DOC is organic acid that reacts with other species in soil and stream solutions. Water exiting the soil

profile enters either the stream or groundwater; a user-specified fraction of this groundwater storage is released to stream flow each day.

Annual denudation rates of common primary and secondary minerals are model inputs, and each mineral can be dictated to dissolve only, to precipitate only, or to do either. The maximum amount of any mineral that can be dissolved within a solution on a given day is calculated by dividing its annual denudation rate by 365. The user specifies the distribution of minerals among the soil layers, groundwater, and stream. For solutions where mineral dissolution occurs, the daily potential denudation rates of each mineral are listed in a PHREEQC EQUILIBRIUM_PHASES reaction. This means minerals can dissolve until they reach equilibrium with the solution, or until the maximum daily amount has been dissolved, whichever comes first. No kinetically limited mineral dissolution reactions are considered. Minerals precipitate when their components are oversaturated in solution.

The production and flushing of DOC in soils influences stream chemistry. In particular, DOC has the capacity to complex with free heavy metal cations, reducing their toxicity (Drever 1982). In the model, DOC concentrates in soil over the winter when soil water flux is low, and is flushed from the soil when water flow increases. Naturally occurring organic acids are modeled using a triprotic analog (H_3Org) (Driscoll et al. 1994, Gbondo-Tugbawa et al. 2001). The total amount of organic analog present is estimated as,

$$\left[Org^{n-} \right]_{Total} = SiteDenDOC \qquad (1)$$

where *SiteDenDOC* (Table 2.1) is site density, which is the moles of organic anion sites per moles of DOC, and Org^{n-} is the organic analog anion in soil solution.

Acid neutralizing capacity (ANC) is calculated as the concentration (μeq/L) of H^+ acceptors minus concentrations of H^+ donors and allows for the contribution of dissolved

inorganic carbon as well as organic solutes that bind H^+ and certain hydroxy-Al and organo-Al complexes (Driscoll et al. 1994, Gbondo-Tugbawa et al. 2001),

$$\begin{aligned} ANC = &[HCO_3^-] + 2[CO_3^{2-}] + [OH^-] - [H^+] \\ &+ \left[Al(OH)^{2+} \right] + 3\left[Al(OH)^{4-} \right] \\ &+ \left[HOrg^{2-} \right] + 2[Org^{3-}] + [AlOrg] \end{aligned} \qquad (2)$$

2.3.4.4 Surface water and snow dynamics

Stream flow is controlled by a number of model parameters to obtain a watershed response (Table 2.1). Rain and snow melt that do not infiltrate the soil surface carry precipitation solutes to stream flow along with dissolved organics leached from surface litter, although a fraction of surface runoff (RO2DEEP) can be routed to groundwater for deferred release into the stream. Water that infiltrates the soil profile leaches organic and inorganic species. DayCent directs a constant fraction (STORMF) of soil drainage to stream flow and (1-STORMF) to groundwater; a constant fraction (BASEF) of groundwater is routed to stream flow. Some of the CO_2 carried from soil solutions and groundwater degasses as it encounters the lower partial pressure of the atmosphere. Geochemical reactions in stream flow and groundwater include the same aqueous reactions defined for soils, except for cation exchange.

Three parameters regulate snowpack accumulation, melt, and sublimation (Table 2.1). Precipitation is added to the snowpack when maximum daily air temperature is below TMELT(1), and snow melts above this temperature. The rate of melt is a function of TMELT(2) and the difference between maximum daily air temperature and TMELT(1). When a snowpack is present, the maximum amount of sublimation is the product of parameter FSUBLIM and a potential evapotranspiration rate calculated by the model as a function of air temperature.

FSUBLIM > 1 is used to account for sublimation by wind that can substantially increase snowpack loss from windy, high elevation environments (Hartman et al. 1999).

Elution causes early melt water to be the most chemically concentrated of the season. Even when ionic concentrations in precipitation are low, snowpacks may accumulate large quantities of ionic species and release these species in a strong ionic pulse (Campbell et al. 1995). The magnitude of the ionic pulse depends on snow depth, rate of melt, and number of melt/freeze cycles in the snowpack (Williams and Melack 1991, Bales 1992), and therefore may vary regionally, spatially within a watershed, and/or from year to year at the same site (Williams and Caine 2001). To simulate elution, the model allows the user to increase the rate of ionic release from the snowpack for a specified duration at the commencement of snowmelt.

2.3.4.5 Dissolved gases

The total amount of dissolved inorganic carbon in soil, groundwater, and stream solutions is regulated in part by equilibrating solutions with $CO_2(g)$. The partial pressure of $CO_2(g)$ in soil and groundwater solutions, pCO_2soil (Table 2.1) was set to $10^{-2.5}$ atm (Lindsay 2001). The stream water solution and the top soil layer are brought to equilibrium with $pCO_2(z)$, where z (meters) is the site elevation. The altimeter equation multiplied by $10^{\log 10 p^{CO2adj}}$ (Table 2.1) defines the value of $pCO_2(z)$ used by the model,

$$pCO_2(z) = pCO_2(0) * e^{-gz/RT} * 10^{\log 10 pCO2adj} \qquad (3)$$

where $pCO_2(0)$ is the pCO_2 at mean sea level ($10^{-3.5}$ atm), g is the gravitational constant (9.81 m s^{-2}), R is the specific gas constant (287.0 J kg^{-1} K^{-1}), and T is the temperature (K).

2.4 Methods

2.4.1 Study area

The 183 ha Andrews Creek watershed is located within the larger Loch Vale watershed, Rocky Mountain National Park, CO. It ranges in elevation from 3200 to 4000m and is dominated by bedrock (57%) and talus (31%) with alpine tundra soils comprising 11%. Andrews Glacier (10 ha) and a small tarn comprise the remaining land cover fractions of the Andrews Creek watershed (Meixner et al. 2000). The tarn was not included in the modeling effort. The hydrology is dominated by annual winter snow that melts during the spring and summer. Discharge appeared to be augmented by glacier and permafrost melt water after year 1997 (Clow et al. 2003). Stream discharge is monitored continuously at a gaging station at the base of the watershed during the ice-free season. Stream water samples are collected weekly for chemical analysis at the same location.

An old-growth Englemann spruce-subalpine fir forest is located just below the Andrews Creek stream gage. The forest is characterized as cool, sheltered, well-drained, with relatively deep soils. Soils are coarse-textured with an overlying organic layer averaging 5cm (Rueth et al. 2003).

Talus slopes in LVWS are the primary ground water reservoir, with a maximum storage capacity equal to or greater than annual discharge (Clow et al. 2003). Groundwater flowing from talus can account for ≥75% of streamflow in Andrews Creek during storms and the winter baseflow period. Ice stored as permafrost (including rock glaciers) is the second largest ground water reservoir in LVWS (Clow et al. 2003).

Average annual precipitation from 1984-2003 measured at the Loch Vale weather station was 106 (stdev 18) cm, approximately 65 percent of which was snow (NADP/NTN 2004). The climate is cold and windy, with a mean annual temperature of 1.5 °C (Baron 2002).

2.4.2 Simulated land cover types

Separate bedrock/talus and tundra sites were simulated and their results combined to derive total watershed response for Andrews Creek. The contribution of each site to total discharge quantity and quality was weighted by the percentage of the watershed occupied by each area represented. The combined bedrock/talus and tundra simulation, hereafter referred to as the combined alpine run, had a 89% contribution from bedrock/talus and 11% from tundra (Meixner et al. 2000). The bedrock/talus simulation represents solid metamorphic and igneous bedrock surfaces and cliffs, talus slopes, and block slopes with a small amount of perennial vegetation. The tundra of Andrews Creek Watershed has moderately deep soils with dry to moist perennial sedge meadows. Tundra vegetation and soil organic matter parameters for DayCent were obtained from a nearby alpine research site, Niwot Ridge (Conley et al. 2000).

Although subalpine forest within LVWS lies primarily below the Andrews Creek outlet, we simulated forest dynamics to further test the biological and soil processes of the model against a rich data set available for this forest. We did not model the entire Loch Vale watershed, nor did we include the forest simulation in Andrews Creek results.

2.4.3 Parameter estimation and initial conditions

Soil layer thickness, pH, clay content, organic matter percentage, and exchangeable cations for tundra and forest soils were initialized with data for a Cryochrept and Cryoboralf,

respectively (Table 2.2; Baron et al. 1992b). For the bedrock/talus simulation, we created a single shallow dense soil layer with very low cation exchange capacity (Table 2.2, 2.3, 2.4). Because measured sulfate adsorption in LVWS was less than 1.2 mmol kg^{-1} and soil PO_4^{3-} concentrations are low (Baron et al. 1992b), sulfate and other anion adsorption reactions were not included in Andrews Creek simulations.

We prescribed different weathering rates to bedrock/talus, tundra, and forest simulations (Table 2.5). Primary mineral weathering reactions in LVWS have been quantified using a combination of traditional mass-balance calculation methods and strontium isotope mixing calculations (Mast et al. 1990, Clow 1992, Mast 1992, Clow et al. 1997). Calcite weathering occurs in fresh talus surfaces, but is not likely in older more weathered soils (Walthall 1985, Clow and Sueker 2000). Silicate mineral weathering has a strong influence on tundra waters (Clow and Sueker 2000), and the influence of sulfide-bearing minerals is significant in Andrews Creek (Campbell et al. 1995). The kinetically-limited dissolution of crystalline minerals can not account for the regulation of SiO_2 in LVWS stream waters, and faster reacting amorphous aluminosilicates may play an important role in regulating SiO_2 concentrations in alpine soils (Clow 1992, Campbell et al. 1995). Walthall (1985) reported that minerals in LVWS forest soils dissolve at four times the watershed average rate. We assumed that silicates and pyrite in tundra soils dissolve at three times the watershed rate, and assigned 100% of calcite weathering to the bedrock/talus site. The 99 moles of oligoclase (Na:Ca = 73:27) are represented as 72.3 moles of albite and 26.7 moles of anorthite. We prescribed amorphous silica dissolution in tundra and bedrock/talus soils to better estimate stream silica concentrations.

2.4.4 Weather data

Precipitation and daily minimum and maximum air temperatures data were taken from the LVWS weather station (3159 m) (LVWS 2004). The median elevation of Andrews Creek basin is ~400 m higher than the weather station, so we applied an environmental lapse rate of 6°C per 1000m (Daly et al. 2002)to account not only for the higher elevation of Andrews Creek basin, but also the shadowing effect of cliff faces and northerly aspect of the catchment that limits solar heating during much of the year (Campbell et al. 1995).

Both weekly and daily precipitation amounts were measured at NADP/NTN site CO98 (NADP/NTN 2004). Weekly measurements were often available when daily precipitation values were missing, particularly during the snow season. In this case we adjusted daily precipitation uniformly for each missing value during the week, so that the weekly sum was equal to the measured weekly amount. When neither daily nor weekly values were recorded, daily precipitation was set to 0.0. A second weather station in Andrews Creek basin was used to fill in missing temperature data using linear regression equations.

2.4.5 Daily wet and dry deposition estimates

Daily wet deposition concentrations were derived from weekly concentrations by assuming individual precipitation events had the same concentrations as the week-long sample. Field pH values were used when possible, otherwise lab pH values were substituted. Missing concentrations of any solute for a particular day of year were assigned the multi-year average concentration for that same day of year.

The composition and proportion of dry deposition varied seasonally and spatially in LVWS (Table 2.6). Quarters 1, 2, 3, and 4 were January-March (winter), April-June (spring),

July-September (summer), and October-December (autumn), respectively. To calculate seasonal dry:wet deposition ratios of NO_3^-, NH_4^+, and S (SO_2 plus SO_4^{2-}), we used the 1995-2002 quarterly dry deposition measurements for site ROM406 of the Clean Air Status and Trends Network (CASTNet) (CASTNET 2004), and the corresponding quarterly wet deposition measurements from NADP/NTN site CO98 in LVWS. The ROM406 site is located within forest at an elevation of 2743 meters, approximately 10 km SE of and 400m lower than NADP/NTN site CO98. According to the CASTNet derived dry:wet ratios (Table 2.6), the highest proportions of NO_3^- dryfall occurred in the summer (0.65) and spring (0.52) quarters, whereas the highest proportions of S dryfall occurred in the winter (0.29) and autumn (0.28) quarters. The dry:wet NH_4^+ ratio was greatest in the winter quarter (0.17). For forest simulations we used these SO_4^{2-}, NO_3^- and NH_4^+ dry:wet ratios. For tundra and bedrock/talus we used one-half these NO_3^- and NH_4^+ dry:wet ratios. Because N deposition is affected by upslope conditions (Baron et al. 1992a), we assumed the treeless high elevation areas of LVWS don't capture as much dryfall nitrogen as forests due to their smaller LAI and relative position upslope of forests. Additionally, the dry:wet ratios for NO_3^- and NH_4^+, derived from (Clow and Mast 1995) for a treeless area in the summer, were much lower than CASTNET/NADP derived ratios while dry:wet SO_4^{2-} ratios were similar (Table 2.6).

We estimated dry:wet ratios for base cations and Cl^- using bulk deposition measurements from two sources (Table 2.6). For each constituent *i*, the dry:wet ratio was calculated as,

$$\frac{bulk\ deposition_i - wet\ deposition_i}{wet\ deposition_i} \qquad (6)$$

where $wet\ deposition_i$ was measured at the nearest NADP/NTN collector. We used measurements of bulk deposition in the LVWS snowpack (Campbell et al. 1995) to estimate the dry:wet ratios of Ca^{2+}, Mg^{2+}, K^+, Na^+, and Cl^- from October to March. For April-September

base cation and Cl^- dry:wet ratios we used measurements of bulk deposition on a granite surface in LVWS, taken at 3300m, above treeline (Clow and Mast 1995). For most of the year, dry deposition estimates for Ca^{2+}, Mg^{2+}, and K^+ were greater or equal to the amount of wet deposition of these cations. Dry deposition of Na^+ and Cl^- were insignificant in the winter.

2.4.6 Calibration

DayCent-Chem was calibrated using Andrews Creek stream chemistry and discharge data for years 1992-1999; years 2000-2003 we used for evaluation. Model calibration required several steps: 1) match simulated net primary production, soil organic matter content, and nitrogen mineralization rates with corresponding observed values, 2) match daily and annual total discharge with measured amounts, 3) match daily stream chemistry with measured concentrations, and 4) match simulated annual volume-weighted mean soil and stream concentrations with measured means.

Since the geochemical calculations are computationally intensive, DayCent was brought to an equilibrium state without utilizing PHREEQC. First, we ran the model for 400 years using background (pre-industrial) inputs of nitrogen (0.04 g N $m^{-2}yr^{-1}$) (Galloway et al. 1996). Next, we ran the model for 30 years with current average deposition rates (0.35 g N m^{-2} yr^{-1}) that varied from year to year as a linear function of precipitation. Finally, we ran the model for years 1984-2003 with the geochemical model calculations. All runs used daily 1984-2003 weather, repeated over and over if necessary.

We tuned the model on uncertain values such as the fraction of mineral denudation in each soil layer, parameters that control watershed average discharge, and pCO_2 of stream water and soil water (Table 2.1) to represent measured 1992-1999 daily stream discharge and stream

chemistry. Stream concentration calibrations were made by visually comparing daily and annual simulated and measured stream discharge and species concentrations. Our goals were to constrain the simulated concentrations within the range of measured concentrations and capture the timing and patterns of flow dilution and flow concentration for each solute. Elution parameters were adjusted to better fit stream Cl^-, SO_4^{2-}, and NO_3^-. The pH of soil and stream solutions was computed as a charge balance in solution.

We computed three separate performance measures for discharge and all solutes to evaluate the model. These included the normalized root mean square error (NRMSE), the normalized mean absolute error (NMAE) (Janssen and Heuberger 1995) and the Nash-Sutcliffe value (Nash and Sutcliffe 1970). A Nash-Sutcliffe value less than zero indicates that the mean of the observation is a better predictor of observed data than the model prediction; values close to 1.0 indicate good agreement.

2.4.7 N(-3)/N(+5) Redox Reactions

DayCent-Chem can be run with or without PHREEQC's N(-3)/N(+5) redox reactions, where N(-3) and N(+5) are the N oxidation states of NH_4^+ and NO_3^-, respectively. Nitrification and denitrification are a part of DayCent's soil processes, and allowing PHREEQC to duplicate these reactions may be redundant or even incorrect. PHREEQC's N(-3)/N(+5) redox was turned off for the tundra and forest simulations with multiple soil layers, but was allowed for the bedrock/talus simulation that describes only a single shallow and dense soil layer.

2.5 Results

2.5.1 Stream discharge and chemistry

The model performed slightly better for calibration years 1992-1999 than for evaluation years 2000-2003 (Table 2.7). Nash-Sutcliffe values, computed for daily discharge and stream concentrations, were closer to 1.0 for 1992-1999 for all values except discharge. Evaluation years corresponded to some of the driest years in Andrews Creek. Overall, model results compared better to measurements for wetter-than-average years than for drier years. Precipitation was above the 1984-2003 106 cm average during 1993-1997. Precipitation was below the average in 1992 and 1998-2003.

Daily stream concentrations were close to measured for Andrews Creek during spring and summer, but the model was less able to reproduce stream chemistry during winter when flow was very low. On the days simulated discharge was less than 0.01 cm (0.02 cfs), modeled stream concentrations were filtered from the graphs (Figures 2.3 b-j). Error terms (NRMSE and NMAE) were smaller and Nash-Sutcliffe values were closer to 1.0 for the majority of solutes when the 16% of the values representing very low flow were not included (Table 2.7).

The model captured total annual flow best through 1997, and after 1997 the model underpredicted annual totals (Figure 2.4a). This underestimate of annual total discharge is reflected in the daily hydrographs on the falling limb of years 1998 and 2000-2003 when simulated flow is below measured flow (Figure 2.3a). Daily simulated discharge followed the hydrographs of measured discharge for Andrews Creek with an R^2 of 0.64 (Figure 2.3a). For most years, the simulated onset of snow melt and the amount and timing of peak flow were close to measured values. The model overpredicted some runoff events in 1994, 1996, 1997, and 2002, and there was a large spike in simulated discharge for late August of 1994.

With the exception of a few outliers, simulated daily ANC was within the range of observed concentrations (Figure 2.3b). For most years through 1997, the model captured the observed increase in stream ANC going into winter, and its subsequent dip during snowmelt. Simulated daily ANC concentrations were particularly sensitive to daily discharge estimates, and were underestimated when discharge was overestimated, and visa versa. Outliers (ANC < 10 $\mu eq\ L^{-1}$) always occurred when there was an abrupt increase in simulated discharge that simultaneously diluted simulated stream base cation (BC) concentrations. Simulated annual volume-weighted mean ANC concentrations were within 12 $\mu eq\ L^{-1}$ of measured values for 1992-1997, but were overestimated by 8-36 $\mu eq\ L^{-1}$ the other years (Figure 2.4b).

Simulated pH tracked simulated ANC (Figure 2.3c) and was within the range of observed values, though a few outliers occurred on days when ANC was also underestimated. Simulated annual volume-weighted mean pH was within 0.2 units of measured except for years 1994 and 2003 when it was 0.4 and 0.3 units greater, respectively, than measured (Figure 2.4c).

Measured NO_3^- was concentrated during initial snowmelt due to elution and soil and ground water flushing, dipped to its minimum concentration during the summer when plants and microbes take up nitrogen, and gradually increased as discharge decreased into autumn. The model captured this pattern of observed NO_3^- concentrations, but sometimes underestimated maximum concentrations or overestimated minimum concentrations (Figure 2.3d). From 1998 to 2003, simulated daily NO_3^- concentrations were higher than observations beginning in August or September until December (Figure 2.3d). Simulated annual volume-weighted mean concentrations of NO_3^- fluctuated around observed concentrations, and were within 8 $\mu eq\ L^{-1}$ of observed concentrations all years (Figure 2.4d). Simulated NH_4^+ concentrations, like measured concentrations, lacked a strong seasonal pattern but were in the range of measured concentrations

(Figure 2.3h). Both simulated and measured annual volume-weighted mean NH_4^+ concentrations were very low and within 2 μeq L^{-1} of each other (Figure 2.4h). Predicted mean annual 1992-1997 inorganic nitrogen export (0.33 g N m^{-2} yr^{-1}) was very close to the measured flux for Andrews Creek (0.32 g N m^{-2} yr^{-1}) (Campbell et al. 2000) (Table 2-8).

The model did especially well at capturing observed daily trends in sulfate concentrations (Figure 2.3e). Like NO_3^-, simulated and measured SO_4^{2-} concentrations were highest during snowmelt, and were at a minimum during the summer. Simulated SO_4^{2-} concentrations for the final third of years 1998, 1999, and 2002 were greater than measured; discharge was underestimated during this time of year in 1998 and 2002. Simulated annual volume-weighted mean concentrations of SO_4^{2-} that did not become more concentrated for drier years as was observed, and were underestimated by 11-16 μeq L^{-1} in 1995, 2001 – 2003. (Figure 2.4e).

Measured Cl^- and BC concentrations followed seasonal patterns similar to NO_3^- and SO_4^{2-}, concentrating during initial snowmelt, diluting through June or July, and gradually concentrating the remaining months of the year (Figures 2.3 f-g). Simulated daily concentrations of Cl^- followed this pattern reasonably well except during 1994 and in the autumn of years 1998, 1999, 2000, and 2002 when simulated concentrations were much higher than observed (Figure 2.3g). Simulated and observed annual volume-weighted mean concentrations of Cl^- were within 1 μeq L^{-1} of each other all years except 1994 **(**Figure 2.4g).

The model underestimated maximum BC concentrations in spring, and overestimated them some years in autumn, but prior to 1998 generally captured the observed pattern of flow dilution during snowmelt and flow concentration during the lower flow periods (Figure 2.3f). Both simulated and observed patterns of silica showed flow dilution during snowmelt and flow concentration during low flow (Figure 2.3i). Simulated daily concentrations of silica tended to

have a wider range of values than were measured, and were particularly higher than observed for a one to two week period at the onset of snow melt, and in autumn of most years after 1997. Simulated annual volume-weighted mean concentrations of base cations (BC) and silica were close to observed values after 1997 **(**Figures 2.4 f-i).

Simulated and measured daily DOC concentrations had the same range of values (Figure 2.3j). Simulated annual volume-weighted mean DOC concentrations were lower than measured DOC (Figure 2.4j). Infrequent measurements of DOC in Andrews Creek may have made this gap between simulated and measured annual DOC appear larger than it actually was.

2.5.2 Combined runs vs. separate runs

Steam chemistry from the combined alpine run approximated measurements better than individual tundra and bedrock/talus runs (Table 2.7). The combined run results had the smallest error terms for pH, NO_3^-, base cations, Si, and NH_4^+. The tundra simulation had the smallest error terms for ANC, SO_4^{2-}, Cl, and discharge, and tundra had a slightly higher R^2 for discharge. The bedrock/talus runs did not have the smallest error term for any solute. Though some biological processes were simulated for bedrock/talus that contributed 89% to stream discharge and chemistry, the greater plant growth, soil organic matter leaching, and soil depth represented by the tundra simulation improved overall results. The 100% bedrock/talus simulation overpredicted the magnitude of daily runoff more often than the combined run did. The contribution of DOC to stream flow (Figures 2.3j, 2.4j) was almost exclusively from the tundra simulation. Because the bedrock/talus run included calcite dissolution (from rock surfaces) and the tundra did not, daily stream BC and ANC concentrations for this simulation were generally higher and further from measurements than those of the combined simulation.

2.5.3 Evapotranspiration, sublimation, NPP, biomass, mineralization, and soil organic matter

2.5.3.1 Tundra

Model estimates of net primary production (NPP) and live biomass for tundra were lower than, but close to, measured values from nearby Niwot Ridge (40° 03′ N 105° 35′ W, ~30 kilometers southwest of LVWS) (Table 2.8). Actual average annual production rates for LVWS tundra are probably lower than those at Niwot Ridge due to shallower soils and steeper slopes at LVWS (Arthur 1992). Simulated above ground NPP for tundra (43 g C m^{-2} yr^{-1}) was at the low end of that measured at Niwot Ridge (44-135 g C m^{-2} yr^{-1}) (Bowman and Fisk 2001), while total NPP (95 g C m^{-2} was less than measured (149-219 g C m^{-2}) (Bowman and Fisk 2001). Year-long simulated aboveground live biomass (0-63.8 g C m^{-2}) was at the low end of Niwot measurements (60-117 g C m^{-2}) (Bowman and Fisk 2001) while belowground live biomass (425-515 g C m^{-2}) was in the middle of the measured range (225-929 g C m^{-2}) (Bowman and Fisk 2001). The model's above-to-belowground biomass ratio at the peak of the growing season was about 1:8, while measured above-to-below ground biomass ratios ranged from 1:3.7 to 1:12 (Bowman and Fisk 2001).

The model did well at estimating N-mineralization and total soil organic matter, but underpredicted total evapotranspiration for tundra (Table 2.8). Simulated N-mineralization rates (2.1 g N m^{-2} yr^{-1}) were very close to those observed on Niwot Ridge (~2.0 g N m^{-2} yr^{-1}) (Bowman 1992) and soil organic matter (9550 g C m^{-2}) was within the range observed: 6700 g C m^{-2} for dry alpine sedge meadows at Niwot Ridge (Seastedt 2001) and 13,000 g C m^{-2} (Conley et al. 2000). Simulated tundra evapotranspiration (ET) (6.1 cm yr^{-1}) was about 26% of a previously approximated amount (23.4 cm yr^{-1}), and sublimation (26.5 cm yr^{-1}) was at the low end of the expected range (26-88 cm yr^{-1}) (Baron and Denning 1992).

2.5.3.2 Bedrock/Talus

The bedrock/talus simulation represented a variety of rock surfaces with minimal plant production where runoff and evaporation are dominant processes. Simulated discharge from the rock surface (91.5 (stdev. 18.4) cm yr^{-1}) was higher than simulated tundra discharge (83.8 (stdev. 13.9) cm yr^{-1}) (Table 2.8). Average annual simulated ET for bedrock/talus (11.7 cm yr^{-1}) was between two previous approximations. Clow and Mast (1995) estimated that ET from a rock surface is approximately 15% of summer precipitation (or approximately 8 cm yr^{-1}), and Baron and Denning (1992) estimated that ET was approximately 17.0 cm yr^{-1}. Simulated sublimation for bedrock/talus (15 cm yr^{-1}) was below the expected range (26-88 cm yr^{-1}) (Baron and Denning 1992).

2.5.3.3 Forest

Simulated net primary production (NPP) and live biomass for forest were lower than, but close to, measured values (Arthur and Fahey 1992) (Table 2.8). Simulated above ground NPP for forest (111 g C m^{-2} yr^{-1}) was lower than was measured (163 g C m^{-2} yr^{-1}), while total simulated NPP (186 g C m^{-2}) was within the measured range (136-340 g C m^{-2}). The range of simulated belowground live biomass (1170-1266 g C m^{-2}) included a measured value (1200 g C m^{-2}), while simulated aboveground live biomass (4270-4408 g C m^{-2}) was lower than measured (5511 g C m^{-2}).

As with tundra, the model did well at estimating N-mineralization and total soil organic matter but underpredicted total evapotranspiration for forest (Table 2.8). The simulated N-mineralization rate for forest (2.1 g N m^{-2} yr^{-1}) was at the low end of measured values (2.0-3.0 g N m^{-2} yr^{-1}) (Arthur 1990, Arthur and Fahey 1992) and soil organic matter (6910 g C m^{-2}) was

close to the mean measured value (6800 g C m^{-2}) (Arthur and Fahey 1992, Baron and Denning 1992), 1992). Simulated forest evapotranspiration (ET) (27.0 cm yr^{-1}) was about 50% of a previously approximated amount (52.5 cm yr^{-1}), while sublimation (20.8 cm yr^{-1}) was also lower than previous estimates (26-88 cm yr^{-1}) (Baron and Denning 1992).

2.5.4 Simulations without biologic calculations

To test model sensitivity to its biological processes, we ran tundra and bedrock/talus simulations that bypassed calculations of SOM decomposition, mineralization, nitrification, denitrification, and plant production. We compared simulated stream chemistry for the tundra simulations with and without biology, and for the combined alpine simulations with and without biology.

Modeled stream NO_3^-, ANC, pH, discharge, and DOC for tundra were sensitive to the model's biological calculations. Results showed that tundra biological processes reduced stream NO_3^- concentrations, and increased stream ANC concentrations, pH, and evapotranspiration. Compared to results for tundra without biology, the tundra run with biology had annual (volume-weighted) mean stream nitrate concentrations that were 3 to 8 μeq L^{-1} (average 6 μeq L^{-1}) less (Figure 2.5a), annual mean ANC concentrations that were up to 10 μeq L^{-1} (average 5 μeq L^{-1}) greater (Figure 2.5b), annual stream pH that was as much as 0.2 units higher (Figure 2.5c), and discharge that was 2 to 7 cm $year^{-1}$ less.

Differences in stream chemistry were less noticeable between the combined runs (11% tundra, 89% bedrock/talus) with and without biology. The combined run without biology had annual mean stream nitrate concentrations that were 0 to 3 μeq L^{-1} more, annual mean ANC that was up to 1.4 μeq L^{-1} less, and discharge that was 0.3 to 1.0 cm $year^{-1}$ more, than the combined

run with biology. The higher annual mean NO_3^- concentrations for the combined runs without biology were attributed primarily to late summer and early autumn nitrate concentrations that were up to 20 μeq L^{-1} greater than were shown by combined run with biology. Since the combined run with biology overestimated NO_3^- concentrations in the late summer and early fall, runs without biology depart further from observations. The lower annual mean ANC concentrations for the combined run without biology were attributed primarily to the lower late summer and early fall ANC concentrations.

2.5.5 Soil solution chemistry

Measurements of interstitial solute concentrations were not available for the tundra soils in LVWS, so we compared simulated tundra soil chemistry to soil chemistry data from Niwot Ridge. Soil water pH values from our tundra simulations were comparable to, but generally higher than, some pH measurements at Niwot Ridge. The Inceptisols on Niwot Ridge were moderately acidic, with average pH ranging from 4.7 to 5.0 in moist meadow and about 5.5 in dry meadow (Seastedt 2001). The simulated volume-weighted mean of soil water pH for the soil profile varied seasonally and ranged from 5.4 to 6.1. Other measurements of soil water pH at Niwot Ridge from June through August (Litaor 1988) averaged 5.7 and were very close to our simulated volume-weighted mean pH for tundra soils (5.8) for these same months.

Average June through August soil water concentrations of Ca^{2+}, Mg^{2+}, Na^+, K^+, and alkalinity at Niwot Ridge (Litaor 1988) were much higher than the concentrations that we simulated for the tundra soils. For these same months, measured volume-weighted mean SO_4^{2-} concentrations (Litaor 1988) were equivalent to those we simulated for tundra (26 μeq L^{-1}). Simulated summer NO_3^- concentrations for tundra soils (14 μeq L^{-1}) were on average 64% of

those measured at Niwot Ridge (22 μeq L^{-1}) (Litaor 1988) that receives greater N deposition (NADP/NTN 2004), but estimated NO_3^- concentrations were not significantly different from measured concentrations.

Simulated forest soil chemistry compared well to measurements for some constituents. Multiple lysimeter measurements from the top 15 cm of soil of three forest plots were available over a 2 to 4 year period, approximately once a week from mid May to September (Rueth et al. 2003). The average of all lysimeter measurements for each day, along with their standard deviations, were plotted against model results averaged for the top 20cm of soil (Figure 2.6). Simulated S and Al soil solution concentrations were close to measurements most days (Figures 2.6 a,b). Modeled Ca and Mg concentrations were generally lower than observations, but for many days were within one standard deviation of measurements (Figures 2.6 c,d). Modeled K and Na concentrations were generally higher than those measured but were within one standard deviation some days (Figures 2.6 e,f). Simulated NO_3-N concentrations were generally higher than measured, but were within one standard deviation some days whereas simulated NH_4-N concentrations were a magnitude larger than measurements (Figures 2.6 g,h).

2.6 Discussion

2.6.1 Model performance

DayCent-Chem replicated seasonal and annual stream chemistry and discharge for Andrews Creek in years with abundant precipitation. In warm, dry years, especially those after 1997, the simulated discharge was lower than actual discharge and solutes were more concentrated than measured values. The discrepancy appears to have more to do with melting of permanent ice in Loch Vale, a function the model does not perform, than model performance.

Streamflow in Andrews Creek is generally 70% to 80% of measured annual precipitation, with the remainder lost via evapotranspiration and sublimation (Clow et al. 2003). From 1997 to 2001 the measured discharge:precipitation ranged 87-101%, and was 114% in 2003. Summer air temperatures in Loch Vale have been the warmest on record since 1997, so while these were years of low precipitation inputs, they were also years with temperatures high enough to raise the permafrost line and melt ice in rock and ice glaciers and permafrost (Clow et al. 2003).

The 1994 spikes in simulated daily and annual Cl^- stream concentrations (Figures 2.3g, 2.4g) resulted from a suspiciously high concentration (and deposition) of Cl^- in the 11/30/1993-12/7/1993 NADP weekly record. This high input of Cl^- to the model was stored in its snowpack and did not show up in simulated streamflow until the onset of snowmelt in 1994. Simulated annual pH dropped in 1994 (Figure 2.4c), reflecting a negative charge imbalance from the high Cl^- concentration (Figure 2.4g). We do not know why measured stream chemistry did not reflect the high Cl^- input that was measured in wet deposition in late 1993.

The simulated discharge spike in late August of simulation year 1994 (Figure 2.3a) has been problematic for at least two other hydrologic models applied to LVWS (Hartman et al. 1999, Meixner et al. 2000). The overprediction of this summer rainfall discharge peak has been attributed to either incorrect precipitation measurements as input to the models or insufficient soil zone storage within the models. The high simulated discharge peak simultaneously caused stream ANC to become negative and pH to drop (Figures 2.3 b,c).

Modeling stream ANC and pH was challenging in part because they were very sensitive to complex silica reactions and to stream pCO_2. While Mast (1992) quantified mineral weathering reactions with incomplete mineral dissolution (i.e. biotite and chlorite to smectite-illite, and oligoclase to kaolinite) it was not possible to describe the stoichiometry of these

incomplete reactions to the PHREEQC model. To mimic the incomplete dissolution of silicates, smectite and kaolinite were allowed to precipitate or dissolve (Dave Parkhurst, personal communication). Prescribing the dissolution of amorphous silica was also required. We increased stream pCO_2 above expected ambient pCO_2 at the elevation of Andrews Creek ($10^{-3.68}$ atm) to improve pH estimates. Increasing stream pCO_2 also improved estimates of annual mean SO_4^{2-}, NO_3^-, NH_4^+, and Si concentrations but elevated simulated stream ANC above observations. Using the AHM model, Meixner et al. (2000) also found that calibrated pCO_2 for Andrews Creek ($10^{-3.4}$ atm) was greater than ambient pCO_2. An analysis of a large number of lakes worldwide showed that boreal, temperate, and tropical lakes were typically supersaturated with CO_2 at concentrations that were often multi-fold greater than atmospheric CO_2 (Cole et al. 1994).

The model did especially well predicting spring and summer sulfate and aluminum soil water concentrations for forests. The simulated summer sulfate concentrations for tundra soil were close to those measured at Niwot Ridge. DayCent-Chem slightly underpredicted base cation concentrations for forest and tundra soils, but this could be due to uncertainties in estimating dry deposition and mineral denudation rates.

Soil and ground water processes are important to describing the stream chemistry of the watershed even though bedrock and talus cover 89% of Andrews Creek. The combined runs produced better results than bedrock-talus simulations alone. The greater water storage capacity of soils and evapotranspiration in tundra tempered the magnitude of daily runoff events, and tundra contributed the primary biological influence on stream chemistry.

2.6.2 Model comparisons

Different approaches to modeling reflect differences in modeling philosophy, differences in hypotheses being tested, and the anticipated model outcomes. Additionally models have computational and data input requirements. "Quantitative models allow the investigator to *observe* patterns embedded in the data, to *synthesize* data on disparate components into an integrated view of ecosystem function, and ultimately to *predict* the future behavior of some aspects of the ecosystem under given scenarios of future external drivers (Canham et al. 2003a, p.1)." DayCent-Chem is mechanistically rich and reflects our desire to capture daily biological, biogeochemical, and geochemical responses to changes in nitrogen availability. It was used for the purposes of this paper to observe and synthesize data; we plan to use it predictively in future efforts.

Four other models have been applied to Andrews Creek or Loch Vale. The Alpine Hydrochemical Mode (AHM) and the Regional Hydro-Ecologic Simulation System (RHESSys) were used to observe, synthesize, and predict (Hartman et al. 1999, Baron et al. 2000, Meixner et al. 2000). CENTURY and MAGIC were used to predict future stream chemistry conditions only (Baron et al. 1994, Sullivan et al. 2005). DayCent-Chem differs from these four models. DayCent-Chem includes explicit biogeochemical processes and computationally intensive geochemical calculations, but does not require complex spatial data processing for initialization and analysis and executes on personal computers well under an hour.

AHM, a lumped conceptual model that was designed specifically to represent daily hydrochemistry of alpine watersheds, was used to predict stream chemical response to doubling of N deposition. Nitrogen equations in the model are fitted to measured stream values, and can not reflect terrestrial nutrient cycling or ecosystem processes below treeline (Meixner et al.

2000). DayCent-Chem and AHM produced very similar results for Andrews Creek, with AHM capturing discharge slightly better, but seasonal change in ANC slightly worse.

RHESSys is a spatial data process and simulation system that computes daily water and carbon budgets of terrestrial ecosystems but does not include geochemical equations. It was applied to Loch Vale, including Andrews Creek, to project changes in watershed hydrology and tundra and forest productivity under climate change (Baron et al. 1994, Hartman et al. 1999). The underlying model structures and data requirements are different than DayCent-Chem, and the purpose completely different, but RHESSys was able to reproduce measured discharge values within 8% of annual flow for two years (1993-1994), compared with 14% for DayCent-Chem for those same years (Hartman et al. 1999).

Two monthly models, CENTURY and MAGIC, have been applied to Andrews Creek and/or Loch Vale (Baron et al. 1994, Sullivan et al. 2005). CENTURY, the parent model of DayCent-Chem, was used to ask questions about ecosystem responses to nitrogen deposition (Baron et al. 1994). As with DayCent-Chem, separate forest and tundra landscape units were simulated. Time series comparisons were not made, but forest and tundra ecosystem C and N pools and N mineralization rates were within the range of measured values. For simulation years 1984-1992, DayCent-Chem and CENTURY estimated similar stream N flux for tundra, but DayCent-Chem had higher stream N flux for forest. MAGIC is a lumped parameter model that has been used extensively to predict the long-term effects of acid deposition on stream water chemistry (Cosby et al. 1985). The dynamics of exchangeable base cations in response to strong acid anion inputs drive soil and stream chemistry; and ecological nitrogen cycling is parameterized with first order rate equations. MAGIC was used as a diagnostic tool to evaluate the sensitivity of Andrews Creek to increases in atmospheric strong acid anion deposition, and

measured data were used only for calibration (Sullivan et al. 2005). While it was impossible to compare DayCent-Chem model output to MAGIC model output at this stage, acidification forecasts with DayCent-Chem are forthcoming.

2.6.3 The importance of including biological processes in atmospheric deposition effects models

Simulated stream chemistry was sensitive to soil organic matter turnover, mineralization, nitrification, denitrification, plant production, and transpiration. Tundra simulations that bypassed these biological calculations showed large increases in annual mean stream NO_3^-, large decreases in annual mean ANC, a slight decrease in annual stream pH, and discharge that was increased because of reduced evapotranspiration. Soil organic matter leaching from tundra provided the only input of DOC to simulated streamflow.

Our comparison of simulations with and without N cycling provides an extreme example of the importance of biological processes, illustrating that even in this Rocky Mountain catchment soils and vegetation influence stream chemistry. Comparisons of DayCent-Chem results for forested catchments with models that take a simpler approach toward N cycling are yet to be made. Those comparisons will yield insight into the role of soils and vegetation in influencing acidification potential from atmospheric deposition. That is an important question of interest to regulatory agencies and resource managers, but it reflects only part of the effects caused by atmospheric deposition. Nitrogen, being an essential nutrient for all living organisms, changes terrestrial ecosystems through eutrophication before acidification occurs. Although the largely unvegetated Andrews Creek basin was not the best place to illustrate how the model represents terrestrial nutrient cycling, DayCent-Chem provides this important information to

allow model users and their audiences to evaluate the full spectrum of environmental effects caused by atmospheric deposition.

2.7 Conclusion

DayCent-Chem, a non-spatial biogeochemical model of intermediate complexity, was able to replicate the seasonal and annual stream chemistry of an alpine catchment, Andrews Creek in Rocky Mountain National Park. The contributions of separate bedrock/talus and tundra simulations were aerially weighted. Simulated stream concentrations of many solutes matched well with observations when the model accurately predicted daily and annual discharge. The model had some difficulty accurately portraying some stream solutes during winter low flow. Parameters that regulated runoff, baseflow, melt, and elution helped to calibrate the model's response to the spatially variable processes.

The model matched spring and summer sulfate and aluminum soil water concentrations for forests, and simulated summer sulfate concentrations for tundra soil. Additionally, model estimates of net primary production, biomass, soil organic matter, and net mineralization rates for alpine tundra and subalpine forest were close to measurements.

Soil and ground water processes are important to describing the stream chemistry of the watershed even though bedrock and talus cover 89% of Andrews Creek. The combined runs produced better results than bedrock-talus or tundra simulations alone. Simulated stream chemistry was sensitive to the model's plant and biological soil processes. Although the tundra simulation contributed only 11% to the combined alpine run, modeling plant and soil processes of tundra improved the model's ability to estimate daily runoff and seasonal stream nitrate

concentrations. We expect the importance of including biological processes in the model to increase for simulations of more vegetated systems.

DayCent-Chem is a daily time-step, process-based model that computes a number of biologic and abiotic processes that respond automatically to climate and deposition inputs. The value of this model beyond the application described here will be to test how strongly terrestrial N cycling influences surface water chemistry. Nitrogen cycling processes that are explicitly described by the model, will be important to evaluating potential ecosystem response to alternative scenarios of deposition and climate change.

2.8 Acknowledgements

We thank D. Parkhurst for his consultation, and D. Campbell, D. Clow, D. Manthorne, and D. Hultstrand of the U.S. Geological Survey, Loch Vale Water Energy and Biogeochemical Budgets (WEBB) project for data; S. Del Grosso and R. Conant reviewed an earlier version of this manuscript. Funding was provided by the U.S. Environmental Protection Agency Clean Air Markets Division, EPA STAR Grant R829640, National Park Service Air Resource Division, and by the U.S. Geological Survey Western Mountain Initiative.

Table 2.1. Fitted parameter values for the bedrock/talus, tundra, and forest simulations.

Parameter	Bedrock/ Talus	Tundra	Forest	Description
siteDenDOC	0.023	0.023	0.046	≥ 0.0, moles of H^+ binding sites per moles organic C
$\log_{10}pCO_2adj$	0.3	0.5	0.25	fixed change in $\log_{10}(pCO_2)$ of surface water (0.5 = √10-fold increase)
$\log_{10}pCO_2soil$	-2.5	-2.5	-2.5	$\log_{10}(pCO_2)$ (atm) in soil solutions
doNredox	1	0	0	1 (true) or (0) false - allow N(-3)/N(+5) redox
TMELT(1)	-4.0	-4.0	0.0	Temperature above which snow melts (ºC)
TMELT(2)	0.05	0.05	0.05	cm snow melted per ºC per day
FSUBLIM	1.0	2.0	1.0	potential sublimation rate multiplier
BASEF	0.05	0.05	0.05	base flow fraction (0-1)
STORMF	0.0	0.0	0.0	storm flow fraction (0-1)
RO2DEEP	0.5	1.0	1.0	fraction of runoff routed to groundwater (0-1)

Table 2.2. Forest soil layer properties and initial exchangeable cations (meq/100g) as measured for a Cryoboralf **(**Baron et al. 1992b**)**.

Layer	Thickness (cm)	Depths (cm)	Description
0	5	0 - 5	Oi: slightly decomposed organic matter
1	5	5 - 10	Oe: decomposed organic matter
2	10	10 - 20	E: very cobbly silt loam
3	15	20 - 35	Bt: extremely cobbly sandy loam
4	20	35 – 55	Bc: extremely stoney loamy sand

Layer	pH	Organic Carbon	Clay	CaX_2	MgX_2	KX	NaX	AlX_3	HX
0	4.84	13.1%		18.4	3.2	0.9	0.1	10.5	1.8
1	4.84	13.1%		18.4	3.2	0.9	0.1	10.5	1.8
2	3.78	2.7%	19.5%	5.0	1.0	0.4	0.1	18.9	1.0
3	3.72	2.5%	28.3%	3.6	0.8	0.2	0.1	25.2	0.7
4	3.74	1.3%	16.2%	2.6	0.6	0.1	0.1	16.2	0.4

Table 2.3. Tundra soil layer properties and initial exchangeable cations (meq/100g) as measured for a Cryochrept (Baron et al. 1992b).

Layer	Thickness (cm)	Depths (cm)	Description
0	2	0 – 2	Oe: moderately decomposed organic matter
1	3	2 – 5	A: black cobbly sandy loam, 20% coarse
2	12	5 – 17	Bw: brown cobbly sandy loam, 30% coarse
3	15	17 – 32	Bw: brown cobbly sandy loam, 30% coarse

Layer	pH	Organic Carbon	Clay	CaX_2	MgX_2	KX	NaX	AlX_3	HX
0	5.0	11.6%	7.0%	36.6	7.2	0.9	0.1	1.5	0.5
1	4.95	2.8%	9.5%	13.0	3.0	0.2	0.1	5.1	0.5
2	4.66	0.9%	12.6%	4.8	2.2	0.1	0.1	12.6	0.2
3	4.66	0.9%	6.1%	4.8	2.2	0.1	0.1	12.6	0.2

Table 2.4. Bedrock/talus soil layer properties and initial exchangeable cations (meq/100g). All numbers were estimated.

Layer	Thickness (cm)	Depths (cm)	Description
0	2	0 – 2	Coarse texture with high bulk density

Layer	pH	Organic Carbon	Clay	Bulk Density (g/cm^3)	CaX_2	MgX_2	KX	NaX	AlX_3	HX
0	5.0	0.0%	25%	2.0	0.3	0.04	0.02	0.01	0.3	0.02

Table 2.5. Annual potential mineral denudation rates for Loch Vale watershed (LVWS) and their distribution over bedrock/talus, tundra, and forest. Tundra (11% of LVWS) had the potential to dissolve minerals at three times the watershed rate. Forest (6% of LVWS) had the potential to dissolve minerals at four times the watershed rate. The remaining mineral dissolution was allocated to bedrock/talus. SiO_2(a), amorphous silica, was added to calibrate stream silica, alkalinity, and pH.

mineral	(Mast 1992) LVWS average (mol ha^{-1} yr^{-1})	Bedrock/Talus (mol ha^{-1} yr^{-1})	Tundra (mol ha^{-1} yr^{-1})	Forest (mol ha^{-1} yr^{-1})
calcite	106	129	0	0
albite (73% of 99 moles oligoclase)	72.3	47	217	289
anorthite (27% of 99 moles oligoclase)	26.7	17	80	107
biotite	29	19	87	116
kaolinite	18	0*	0*	0*
chlorite	7	5	21	28
pyrite	6	4	18	24
smectite	0	0*	0*	0*
SiO_2(a)	0	153	153	N/A

*Mineral allowed to precipitate only

Table 2.6. Estimated dry:wet deposition ratios for LVWS. Quarters 1, 2, 3, and 4 are winter (Jan-Mar), spring (Apr-Jun), summer (Jul-Sep), and autumn (Oct-Dec), respectively. The ratios in boldface were used for the forest simulation. The same wet:dry ratios were used for the alpine and bedrock/talus simulations except that NO_3^-. and NH_4^+ dry:wet ratios were halved.

	Quarterly[a] (1,2,3,4)	Oct-Mar[b]	Apr-Sep[c]
NO_3^-	0.29, 0.52, 0.65, 0.39	0.25	0.13
NH_4^+	0.17, 0.13, 0.14, 0.13	0.5	consumption in bulk collector
SO_4^{2-}	0.29, 0.23, 0.27, 0.28	0.29	0.23
Ca^{2+}		2.5	1.71
Mg^{2+}		1.0	3.89
Na^+		insignificant	0.40
K^+		very small	3.33
Cl^-		insignificant	0.21

[a] Computed from CASTNET ROM406 and NADP CO98 data
[b] Campbell et al. 1995 (WY1992): dry:wet computed as ($snowpack_{max}$ - $NADP_{Oct-Mar}$) / $NADP_{Oct-Mar}$
[c] Clow and Mast 1995 (Jul. 5 - Aug. 19, 1994): dry:wet computed as (bulk dep - NADP) / NADP

Table 2.7. Nash-Sutcliffe (Nash-Sut) and normalized mean absolute mean (NMAE) values for daily stream concentrations and discharge. The leftmost column of numbers represent calibrated and evaluation years, respectively. The next four columns represent non-filtered and filtered values. Non-filtered values include all days measurements were available, and filtered include only days simulated discharge was ≥ 0.01 cm. The rightmost six columns represent combined run vs. tundra vs. bedrock/talus runs. Normalized relative mean squared errors (NRMSE) showed the same trends as NMAE and are not included here.

	Combine Run: Calibrated vs. evaluation years		**Combined Run 1992-2003: Non-filtered vs. Filtered**				**1992-2003 Runs: Combined run vs. individual tundra and bedrock/talus runs**					
	1992-1999	2000-2003	Non-filtered	Filtered	Non-filtered	Filtered	Combined	Tundra	Rock	Combined	Tundra	Rock
	Nash-Sut	Nash-Sut	Nash-Sut	Nash-Sut	NMAE	NMAE	Nash-Sut	Nash-Sut	Nash-Sut	NMAE	NMAE	NMAE
pH	-1.84	-3.34	-1.76	-1.65	0.03	0.03	-1.76	-3.38	-1.79	0.03	0.04	0.03
NO_3	-2.94	-14.88	-4.01	-3.05	0.57	0.48	-4.01	-4.79	-5.34	0.57	0.71	0.62
ANC	-2.40	-9.44	-3.88	-5.72	0.47	0.46	-3.88	-2.28	-6.02	0.47	0.33	0.57
SO_4	-1.04	-3.59	-1.39	-1.57	0.36	0.36	-1.39	-0.63	-3.44	0.36	0.26	0.50
Cl	-2.82	-3.05	-2.77	-3.10	0.62	0.68	-2.77	-1.87	-4.05	0.62	0.52	0.74
Ca	-3.87	-8.59	-4.15	-1.70	0.44	0.31	-4.15	-11.25	-4.31	0.44	0.93	0.45
Mg	-3.35	-9.27	-4.05	-2.39	0.50	0.38	-4.05	-7.82	-4.80	0.50	0.82	0.53
K	-1.91	-5.94	-2.29	-2.98	0.51	0.52	-2.29	-6.26	-3.40	0.51	0.83	0.56
Na	-1.86	-5.96	-2.29	-1.91	0.35	0.30	-2.29	-9.03	-5.14	0.35	0.73	0.51
BC	-2.95	-7.66	-3.34	-1.46	0.39	0.27	-3.34	-5.57	-4.12	0.39	0.59	0.42
Si	-4.33	-7.45	-4.77	-4.85	0.38	0.33	-4.77	-5.26	-8.76	0.38	0.43	0.50
Q	0.58	0.63	0.60	0.52	0.49	0.47	0.60	0.65	0.58	0.49	0.45	0.50
NH_4	-1.15	-15.64	-1.93	-0.71	1.81	1.40	-1.93	-65.80	n/a	1.81	10.97	n/a

Table 2.8. Simulated and observed annual water fluxes, annual nitrogen fluxes, annual NPP, annual range of live biomass, and average soil organic matter. Standard deviations are shown in parentheses. Mean annual precipitation from 1984-1999 was 109.8 cm, and from 1992-1999 was 117.5 cm. Years prior to 2000 are summarized since data were measured before then.

Average Annual Values (1984-1999 except where indicated)	Simulated Tundra	Observed Tundra	Simulated Bedrock-Talus	Observed Bedrock-Talus	Simulated Combined Run	Observed Andrews Creek	Simulated Forest	Observed Forest
Discharge (cm/yr), 1992-1999	83.8 (13.9)	n/a	91.5 (18.4)	n/a	90.6 (17.9)	96.0 (13.4)	59.8 (16.8)	n/a
ET (cm/year)	6.1 (1.9)	23.4 [b]	11.7 (3.9)	17.0[b], 15% summer precip [c] (~8cm)	11.0 (3.6)	n/a	27.0 (6.1)	52.5[b]
Sublimation (cm/yr)	26.5 (7.1)	26-88 [b]	15.0 (4.2)	26-88 [b]	16.3 (4.5)	n/a	20.8 (5.4)	26-88 [b]
Stream N ($gN/m^2/yr$), 1992-1997	0.29 (0.08)	n/a	0.34 (0.06)	n/a	0.33 (0.06)	0.32 [d]	0.32 (0.1)	n/a
Net Mineralization ($gN/m^2/yr$)	2.1 (0.7)	~2.0 [a]	0.02 (0.01)	n/a	x	n/a	2.1 (0.3)	2.0-3.0 [h]
NPP above ground	43.0 (9.3)	44-135 [f]	8.8 (0.2)		x	n/a	111 (24)	163 [h*]
NPP total ($gC/m^2/yr$)*	95.1 (24.3)	149-219 [f]	1.3 (0.4)	n/a	x	n/a	186 (43)	136-340 [h*]
above ground live biomass (gC/m^2)*	0 - 63.8	60-117 [f]	x	n/a	x	n/a	4270-4408	5511 [h*]
below ground live biomass (gC/m^2)*	425 - 515	225-929 [f]	x	n/a	x	n/a	1170-1266	1200 [h*]
soil organic matter (gC/m^2)	9,550	6700 [g], 13,000 [e]	17.7	n/a	x	n/a	6910	6800 [h]

[a] Bowman 1992, [b] Baron and Denning 1992, [c] Clow and Mast 1995, [d] Campbell et al. 2000, [e] Conley et al. 2000, [f] Bowman and Fisk 2001, [g] Seastedt 2001; [h] Arthur and Fahey1992.
* Observed values published in grams of biomass were divided by 2.25 to convert to grams of carbon (gC). Observed NPP and biomass for tundra include both dry and moist meadows; n/a (not available); x (not reported).

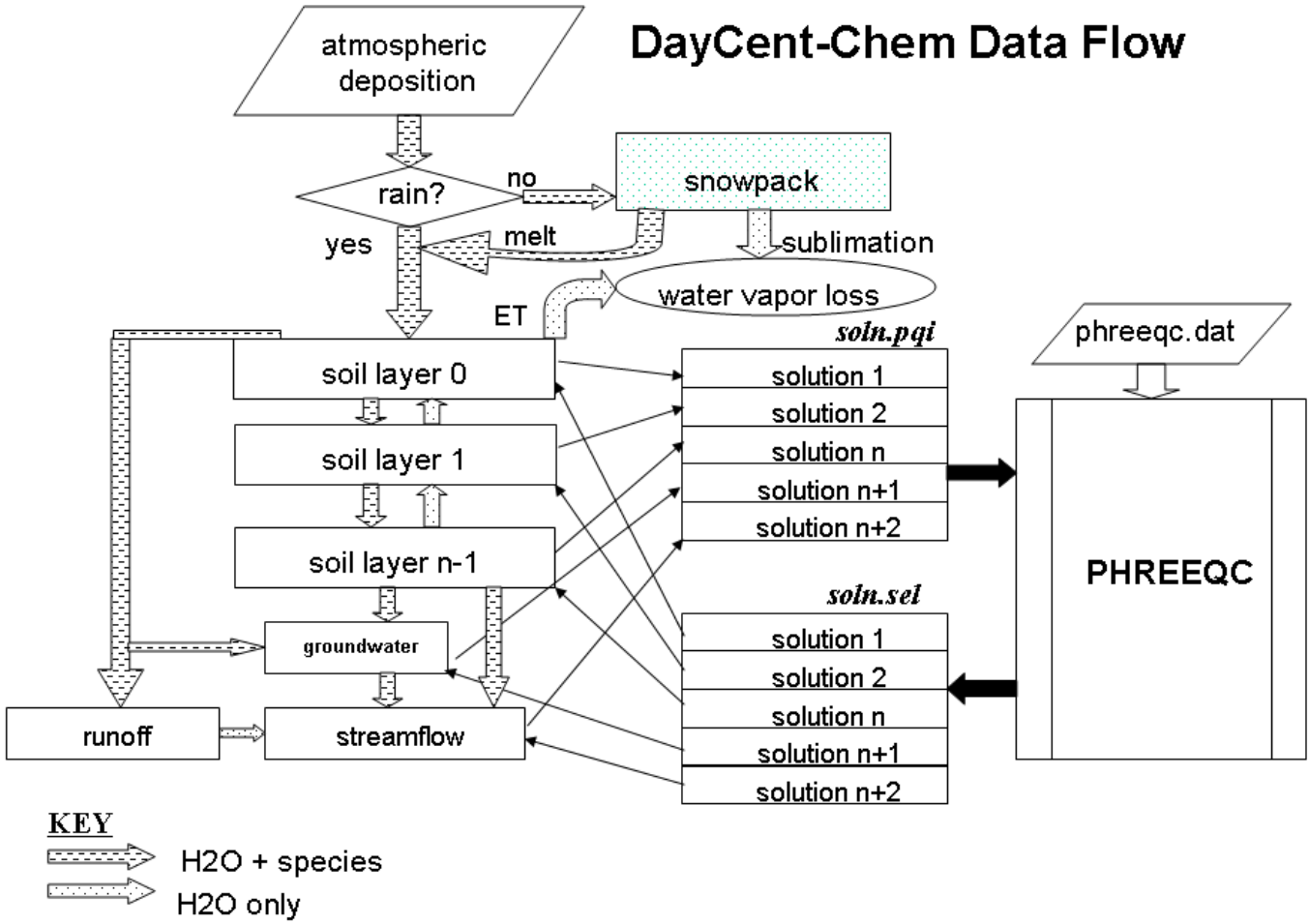

Figure 2.1. Data flow within the DayCent-Chem model.

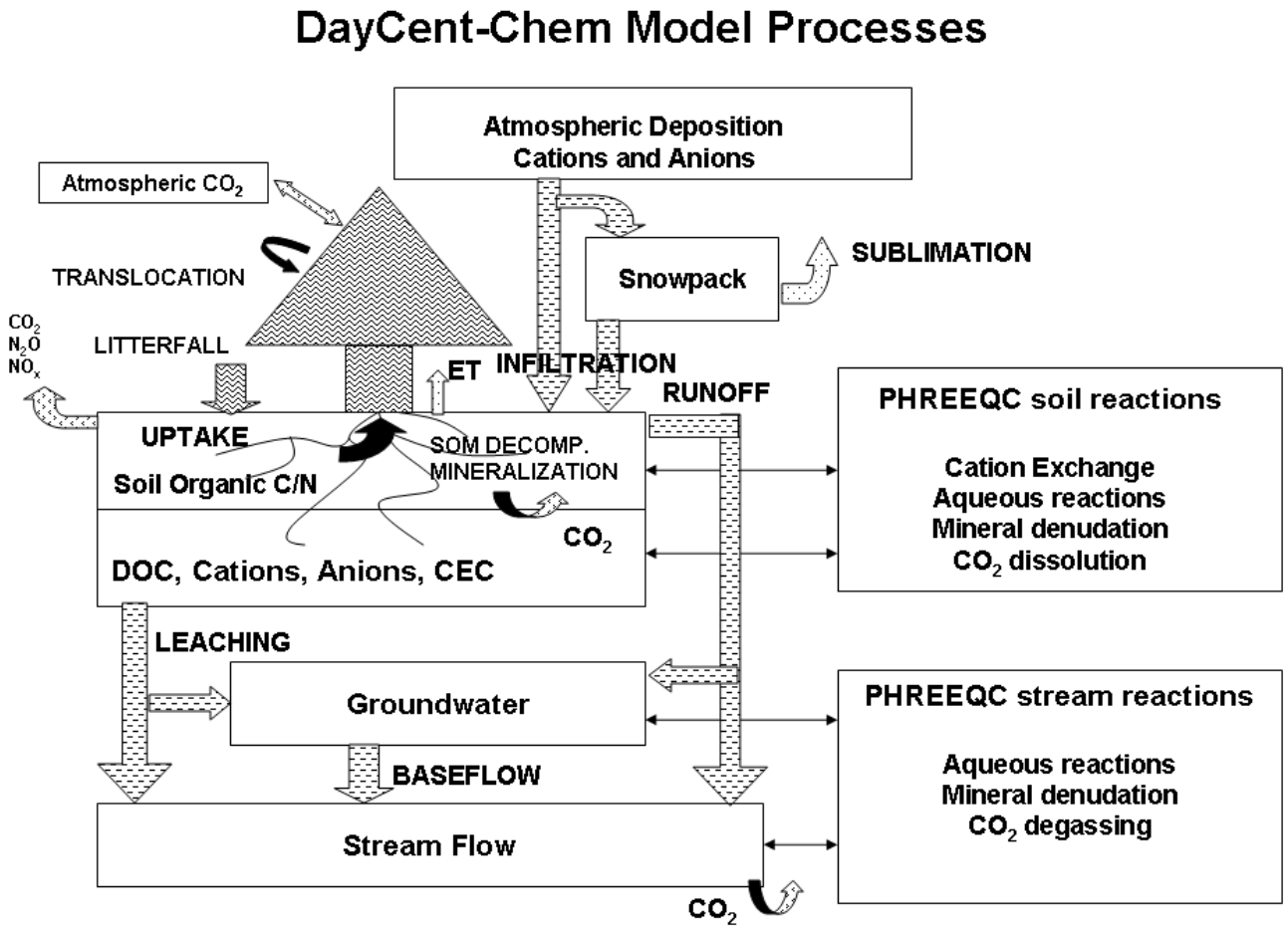

Figure 2.2. DayCent-Chem model processes.

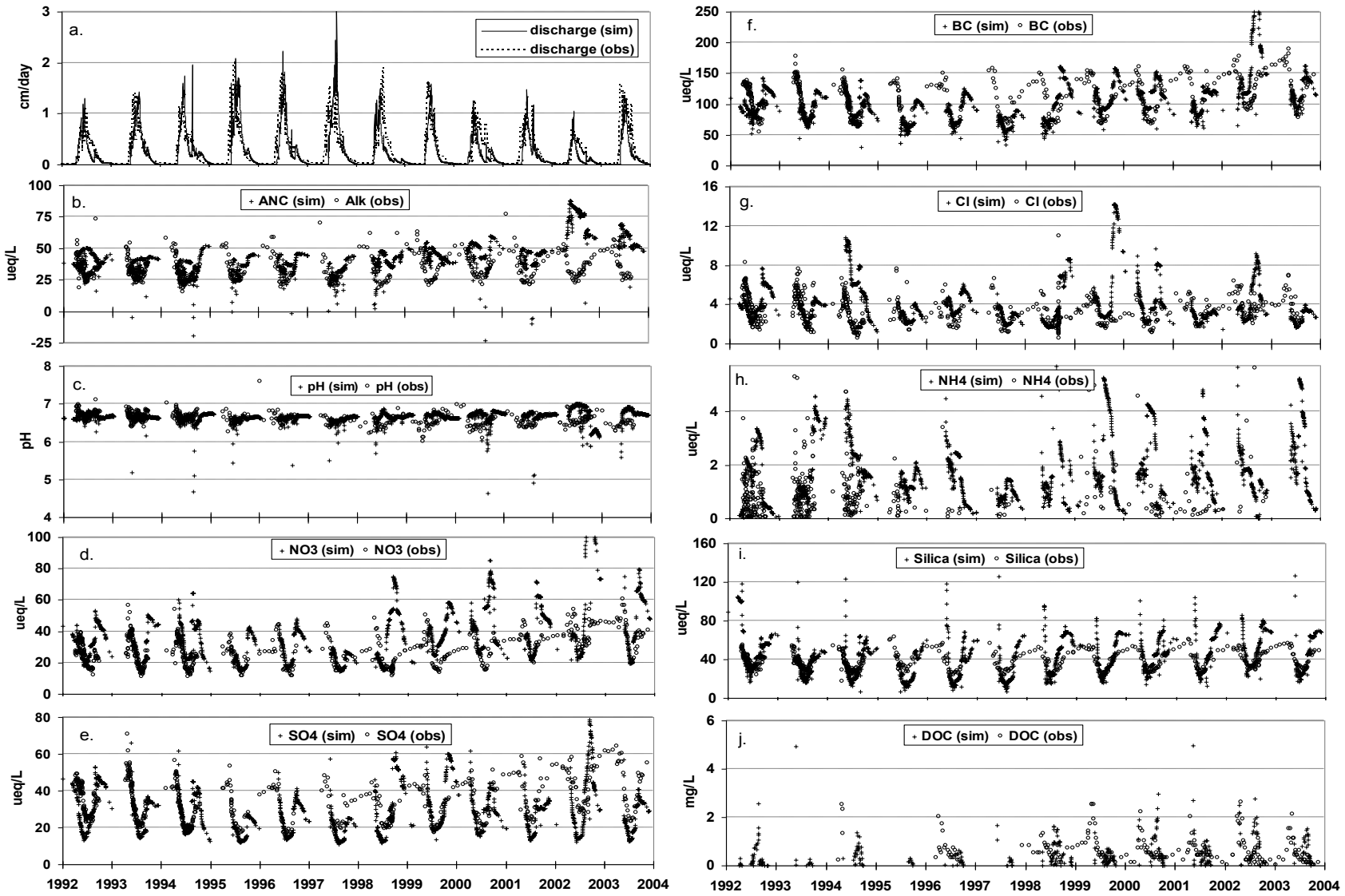

Figure 2.3. Daily discharge and solute concentrations as simulated for the combined alpine run (solid lines or plus signs) and observed in Andrews Creek (dashed lines or open circles): (a) discharge; (b) ANC; (c) pH; (d) NO_3^- (e) SO_4^{2-}; (f) base cations (Ca+Mg+K+Na); (g) Cl^-; (h) NH_4^+; (i) silica; (j) DOC. Observed NH_4^+ concentrations (h) were not available for 1998 and 2003.

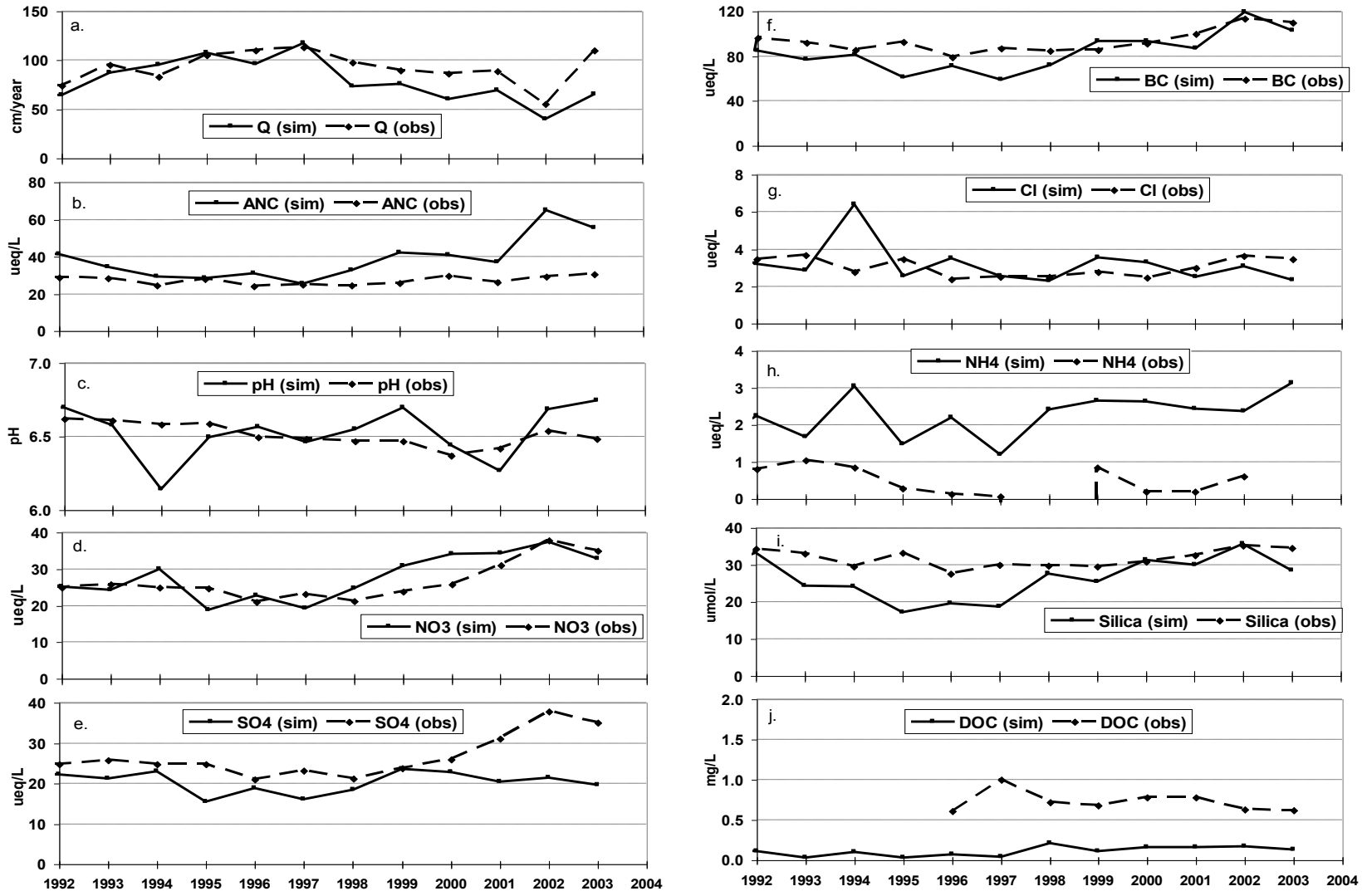

Figure 2.4. Annual mean discharge and annual volume-weighted mean solute concentrations as simulated for the combined alpine run (solid lines) and observed in Andrews Creek (dashed lines): (a) discharge; (b) ANC; (c) pH; (d) NO_3^-; (e) SO_4^{2-}; (f) base cations(Ca+Mg+K+Na); (g) Cl^-; (h) NH_4^+; (i) silica; (j) DOC. Observed NH_4^+ concentrations (h) were not available for 1998.

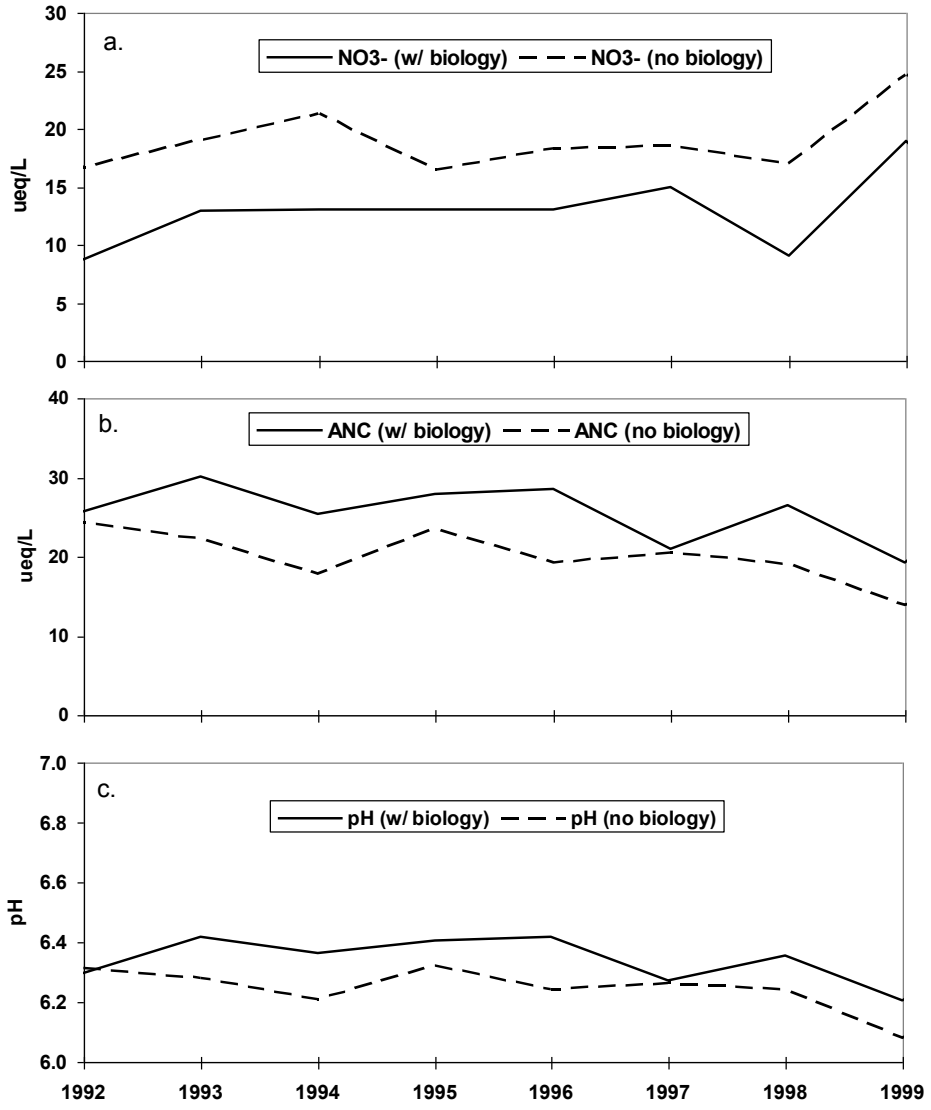

Figure 2.5. Annual volume-weighted mean concentrations for tundra runs with (solid lines) and without (dashed lines) biological calculations: (a) NO_3^-; (b) ANC; (c) pH.

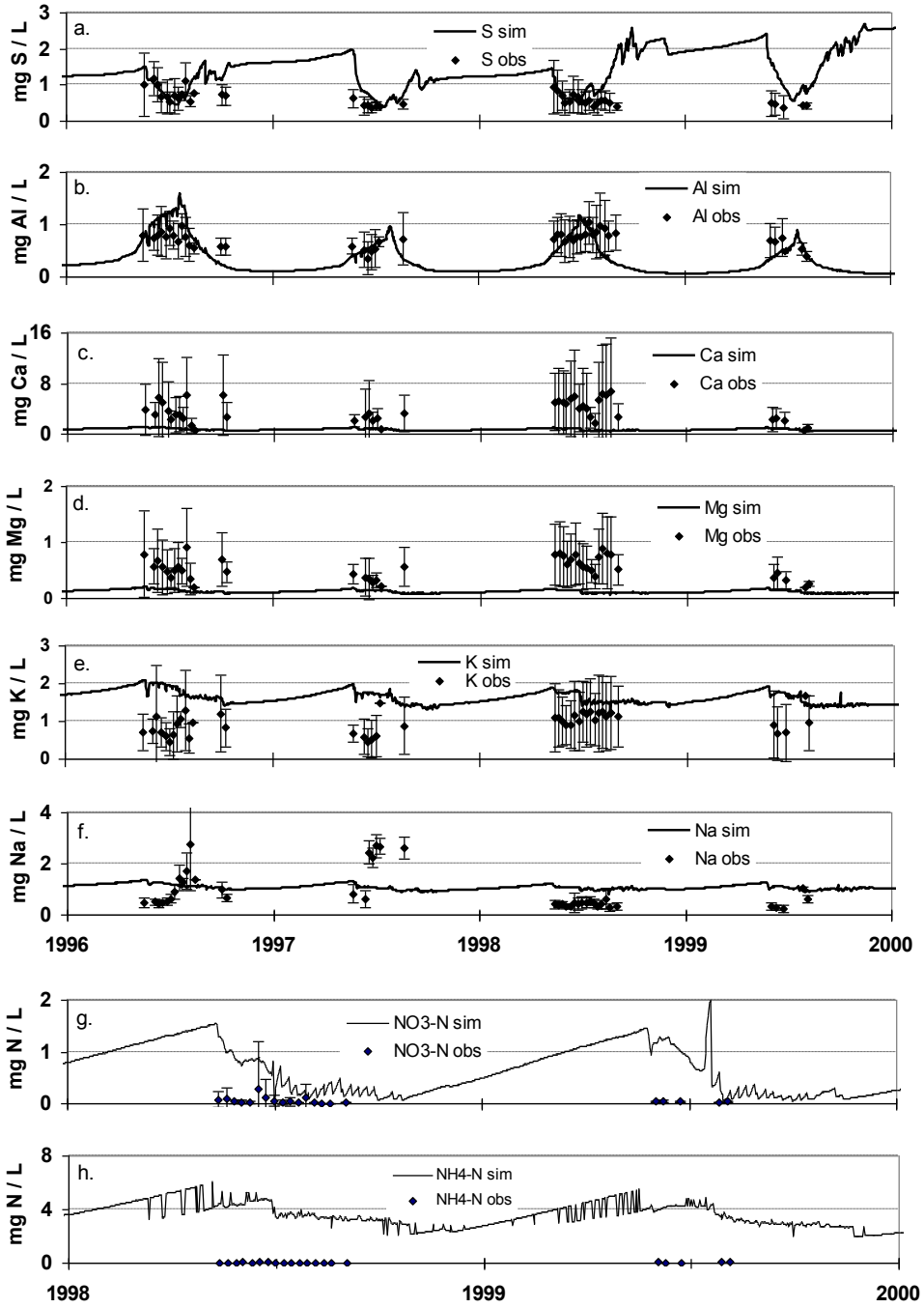

Figure 2.6. Simulated forest soil solution concentrations integrated for the top 20 cm (solid lines), and mean of measured values for the top 15 cm (black dots): (a) S; (b) Al; (c) Ca; (d) Mg; (e) K; (f) Na (g) NO_3-N; (h) NH_4-N. Note graphs for NO_3-N and NH_4-N show years 1998-2000, while all the others show 1996-2000. Error bars on measured values show ± one standard deviation.

3 MODELING STREAM ACIDIFICATION FROM EXCESS NITROGEN DEPOSITION IN AN ALPINE WATERSHED[2]

3.1 Chapter Overview

Because nitrogen is a major nutrient as well as a potential cause of acidification and eutrophication, we developed a model, DayCent-Chem, that simulates plant and soil nutrient cycling as well as soil and water chemical equilibrium. We modeled how much nitrogen deposition it takes to acidify an alpine watershed, and whether the rate at which deposition increases matters. Forty-eight year deposition scenarios included control runs with recent nitrogen deposition amounts (2.0 to 4.5 kg N ha^{-1} yr^{-1}) and scenarios with low, medium, and high rates of N deposition increase. Andrews Creek is not currently acidified, nor did it acidify in control model runs. Episodic acidification occurred when total nitrogen deposition averaged 6.6 kg N ha^{-1} yr^{-1}. Once nitrogen deposition exceeded 7–8 kg N ha^{-1} yr^{-1}, the model predicted yearly episodic acidification. Chronic acidification occurred at 14–15 kg N ha^{-1} yr^{-1}. As N deposition increased, annual volume-weighted mean acid neutralizing capacity (ANC) decreased logarithmically, and the number of days per year with negative ANC increased as a cubic function. Simulated alpine tundra production and soil organic matter turnover increased slightly with N deposition, but production was limited by the harsh alpine climate. The rate of N deposition increase was less important than the annual cumulative amount of N deposition.

---

[2]*Melannie D. Hartman[a], Jill S. Baron[b], DennisS. Ojima[a]*
[a]Natural Resource Ecology Laboratory, Colorado State University, Fort Collins, CO 80526-1499, USA
[b]U.S. Geological Survey, Natural Resource Ecology Laboratory, Colorado State University, Fort Collins, CO 80526-149, USA

3.2 Introduction

Ecosystem response to atmospheric nitrogen deposition is a topic of great interest to federal land managers who have a responsibility to protect Class I areas, national parks and wilderness areas granted special air quality protections under Section 162(a) of the federal Clean Air Act, from ecosystem degradation due to atmospheric deposition of pollutants. Excess N deposition will cause lake and stream acidification in a process similar to that caused by sulfate deposition, with an important difference. Because nitrogen is a critical plant nutrient, any realistic projection of nitrogen-caused acidification must include understanding ecosystem nutrient cycling. Nitrogen export is a function of both deposition and internal nitrogen-cycling processes, including plant uptake and nitrogen immobilization in soil organic matter.

N emissions are high and increasing along the Colorado Front Range due to population, industrial, and agricultural growth (Baron et al. 2004). Four-fifths of Colorado's 5 million people live along the Front Range, and the population is projected to increase more than 50% from 2010 to 2040 (CDLA 2012). In order to jointly address geochemical impacts of N deposition and ecosystem level modifications to N cycling, we developed a hybrid model, DayCent-Chem, to capture these interactions. DayCent-Chem simulates the effects of N deposition on biological assimilation, soil organic matter composition, acid neutralization capacity (ANC) of surface waters, pH, aluminum mobilization, base cation depletion, and base cation flux. DayCent-Chem operates at a daily time step, enabling it to be used to investigate potential for episodic as well as chronic acidification of surface waters. Previously, we calibrated the model to observed data for alpine Andrews Creek watershed in Rocky Mountain National Park (Hartman et al. 2007). We asked whether the presence of terrestrial vegetation, microbial activity, and soil organic matter influenced model output. Here we report DayCent-

Chem's response to nitrogen deposition scenarios and ask: 1) How much N deposition causes episodic and chronic acidification? 2) When will acidification occur under a set of plausible N deposition scenarios? 3) How will tundra respond to increased N deposition?

In evaluating the effects of N deposition in Andrews Creek we looked at ANC. Acid neutralizing capacities of 20, 50, and 100 μeq L^{-1} have been suggested as thresholds for changes in invertebrate and fish populations and in the individual condition of species (Baker et al. 1990, Bulger et al. 2000). The 1992-2002 annual VWM ANC values for Andrews Creek, 24-30 μeq L^{-1}, identify Andrews Creek as extremely acid sensitive (Musselman and Slauson 2004).

3.3 Experimental Section

3.3.1 Model Description

DayCent-Chem is a model built from the existing DayCent (Parton et al. 1998, Del Grosso et al. 2001) and PHREEQC (Parkhurst and Appelo 1999) models. DayCent is a daily time step, process-based biogeochemical model of intermediate complexity that computes site-level water, carbon, and nitrogen dynamics for grasslands, crops, forests, shrublands, and savannas. PHREEQC provides low-temperature aqueous geochemical equilibrium calculations including speciation, CO_2 dissolution, mineral denudation, and cation exchange. Ion-exchange reactions are modeled with the Gaines-Thomas convention and equilibrium constants derived from Appelo and Postma (1993). DayCent-Chem does not utilize PHREEQC's sulfate adsorption and surface complexation reactions.

Inputs to the model include daily precipitation amount and solute concentrations, daily minimum and maximum air temperatures, and daily dry to wet ratios that specify the combined amount of deposition from gas, particulates, and aerosols. DayCent-Chem computes soil water

fluxes and concentrations, stream flow and chemistry, plant production and uptake, soil organic matter decomposition, mineralization, nitrification, and denitrification (Figure 2.2). The model can simulate one type of herbaceous and/or one type of woody vegetation simultaneously, with plant growth that depends plant type characteristics, plus temperature, moisture and nutrient limitations. Snowmelt and rainfall that infiltrates the soil moves upward or downward in one dimension through a multi-layered soil profile before entering the aquifer or stream (Figure 2.2). A full description of the coupled model and its verification for Andrews Creek watershed is found in Hartman et al. (2007).

Acid neutralizing capacity is calculated as the concentration ($\mu eq\ L^{-1}$) of H^+ acceptors minus concentrations of H^+ donors and allows for the contribution of dissolved inorganic carbon as well as organic solutes that bind H^+ and certain hydroxy-Al and organo-Al complexes. Naturally occurring organic acids are modeled using a triprotic analog, H_3Org (Driscoll et al. 1994, Gbondo-Tugbawa et al. 2001).

3.3.2 Study area

Andrews Creek watershed (183 ha) is an alpine subcatchment within Loch Vale Watershed (LVWS), about 80km northwest of Denver, Colorado. It ranges 3200– 4000 m in elevation and is dominated by granite and gneiss bedrock (57%) and talus (31%) with alpine tundra and wet meadow soils comprising 11%; less than 1% of the watershed is forested. Andrews Glacier (10 ha) and a small tarn at its foot comprise the remaining land cover (Meixner et al. 2000). Our simulated stream concentrations represented an 89% contribution from bedrock/talus, and an 11% contribution from tundra; the tarn is < 1 ha and its processes were not modeled. The annual hydrologic cycle is dominated by a cold snowpack that melts May-July.

After snowmelt, shallow ground water reservoirs contribute the majority of stream flow (Clow et al. 2003).

Average annual precipitation from 1984– 1999 (data from years we used for this modeling exercise) was 109 cm, approximately 65 percent of which was snow (NADP/NTN 2004). Dry deposition estimates for NO_3^-, NH_4^+, and SO_4^{2-} were taken from CASTNet site ROM406 (CASTNET 2004). Dry deposition estimates for base cations and Cl^- were taken from measurements in Loch Vale watershed (Campbell et al. 1995, Clow and Mast 1995). Species specific dry:wet ratios were calculated from dry deposition estimates and varied seasonally but not from year to year (Hartman et al. 2007).

Over the past two decades, annual volume-weighted mean (VWM) concentrations of NH_4^+ and NO_3^- in precipitation increased at two high elevation NADP/NTN monitoring sites on the east side of the Continental Divide adjacent to Colorado's Front Range (Campbell et al. 2000, Baron 2006). Concentrations of N in precipitation increased 6.5% yr^{-1} (0.6 μeq $L^{-1}yr^{-1}$) and 3.0% yr^{-1} (0.2 μeq $L^{-1}yr^{-1}$) for NH_4^+ and 2.5% yr^{-1} (0.3 μeq $L^{-1}yr^{-1}$) and 4.6% yr^{-1} (0.7 μeq $L^{-1}yr^{-1}$) for NO_3^- for Loch Vale (NADP CO98) and Niwot Saddle (NADP CO02), respectively, between 1994 and 2003. The rate of increase was lower in the preceding decade. The two sites showed independent wet N deposition trends in 1994– 2003; Loch Vale deposition decreased due to declining precipitation, while Niwot Saddle deposition increased due to increasing precipitation. Dry deposition of inorganic N measured at CASTNet site ROM406, 10km SE of LVWS, showed a decreasing trend of 2.9% yr^{-1} (0.03 kg N ha^{-1} yr^{-1}) from 1995– 2002 (CASTNET 2004). Total SO_4^{2-} deposition in LVWS was relatively low and decreased slightly over time. Wet deposition averaged 2 kg S $ha^{-1}yr^{-1}$ from 1984 to 2003, and dry deposition of SO_2 and SO_4^{2-} averaged 0.4 kg S $ha^{-1}yr^{-1}$ from 1995 to 2002.

Measured ANC in Andrews Creek is naturally low due to minimal soil development and the resistant granite and gneiss bedrock that underlies the watershed, making the watershed susceptible to episodic acidification especially during snowmelt (Campbell et al. 1995). Daily measurements of ANC in Andrews Creek from 1992 to 1999 ranged 15– 70 μeq L^{-1} with the lowest values occurring during snowmelt in June or July each year (Figure 3.1). From 1992 to 1999, annual VWM stream concentrations averaged 26 μeq L^{-1} for ANC, 24 μeq L^{-1} for NO_3^-, 0.5 μeq L^{-1} for NH_4^+, and 26 μeq L^{-1}, for SO_4^{2-} (LVWS 2004).

3.3.3 Nitrogen deposition scenarios

We conducted three sets of nitrogen deposition scenarios (Sets 1– 3), each with four 48-year simulations of differing N deposition rates, for a total of twelve simulations. Each set had its own unique weather sequence, and included a control run (+0.0%) and scenarios with low (+1.25%) , medium (+2.5%), and high (+5.0%) annual increases of N deposition relative to the control run. At the end of 48 years the low, medium, and high scenarios had 60%, 120%, and 240% more N deposition, respectively, than the control run. Increases in wet N deposition were computed by increasing the input concentrations of NO_3^- and NH_4^+ to the model. For the low, medium, and high scenarios input concentrations increased 0.2, 0.4, and 0.8 μeq $L^{-1}yr^{-1}$, respectively, reflecting extant concentration increases. Dry deposition inputs of NO_3^- and NH_4^+, computed from dry:wet ratios, were proportional to their wet deposition inputs.

A 48-year control run was created by concatenating precipitation chemistry and weather records from 1984–1999 three times, then randomizing the order of the years. The three control runs differed only in the order of these years; over the 48-year simulation, the average deposition for each control run was the same at 3.5 kg N ha^{-1} yr^{-1}. The average annual change in N or S

deposition was within ±0.1% of the 48-year mean deposition amount in all control runs. For each set, all scenarios began with the same initial N deposition, 3 to 4 kg N ha^{-1} yr^{-1}, and then diverged according to the weather patterns. After 48 years, N deposition increased to as much as 7.2, 9.9, and 15.3 kg N ha^{-1} yr^{-1} in the low, medium, and high scenarios, respectively. On any given simulation day, all scenarios in a set had the same precipitation amount and air temperatures. Simulation years for the 48-year scenarios were labeled 2000 to 2047.

Total NO_3-N deposition was 66% and total NH_4-N deposition was 34% of total inorganic N deposition for all runs. Organic N deposition has not been measured in Andrews Creek, and we assumed it was insignificant. At a similar alpine basin at Niwot Ridge, organic N was estimated at 16% of total precipitation N, but there was little net retention of organic N in the watershed (Williams et al. 2001). Precipitation concentrations and dry deposition of all other species (base cations, SO_4^{2-}, Cl^-, and H^+) in any low, medium, and high scenario were equivalent to those of control run in the same set. Wet plus dry SO_4^{2-} deposition for all runs averaged 2.7 kg S ha^{-1} yr^{-1}.

Simulated ANC values that were unrealistically low due to overestimated discharge were eliminated (for example, Figure 3.1a). This resulted in the exclusion of 53 out of 17,532 simulation days in each scenario.

3.4 Results

3.4.1 Episodic acidification

Acidification of Andrews Creek did not occur with deposition values of 2.0– 4.5 kg N $ha^{-1}yr^{-1}$ (the 1984-1999 measured levels of deposition), but the stream became episodically acidic (daily ANC $\leq$ 0 μeq L^{-1}) during spring snowmelt when deposition reached 6.3– 7.1 kg N $ha^{-1}yr^{-1}$.

An example from Set 1 contrasts the relative impacts of increasing N deposition (Figure 3.2). The first years of episodic acidification were 44, 28, and 19 years from present (simulation years 2044, 2028, and 2019) for low, medium and high rates of deposition increase, respectively (Figure 3.2). The amount of N in kg N $ha^{-1}yr^{-1}$ that caused episodic acidification for the three medium (6.3, stdev. 0.1) and three high scenarios (6.6, stdev. 0.4) was significantly less than for the three low (7.1, stdev. 0.0) scenarios, and averaged 6.6 (stdev. 0.4) kg N $ha^{-1}yr^{-1}$ for all nine scenarios (Table 3.1).

Because inter-annual variability in deposition for the scenarios ranged up to 5 kg N ha^{-1} yr^{-1}, multi-year deposition averages were more diagnostic of the amount of N deposition that brought ANC ≤ 0 at least once every year. This N deposition threshold was similar for medium and high scenarios, and not seen in the low scenarios. For Set 1, annual recurrence of episodic acidification began 44 and 27 years from present (simulation years 2044 and 2027) for medium and high rates of N deposition increase (Figure 3.2) when deposition was 6.8 – 8.0 kg N $ha^{-1}yr^{-1}$ (Table 3.1). Results were similar for Sets 2 and 3.

3.4.2 Mean annual ANC values

Annual VWM ANC decreased with increasing N deposition, while the frequency of acidification increased (Figure 3.3). Annual VWM ANC increased only 0.01 μeq L^{-1} yr^{-1} for the control runs, decreased 0.2 μeq L^{-1} yr^{-1} for the low scenarios, 0.4 μeq L^{-1} yr^{-1} for the medium scenarios, and 0.6 μeq L^{-1} yr^{-1} for the high scenarios. As N deposition increased, simulated annual VWM ANC decreased logarithmically with an R^2 of 0.81 (Figure 3.3a), and the number days per year that acidification occurred increased as a cubic function with an R^2 of 0.73 (Figure 3.3b). Deposition of 15 kg N $ha^{-1}yr^{-1}$ caused the stream to be acidified for over two months

(Figure 3.3b). Daily stream ANC values of 0 to 20 μeq L^{-1} were associated with daily stream pH of 5.2 to 6.5 (data not shown).

The average amount of N deposition (kg N $ha^{-1}yr^{-1}$) required to lower annual mean ANC to 20 μeq L^{-1} was 6.0 (stdev. 1.5), 7.4 (stdev. 1.1) , and 7.4 (stdev. 0.8) for the low, medium, and high scenarios, respectively, and averaged 7.1 (stdev. 0.4) for all nine scenarios. These deposition amounts were not significantly different from one another (Table 3.1).

3.4.3 Tundra Soil and Vegetation Processes

The tundra vegetation and soils retained 40% or less of atmospheric N deposition each year in all simulations. The N that passed through tundra soils increased base cation flux but did not affect tundra soil base saturation. The measured base cation exchange varied with depth from 7.2 to 44.8 meq/100g (Walthall 1985) and was hundreds of times greater per unit area than the annual mean base cation flux. Base cation flux from tundra soils was 370 eq $ha^{-1}yr^{-1}$, or 21% greater at the end of the high scenarios than for the control runs (305 eq $ha^{-1}yr^{-1}$) (Table 3.2). The percent base saturation was 45% for all scenarios and did not change with increased NO_3^- or NH_4^+ deposition. Soil water pH and ANC did not show an increasing or decreasing trend with N deposition.

Tundra plant and soil organic matter processes responded linearly to the amount of N deposition increase. We report only the trends for the control runs and high scenarios in Table 3.2. Tundra productivity increased only slightly with nitrogen deposition. End-of-simulation net primary production (NPP) for high scenarios was 154 g C m^{-2} yr^{-1}, or 12% greater than NPP at the end of the control runs (137 g C m^{-2} $year^{-1}$) primarily due to increased above-ground production (Table 3.2). The cold climate (mean annual temperature of -1ºC) limited simulated

tundra productivity both directly by air temperature and indirectly by prolonging snow cover. Above- and below-ground C:N ratios barely changed by the end of the high rate of increase scenarios. Soil organic carbon at the end of the high scenarios was only 65 g C m^{-2} greater than for the control runs (10,630 g C m^{-2}).

There was a slight accumulation of soil organic and inorganic N in tundra soils with increasing N deposition (Table 3.2). Soil organic N was 3 g N m^{-2} greater at the end of the high scenarios than for the control runs (556 g N m^{-2} $year^{-1}$), while inorganic soil N for the high scenario (0.24 g N m^{-2}) was 60% greater than for the control runs (0.15 g N m^{-2}). With increased N deposition, net N mineralization rates did not change, net nitrification increased by 30% (from 0.60 to 0.78 g N m^{-2} $year^{-1}$), and plant uptake increased 14% (from 2.9 to 3.3 g N m^{-2} $year^{-1}$) (Table 3.2). Denitrification increased with N deposition but was insignificant to the nitrogen budget.

3.5 Discussion

Acid inputs to Andrews Creek from wet and dry deposition are neutralized by cation exchange processes in soil and talus and by alkalinity derived from kinetically-limited mineral weathering. In spring, the elution of nitrate and sulfate from the snowpack and concurrent rapid flushing of melt water through soil deliver *in situ* nitrogen, organic acids, and inorganic anions to the stream, reduce soil water hydrologic residence times, and dilute soil and stream water alkalinity (Campbell et al. 1995). Our scenarios showed that increased nitrogen deposition above current amounts will exceed the buffering capacity of Andrews Creek, particularly during spring snowmelt, and that the stream will be acidified a greater number of days as N deposition increases. Episodic deposition first occurred between 6.3 and 7.1 kg N $ha^{-1}yr^{-1}$ (Table 3.1). The

amount of N deposition that leads to negative stream ANC could be even lower in less buffered watersheds. Williams and Tonnessen (2000) reported negative stream ANC during snowmelt in two high elevation headwater catchments near Niwot Ridge, CO, at 2.5 to 3.5 kg wet N $ha^{-1}yr^{-1}$. These catchments are about 500m higher than Andrews Creeks catchment, and less vegetated. Seasonal maximum stream ANC at these Niwot Ridge sites was 21 μeq L^{-1}, compared with > 50 μeq L^{-1} for Andrews Creek (Figure 3.1).

Annual VWM ANC ≤ 20 μeq L^{-1} can cause sub-lethal to lethal effects on stream biota (4,5) and has been an indication of susceptibility to episodic acidification (26). In our model results episodic acidification occurred with less deposition (6.6, stdev. 0.4 kg N $ha^{-1}yr^{-1}$) than those that lowered annual VWM ANC to 20 μeq L^{-1} (7.1, stdev. 0.4 kg N $ha^{-1}yr^{-1}$), suggesting that annual mean concentrations of ANC may not be a sensitive enough measure of the potential for at least episodic acidification. Rainbow and native cutthroat trout are spring spawners, and both species are sensitive to even slight declines of stream pH that allow an increase in soluble monomeric aluminum (Woodward et al. 1989, Baker et al. 1990).

Our model results were very similar to those produced by another acidification model, MAGIC, that operates at a monthly timestep. Nitrogen deposition scenarios using MAGIC with a combination of vegetated, non-vegetated, and lake compartments predicted 7.8 kg N $ha^{-1}yr^{-1}$ would cause annual VWM ANC ≤ 20 μeq L^{-1} in Andrews Creek within 50 years (Sullivan et al. 2005), compared with the DayCent-Chem value of 7.1 (stdev. 0.4) kg N $ha^{-1}yr^{-1}$ (Figure 3.3a, Table 3.1). Chronic acidification occurred in MAGIC at 13.9 kg N $ha^{-1}yr^{-1}$, compared with 14.6–15.3 kg N $ha^{-1}yr^{-1}$ from DayCent-Chem (Figure 3.3a).

With increased N deposition, the model showed small changes in plant biomass, plant N uptake, and above-ground plant C:N ratios, negligible changes in net N mineralization, but

notable increases in net nitrification. These results are similar to measurements from a 6-year fertilization experiment in Colorado alpine tundra where total N deposition (ambient + amendments) ranged 6– 66 kg N ha^{-1} yr^{-1}. With increased N fertilizer amounts, plant tissue N concentration, community composition, and net nitrification rates changed much more than overall community biomass (Bowman et al. 2006). Based on field experiments, Bowman et al. (2012) conclude that N critical loads under 10 kg ha^{-1} yr^{-1} are needed to prevent future acidification of soils and surface waters, and recommend N critical loads for vegetation at 3 kg N ha^{-1} yr^{-1} as important for protecting natural plant communities and ecosystem services in Rocky Mountain National Park.

The range of total N deposition in our high scenarios, 3.5 to 15 kg N ha^{-1} yr^{-1}, overlapped N deposition used by Baron et al. (1994) to model the response of tundra under a range of deposition amounts (0.2 to 16 kg N ha^{-1} yr^{-1}). This earlier paper used CENTURY, the monthly version of DayCent. Stream N export increased from 1.8 to 9.0 kg N ha^{-1} yr^{-1} as deposition increased from 3.5 to 15.0 kg N ha^{-1} yr^{-1}, similar to our stream export of 3.0 to 9.0 kg N ha^{-1} yr^{-1} under the same range of deposition. Baron et al. (1994) also found that tundra ecosystem processes responded only slightly to an increase in N deposition.

The rate of N deposition increase was not as important as the amount of deposition for bringing about acidification. The amount of N deposition that caused the first episode of acidification was 0.5– 0.8 kg N ha^{-1} yr^{-1} less for the medium and high scenarios than for the low scenarios (Table 3.1), but this difference is within inter-annual variability in N deposition for Andrews Creek. This mild response to the rate of deposition increase was related to the limited ability of the predominantly unvegetated watershed to assimilate nitrogen and to the intensity of acidic inputs from melting snow that exceed the watershed's capacity to neutralize acidic inputs.

Rapid response of water chemistry, but few corresponding ecological responses, were observed in European and American fertilization experiments when soil organic matter C:N ratios in coniferous forests were less than 24 (Emmett et al. 1998, Rueth et al. 2003). Our simulated tundra soil C:N ratio of 19 was similarly low. The timing and asynchrony between nitrogen inputs and plant demand may have also determined response to N inputs (Matson et al. 2002). Only about 30% of N input to the model occurred during the June-August growing season. Rapid snowmelt and flushing of N through shallow and coarse soils leaves limited opportunities for biological cycling of N, as isotopic analyses has shown for the high Sierra Nevada (Sickman et al. 2003).

Because alpine watersheds are controlled by the ecological processes in harsh climate, there is limited capacity for the sparse vegetation and soils to take up and store nitrogen. We expect the nutrient cycling capabilities of DayCent-Chem to become more important in less climatically-challenged ecosystems. Both MAGIC and DayCent-Chem suggest episodic acidification will occur with only a slight increase in N deposition amounts, from current values of 2.0–4.5 to 6.6–8.0 kg N $ha^{-1}yr^{-1}$. Field experiments showed that N critical loads under 10 kg $ha^{-1}yr^{-1}$ are needed to prevent future acidification of soils and surface waters in alpine communities in Rocky Mountain National Park (Bowman et al. 2012). In our worst case scenario, where N deposition increased at a rate of 5% yr^{-1}, episodic acidification will begin sometime between 15 and 19 years from present.

3.6 Acknowledgements

We thank K. Weathers and D. Burns for reviewing an earlier version of this manuscript. Funding was provided by the U.S. Environmental Protection Agency, National Park Service, and by the U.S. Geological Survey Western Mountain Initiative.

Table 3.1. Summary for the three sets of scenarios, including timeline and deposition associated with acidification. Deposition associated with the commencement of annual recurring acidification is three-year running average mean deposition. The numbers in parenthesis are standard deviations. "Years from present" equals the number of years from the beginning of the scenarios (year 2000).

	Rate of N deposition increase	Years from present	Average deposition kg N ha^{-1} yr^{-1}
First occurrence of episodic acidification (daily ANC $\leq$ 0 μeq L^{-1})	control	-	-
	low	44-45	7.1 (0.0)
	medium	28-30	6.3 (0.1)
	high	15-19	6.6 (0.4)
	scenario average		6.6 (0.4)
First occurrence of annual VWM ANC $\leq$ 20 μeq L^{-1}	control	-	-
	low	30-44	6.0 (1.5)
	medium	27-34	7.4 (1.1)
	high	16-19	7.4 (0.8)
	scenario average		7.1 (0.4)
Commencement of annual recurring acidification	control	-	-
	low	-	-
	medium	43-44	6.8 - 7.7
	high	26-33	7.0 - 8.0

Table 3.2. Trends in tundra soil and vegetation response to N deposition. Numbers in parenthesis are percentage change when the trend of the scenarios with high rate of N deposition increase were compared to the control runs.

	End of Control runs	End of scenarios with high rate of N deposition increase	
Base Cation flux (eq $ha^{-1}yr^{-1}$)	305	370	(21%)
NPP (g C m^{-2} yr^{-1})	137	154	(12%)
Above-ground plant C:N	22	21	(-5%)
Below-ground plant C:N	48.5	48.0	(-1%)
Soil organic matter C (g m^{-2})	10,630	10,695	(< 1%)
Soil organic matter N (g m^{-2})	556	559	(< 1%)
Inorganic N (g m^{-2})	0.15	0.24	(60%)
Net mineralization (g N m^{-2} yr^{-1})	2.9	3.0	(3%)
Net nitrification (g N m^{-2} yr^{-1})	0.60	0.78	(30%)
Plant uptake (g N m^{-2} yr^{-1})	2.9	3.3	(14%)

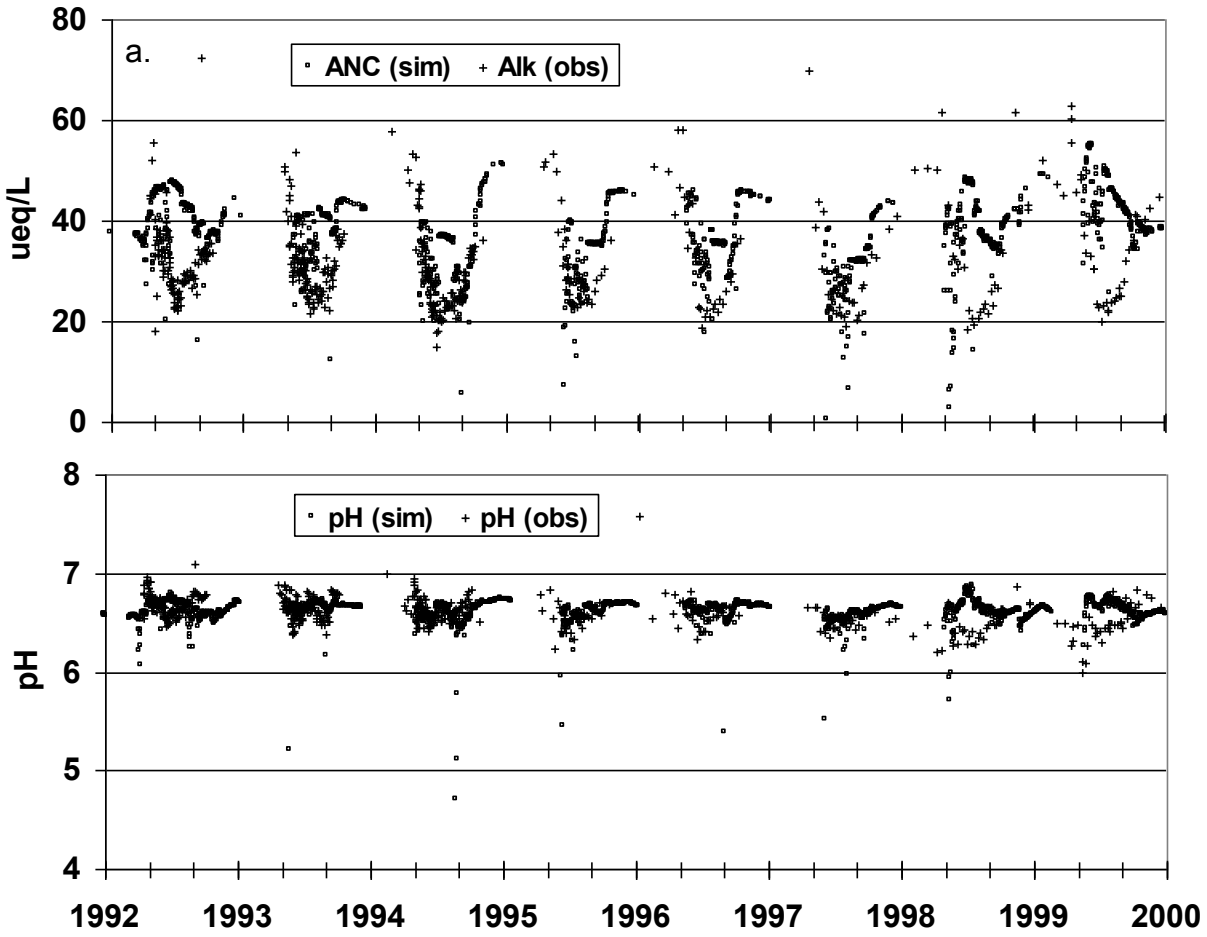

Figure 3.1. Simulated daily stream concentrations versus observed stream concentrations for Andrews Creek from 1992 thru 1999: (a) ANC; (b) pH.

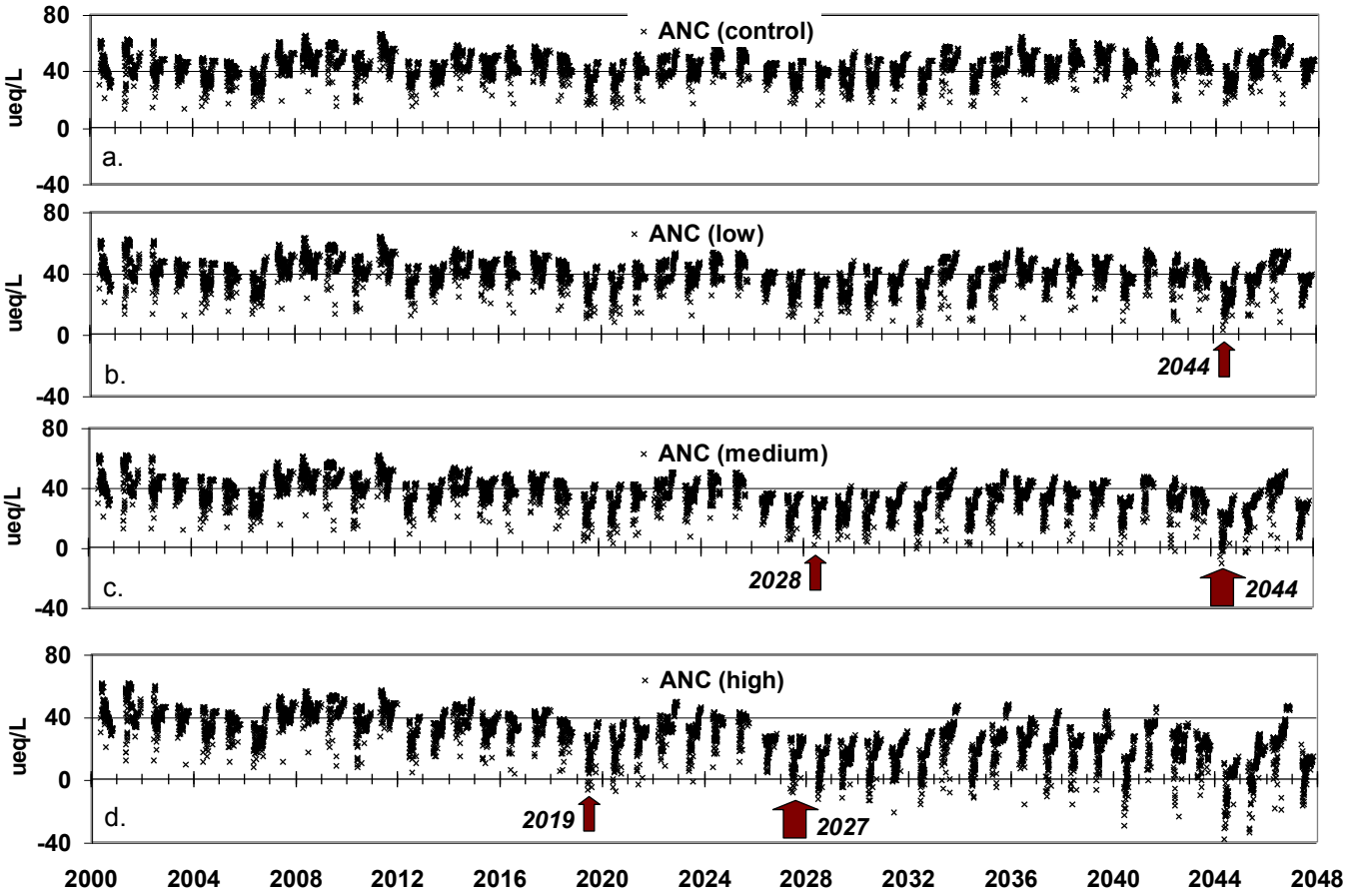

Figure 3.2. Daily simulated ANC values for the scenarios in Set 1: (a) control run; (b) low rate of N deposition increase; (c) medium rate of N deposition increase; (d) high rate of N deposition increase. Small arrows point to the first year that acidification occurred (daily ANC $\leq$ 0 μeq L^{-1}), and large arrows point to the commencement of recurring annual episodic acidification.

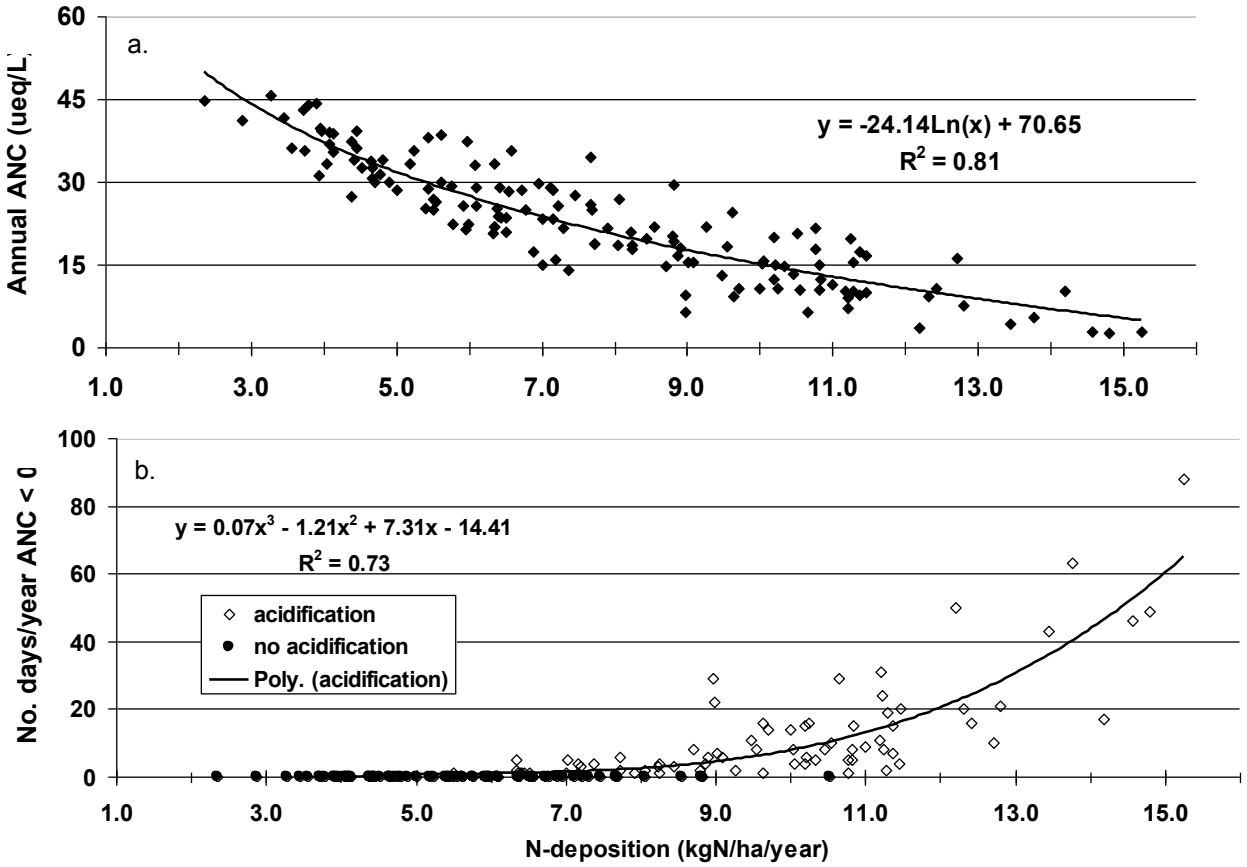

Figure 3.3. Results of the three high (+5.0%) scenarios: (a) The relationship between annual total N deposition to annual volume-weighted mean ANC was described as a logarithmic function with an R^2 of 0.81; (b) The relationship between total N deposition to the number of days per year that ANC ≤ 0 μeq L^{-1} was described as a cubic function with an R^2 of 0.73. Points labeled "acidification" are those where No. of days > 0, and "no acidification" indicates points where No. of days = 0. The curve was fit to the "acidification" points.

4 COMBINED EFFECTS OF WARMING AND ATMOSPHERIC NITROGEN DEPOSITION ON NET ECOSYSTEM PRODUCTION, GREENHOUSE GAS FLUX AND WATER QUALITY IN NINE UNITED STATES MOUNTAIN ECOSYSTEMS[3]

4.1 Chapter Overview

Concurrent changes in climate, atmospheric nitrogen (N) deposition, and increasing levels of atmospheric carbon dioxide (CO_2) affect ecosystems in complex ways. The DayCent-Chem model was used to investigate the combined effects of these human-caused drivers of change over the period 1980-2075 at seven forested montane and two alpine watersheds in the United States. Net ecosystem production (NEP) increased linearly with increasing N deposition for six out of seven forested watersheds; warming directly increased NEP at only two of these sites. Warming reduced soil organic carbon storage at all sites by increasing heterotrophic respiration. At most sites, warming together with high N deposition increased nitrous oxide (N_2O) emissions to negate the greenhouse benefit of soil carbon sequestration. Over the simulation period, N was the main driver of change to net ecosystem greenhouse gas flux, but the N contribution to ecosystem carbon content averaged across forests was only 6-7% and was negligible for the alpine. Two levels of CO_2 fertilization produced only minor differences in greenhouse gas sequestration. Stream nitrate (NO_3^-) fluxes increased sharply with N-loading, primarily at three watersheds where initial N deposition values were high relative to terrestrial N uptake capacity. The simulated results displayed fewer synergistic responses to warming, N-loading, and CO_2 fertilization than

[3]*Melannie D. Hartman[a], Jill S. Baron[b], Holly A. Ewing[c], Kathleen C. Weathers[d]*
[a]*Natural Resource Ecology Laboratory, Colorado State University, Fort Collins, CO 80526-1499, USA*
[b]*U.S. Geological Survey, Natural Resource Ecology Laboratory, Colorado State University, Fort Collins, CO 80526-149, USA*
[c]*Program in Environmental Studies, Bates College, Lewiston, ME 04240, USA*
[d]*Cary Institute of Ecosystem Studies, 2801 Sharon Turnpike, Millbrook, NY 12545, USA*

expected. Overall, simulations with DayCent-Chem suggest individual site characteristics and historical patterns of N deposition are important determinants of forest or alpine ecosystem responses to global change.

4.2 Introduction

Natural biogeochemical cycles of carbon (C) and nitrogen (N) have been strongly altered by land use change and human industrial and agricultural emissions, and the expected trend is for an increase in these emissions around the world (Sutton et al. 2011). Average atmospheric carbon dioxide (CO_2) in 2008 was 385 ppm, 38% above pre-industrial levels (Le Quéré et al. 2009), while the amount of available reactive nitrogen (Nr) in 2008 was 126% greater than that derived from natural biological nitrogen fixation and lightning (Schlesinger 2009). Global annual N deposition is predicted to increase another two- or threefold in the coming years (Lamarque et al. 2005). Emissions of CO_2 increased nearly 30% between 2000 and 2008, a trajectory coincident with the most carbon-intensive scenarios proposed by the Intergovernmental Panel on Climate Change (Le Quéré et al. 2009). The increase in atmospheric CO_2 is the largest contributor to human-induced climate change, and is controlled not only by emissions but by the strength of terrestrial and ocean sinks for C (Canadell et al. 2007). Terrestrial ecosystems are estimated to remove nearly three gigatons (Gt) of CO_2 from the atmosphere each year, playing a strong role in carbon uptake and storage in above- and belowground biomass (Canadell and Raupach 2008). The storage capability of terrestrial biomass and soils is therefore critical to mitigating the climate change effects of increasing CO_2.

Recent papers report increased C sequestration in forests and grasslands from CO_2 and N fertilization, yet the strength of the response depends on interdependent factors that vary by location and climate, vegetation types, degree of C or N saturation, and interactions

of stressors (Bedison and McNeil 2009, Campbell et al. 2009, Janssens and Luyssaert 2009, McMahon et al. 2010, Thomas et al. 2010, Chen et al. 2011). The C-N links in forests and grasslands that regulate terrestrial C storage and cycling include effects on photosynthesis from CO_2 and N stimulation, the allocation of C to above- and belowground biomass, and stimulation or suppression of microbial decomposition and respiration (Janssens and Luyssaert 2009, Liu and Greaver 2010, McMahon et al. 2010).

Empirical studies and meta-analyses of ecosystem responses to changes in climate, CO_2, and N deposition, either singly or combined, most often present results for one or two response variables. Rates of forest growth and productivity, aboveground biomass (Boisvenue and Running 2006, Bedison and McNeil 2009, McMahon et al. 2010, Thomas et al. 2010), and belowground C dynamics (de Vries et al. 2009, Liu and Greaver 2010) are among those described. Ecosystem models can offer a more comprehensive evaluation of multiple interacting or counteracting drivers and response variables (eg. Canham et al. 2003a). When validated against long-term data sets they provide a powerful way to project ecosystem responses to multiple global change drivers and have been used to test assumptions about the direct and indirect effects of climate change on ecosystems. Studies in a northern hardwood ecosystem (Campbell et al. 2009) and coniferous forests in the Rocky Mountains (Boisvenue and Running 2010) and Austria (Eastaugh et al. 2011), for example, underscore the importance of understanding the interaction of N deposition with climatic change and the need to address spatial variability in developing scenarios about how global change will affect ecosystem processes.

Our objectives here address many of these concerns through evaluation of the coupled ecosystem and biogeochemical responses in montane and alpine ecosystems in the U.S. to climate warming, increased or decreased atmospheric N deposition, and CO_2 fertilization. We used the ecosystem model DayCent-Chem to compare biogeochemical responses in nine

primarily montane catchments across a range of U.S. climates and N deposition histories. DayCent-Chem is a process-based ecosystem nutrient cycling model that simulates CO_2 fertilization effects while accounting for water, temperature, and nutrient N, phosphorus (P), and sulfur (S) constraints on plant growth and soil organic matter cycling (Hartman et al. 2007, Hartman et al. 2009). We developed site-specific scenarios of climate and N deposition, under two CO_2 concentrations that are within predicted ranges for the period 2001-2075 and used them to explore changes in C allocations to above- and below-ground biomass and soil organic matter, NEP, net greenhouse gas (GHG) flux, nitrous oxide (N_2O) emissions, and stream nitrate (NO_3^-) chemistry.

4.3 Methods

4.3.1 Study Sites

Our study sites were instrumented watersheds from four U.S. National Parks and four Long Term Ecological Research (LTER) areas (Table 4.1). The sites ranged in elevation at their outlets from 129 m to 3515 m and included two sites each from New England (Hubbard Brook LTER, NH (HBR) and Acadia National Park, ME (ACAD)), southern Appalachia (Coweeta LTER, NC (CWT) and Great Smoky Mountains National Park, NC (GRSM)), Cascades (HJ Andrews LTER, OR (HJA) and Mount Rainier National Park, WA (MORA)), and Rocky Mountains (Rocky Mountain National Park, CO (ANDCRK) and Niwot Ridge LTER, CO (NWT)) (Hartman et al. 2009). Two forested watersheds of different stand age at the HJ Andrews Experimental Forests were modeled: HJA (young) was clear-cut in 1975, and HJA (old) has trees >500 years. All sites were forested except for the Rocky Mountain locations. Detailed descriptions and model parameterization/validation for each site are found in Hartman et al. (2009).

4.3.2 DayCent-Chem Model

DayCent-Chem is a variation of CENTURY (Hartman et al. 2007). The CENTURY models specialize in C and N cycling by incorporating detailed mechanistic representations of plant nutrient and water uptake, soil microbial activities, and soil organic matter. They have been widely applied to grasslands, forests, and agricultural lands around world (Parton et al. 1993, Baron et al. 1994, Pan et al. 1998, Parton and Silver 2007). DayCent-Chem is constructed from DayCent, the daily-timestep version of CENTURY (Parton et al. 1998), and PHREEQC, a low-temperature aqueous geochemical model (Parkhurst and Appelo 1999) that allows prediction of stream and soil water chemistry for a number of solutes. A full model description is found in Hartman et al. (2007).

DayCent-Chem computes ecosystem dynamics, including soil water fluxes, snowpack and stream dynamics, plant production and nutrient uptake, litterfall, soil temperature with depth, soil organic matter decomposition, mineralization, nitrification, and denitrification, while utilizing PHREEQC's low-temperature aqueous geochemical equilibrium calculations, including CO_2 dissolution, mineral denudation, and cation exchange, to compute soil water and stream chemistry. Inputs to DayCent-Chem include daily precipitation amount and solute concentrations, daily minimum and maximum air temperatures, and the daily dry deposition from gas, particulates, and aerosols (specified either with a dry-to-wet deposition ratio or an absolute amount of dry deposition).

4.3.3 Nitrogen Processing

We computed both direct soil N_2O emissions and indirect N_2O from N leaching/runoff to surface waters. The trace gas submodel computes direct soil N_2O and nitrogen (di)oxide (NO_x) emissions as the intermediate products of denitrification and nitrification reactions (Parton et al. 1996, Del Grosso et al. 2000a, Parton et al. 2001). The denitrification submodel

assumes that N gas from denitrification is controlled by soil NO_3^-, heterotrophic CO_2 respiration (a surrogate for labile C availability), and oxygen (O_2) availability (determined by water-filled pore space and soil physical properties that control gas diffusivity). Soil nitrification rates are controlled by soil ammonium (NH_4^+) concentration, water content, soil temperature, and pH. Indirect N_2O from N leaching/runoff was calculated as 0.0075 kg N_2O-N per kg N leached runoff (IPCC/WMO/UNEP 2000). We computed cumulative N_2O emissions by summing both direct and indirect annual N_2O fluxes from 1980 to 2075. To enable comparison of sequestration of GHG (as ecosystem C accumulation in above- and below-ground biomass and SOM) with emission of GHG in the form of N_2O, we calculated the CO_2-C equivalents for N_2O flux assuming that 1 kg N_2O had the 100-year warming potential of 296 kg of CO_2 (Ramaswamy 2001).

4.3.4 Carbon dynamics

DayCent calculates a CO_2 effect on plant (primary) production, water-use efficiency, and plant C:N ratios. Model parameters relating to CO_2 fertilization were developed for the CENTURY model during the Vegetation Ecosystem Mapping and Analysis Project (VEMAP) (Pan et al. 1998). As described in the equations (1) and (2) below, the CO_2 fertilization effect was described relative to atmospheric CO_2 doubling from 350 to 700 ppm.

The potential net primary production at time t, NPP[t], was calculated as,

$$NPP[t] = NPP[0]\left(1 + \frac{\beta_1 \log_{10}\left(\frac{CO_2[t]}{CO_2[0]}\right)}{\log_{10}(2)}\right) \quad (1)$$

where $\beta 1 \geq 0$, $CO_2[0] = 350$ ppm, and NPP[0] equals the potential net primary production at 350 ppm. For plant types used in this exercise, $0.20 \leq \beta 1 \leq 0.25$, meaning that a CO_2

concentration of 700 ppm would increase potential production by 20% – 25%. Actual simulated net primary production was less than or equal to NPP[t] and depended on water and nutrient availability.

Similarly transpiration at time t, Transp[t], was reduced as CO_2 increased,

$$Transp[t] = Transp[0]\left(1 + \frac{\beta_2 \log_{10}\left(\frac{CO_2[t]}{CO_2[0]}\right)}{\log_{10}(2)}\right) \quad (2)$$

where $\beta 2 \leq 0$, $CO_2[0] = 350$ ppm, and Transp[0] is the amount of transpiration at 350 ppm. For plant types used in this exercise, $-0.25 \leq \beta 2 \leq -0.20$, which means that doubling CO_2 concentration (from 350 ppm to 700 ppm) would decrease transpiration by 20% – 25%.

Site-specific vegetation parameters specify a range of allowable plant tissue C:N ratios and therefore regulate the amount of N uptake per unit of C fixed in the model. Using relationships similar to the one described above for NPP, the model can simulate increased plant nitrogen-use (NUE) and maximum C:N ratios of plants. For this exercise, both minimum and maximum C:N ratios of plants were set to increase by 20% – 25% with a CO_2 doubling, based upon VEMAP simulations. The difference between minimum and maximum C:N ratios remained constant.

4.3.5 Pre-scenario characterization of ecosystem fluxes and storage

DayCent-Chem was parameterized for each site as part of an extensive data gathering and collaborative modeling effort (Hartman et al. 2009). Model results were compared to measured ecosystem pools and fluxes, and stream chemistry. The number of measured variables available for comparison varied by site and ranged from 22 for NWT and MORA to 79 for GRSM (Hartman et al. 2009).

While each of the two sites in a region were proximal to each other, pre-scenario simulations of ecosystem fluxes and C storage showed differences due to site-specific elevation, climate, atmospheric N deposition, and stand history (Hartman et al. 2009) (Table 4.2). GRSM had the highest annual productivity, heterotrophic respiration, soil organic matter carbon, N mineralization, and stream NO_3^- of all sites. Other sites with high production and respiration were CWT and ACAD; all three of them are located in eastern North America. Net ecosystem production (NEP), the difference between NPP and heterotrophic respiration, was greatest at ACAD, GRSM, and HJA (old). For the alpine sites, 90% of total ecosystem C was in belowground biomass and soil organic matter. For all forested sites except HJA (young), aboveground C was 53 – 66% of total ecosystem C. The flux of N_2O from ANDCK and NWT was among the highest, and stream NO_3^- fluxes at these alpine sites were moderately high compared with the other sites. Rates of NPP, Rh, N-mineralization and N_2O flux for HJA (young) were similar to rates in HJA (old), and intermediate in rates compared with the other sites. Soil organic matter and belowground plant residue (SOM C) for the young stand was among the lowest of all sites, while NEP was among the greatest for the old-growth HJA forest. Stream NO_3^- fluxes at both HJA sites were the lowest of all sites reported. MORA was the other site with extremely low stream NO_3^-, as well as low pre-scenario rates of N mineralization and N_2O flux.

Model scenarios

We compared current with future conditions for each site under plausible increases in temperature, N deposition, and atmospheric CO_2, as described below. All treatments were adjusted gradually over the simulation period. Each site was run under "NO WARM" and "WARM," "LOW N" and "HIGH N," and "MEDIUM" and "HIGH" atmospheric CO_2 scenarios that resulted in six scenarios for each site (Table 4.3). We did not pair the HIGH atmospheric CO_2 concentrations with a NO WARM scenario in the same simulation. Our

scenarios ran from the beginning of measured records for each site (earliest at HBR was 1979, latest at MORA was 1990) to 2075.

Each simulation had three stages: 1) a spin-up; 2) a period with measured inputs; and 3) a period with scenario inputs. The 500- to 1000- year spin-up run brought long-term C stores to quasi-equilibrium. For this stage the measured meteorological record for the site, which was much shorter than 100 years, was repeated many times, and N deposition was set at background levels (0.5 kg N ha^{-1} yr^{-1}) (Holland et al. 1999) until simulation year 1900 when N deposition was ramped linearly to reach measured amounts. HJA (young) was spun up as for HJA (old) site until 1975, when 95% of above-ground biomass was removed. For the next stage, the model was driven by measured atmospheric deposition, daily weather, and CO_2 concentrations; this stage started sometime between 1979 and 1990, depending on data availability for each site and ended with simulation year 2000. Simulations for years 2001-2075 were driven by the scenarios in daily climate, N deposition, and atmospheric CO_2. The six simulations for each site were identical from the start of the spin-up to the end of year 2000 before they branched off into the scenario inputs in 2001.

Climate scenarios for 2001 – 2075

Climate warming (WARM) scenarios were taken from Leung and Qian (2005). The scenarios were derived from MM5 (Penn State/NCAR Mesoscale Model) downscaled projections of the NCAR/DOE Parallel Climate Model (PCM) for 1976 – 2075 (Leung et al. 2003, Leung and Qian 2005). Control runs came from a 1975-1996 PCM simulation of historical climate using historical greenhouse gas emissions. Future climate PCM runs were initiated in 1995 with ocean data assimilation and a business-as-usual emissions scenario for greenhouse gases and aerosols, which produced about 1% increase in greenhouse gas concentrations per year. MM5 is a regional climate model that was used to dynamically downscale control and future simulations using a nested model configuration that yielded

climate at 36 km spatial resolution. Climate files were extracted based on latitude and longitude from the larger data set. Meteorological data measured at each site were compared to MM5 climate files for overlapping years. MM5 daily temperatures and precipitation were systematically adjusted using equations 3 – 6 across all years (including those beyond the instrumental record) so that there was a match between the years of measurement and the early model years and the resulting annual means were consistent with observed weather.

To compute daily scenario temperatures ($Tscen_{daily}$), ΔT was calculated as the average difference between mean annual observed temperature ($Tobs_{annual}$) and mean annual MM5 temperature ($TMM5_{annual}$), where n is the number of years observations were available. This procedure was done separately for minimum and maximum air temperatures.

$$\Delta T = \frac{1}{n}\sum (Tobs_{annual} - TMM5_{annual}) \quad \text{(for years 1976 – 2005)} \qquad (3)$$

$$Tscen_{daily} = TMM5_{daily} + \Delta T \qquad \text{(for years 2001 – 2075)} \qquad (4)$$

To compute daily scenario precipitation ($Pscen_{daily}$), ΔP was calculated as the average annual ratio of annual observed precipitation ($Pobs_{annual}$) to annual MM5 precipitation ($PMM5_{annual}$), where n is the number of years observations available.

$$\Delta P = \frac{1}{n}\sum \frac{Pobs_{annual}}{PMM5_{annual}} \qquad \text{(for years 1976 – 2005)} \qquad (5)$$

$$Pscen_{daily} = \Delta P \times PMM5_{daily} \quad \text{(for years 2001 – 2075)} \qquad (6)$$

The resulting WARM scenarios for all sites showed a 0.02 – 0.03 °C yr^{-1} increase in average annual temperature, resulting in a 2-3 °C increase by 2075, depending on the site.

Each site-specific NO WARM scenario was derived from observed weather by randomly shuffling and repeating year-long segments of daily meteorological records. The NO WARM scenario had no temperature trend. For all sites, the difference in annual mean

precipitation between the WARM and NO WARM scenarios was not significantly different, and neither scenario showed a decline or increase in annual precipitation over time.

Nitrogen scenarios for 2001 – 2075

All simulations used site-specific measured total inorganic N deposition (data sources listed in Hartman et al. 2009, CASTNET 2013, NADP/NTN 2013) through 2000. We did not consider the effects of S deposition in this study. Site-specific LOW N or HIGH N deposition scenarios were applied from 2001-2075 (Table 4.1). The LOW N deposition scenarios were based on U.S. EPA projections of deposition of wet and dry inorganic N species simulated for 36-km grid cells across the U.S. by the U.S. EPA Community Multiscale Air Quality (CMAQ v4.5) Modeling System (CMAQ 2005). CMAQ provided a '2001 Base Case', that was validated against measurements, and the total annual deposition of each chemical species for 2010, 2015, 2020 based on projected effects of the EPA Clean Air Interstate Rule, CAIR, which caps sulfur dioxide (SO_2) and NO_x emissions. Daily wet and dry deposition inputs were created with linear interpolation of annual deposition amounts for the years between 2001, 2010, 2015, and 2020. Deposition amounts from 2020 were applied to each subsequent year to 2075. Daily deposition was calculated as annual deposition divided by 365. We scaled up the 2001, 2010, 2015, and 2020 N deposition amounts in the CMAQ scenario for two sites, GRSM and NWT, because CMAQ simulated deposition in 2001 was much lower than measured 2001. The adjustments were made by scaling CMAQ results to match measured results, and that scalar was then applied to all subsequent years for each chemical solute.

The HIGH N scenario was created by increasing annual simulated 2001 deposition amounts by 1% each year to 2075. After 75 years annual deposition was 1.75 times as great as it was simulated to be in 2001. Daily deposition amounts were the annual amount divided by 365.

4.3.6 Atmospheric CO_2 scenarios

Atmospheric CO_2 concentration was equal to the annual mean measured concentration at Mauna Loa for all scenarios and all sites through simulation year 2000 (for example, 339 ppm in 1980 and 369.4 ppm in 2000, ftp://ftp.cmdl.noaa.gov/ccg/co2/trends/co2_annmean_mlo.txt). Starting with year 2001, annual atmospheric CO_2 concentrations were ramped to one of two potential future concentrations. For two of the six simulations, the 2075 CO_2 concentration reached 780 ppm. This "HIGH CO_2" scenario was based on A1F1, the highest CO_2 emissions scenario from the Special Report on Emissions Scenarios (SRES) (Nakicenovic 2000). For the other four simulations, the 2075 CO_2 concentration reached 600 ppm. This "MEDIUM CO_2" scenario was based on the older IPCC IS92a business-as-usual projection (IPCC 1996) which was in the middle of the range of SRES atmospheric CO_2 projections. CO_2 concentrations were incremented annually by a constant amount in order to reach either 780 or 600 ppm.

4.3.7 Mean Percent Differences

The mean percent differences between responses to individual scenarios for above- and below-ground live biomass C, SOM C, N-gas flux, N mineralization rate, and stream NO_3^- flux were calculated by subtracting the percent changes from base conditions for the last ten years of simulations (2065-2075) (Tables 4.4, 4.6) for pairs of scenarios, then averaging the differences for HIGH N minus LOW N, WARM minus NO WARM, and HIGH CO_2 minus MEDIUM CO_2 scenarios. For example, the mean percent difference for HIGH N – LOW N was computed by (1) subtracting the percent change from base conditions for LOW N NO WARM from the percent change for HIGH N NO WARM, (2) subtracting the percent change from base conditions for LOW N WARM from the percent change for HIGH N WARM, then (3) averaging these two differences.

4.3.8 Response Ratios

Response ratios for each site and scenario were calculated to compare the effect of different treatments on total ecosystem C content from the beginning to end of the simulations. The response ratios were determined by dividing total ecosystem C at year 2075 (less the CO_2-C equivalent lost as N_2O from 2001 – 2075) by total ecosystem C at base conditions.

4.3.9 Nitrogen Use Efficiency

We also calculated metrics for NUE and net ecosystem greenhouse gas (GHG) flux. Nitrogen use efficiency (NUE, g C g N^{-1}), the increase in NEP (g C) for every 1 g increase in N deposition, was calculated as the slope of regression line when NEP was plotted against N deposition. We considered NUE only for the HIGH N scenarios; for each LOW N scenario the amount of N deposition was nearly constant throughout the simulation.

4.3.10 Net Ecosystem Greenhouse Gas Flux

We computed the net ecosystem GHG flux by subtracting cumulative N_2O emissions expressed as CO_2-C equivalents (g CO_2-Ce m^{-2}) from 1980 to 2075 from total ecosystem C accumulation (aboveground C, belowground C, and SOM C, g C m^{-2}) over the same period. Positive values identified terrestrial systems that were net GHG sinks, and negative values those that were a net GHG source.

4.4 Results

We focus here on (1) whether ecosystem responses revealed synergistic interaction among N deposition, warming, and elevated CO_2 as drivers of change, (2) whether there were differences in the magnitude of ecosystem responses over the course of the simulation as a

function of the driving factors N deposition, warming, and CO_2, and (3) how site-specific characteristics affected ecosystem responses.

4.4.1 Aboveground Biomass C Responses to Individual and Cumulative Drivers

Once the baseline C accumulation over time was factored out, N deposition and warming appeared to have the greatest supplemental effect on aboveground C (aboveground live and dead plant material and plant residue) accumulation in these systems. When the aboveground C values were compared between the base conditions (Table 4.2) and the model output from 2075 for the different scenarios (Table 4.4), aboveground C was seen to have increased over base values. The increase in aboveground C was slight for GRSM and ANDCK, and greatest in the aggrading forest, HJA (young). HIGH N stimulated aboveground C accrual at all sites, with the greatest stimulation of HIGH N over LOW N at HBR, CWT, and HJA (young) (Figure 4.1). Aboveground C was also stimulated with WARM scenarios at HBR, but had a negligible or negative response at all other sites. At HJA (young) and the two alpine sites WARM scenarios reduced the amount of aboveground C accumulation compared with NO WARM by 10 – 20% (Figure 4.1).

Aboveground biomass C production was greater in the HIGH N WARM scenario than scenarios of either HIGH N or WARM but only at those forest sites with the lowest annual mean temperature: HBR, ACAD, and MORA (Table 4.4). For all other sites there was no enhanced response. The difference in aboveground C accumulation between the MEDIUM CO_2 and HIGH CO_2 scenarios was <5% for all sites (Figure 4.1).

4.4.2 Belowground Biomass C Responses to Individual and Cumulative Drivers

Across sites, belowground biomass C responses were generally smaller percentages of the baseline than aboveground biomass responses and no single driving factor stood out as

responsible for large changes. Belowground biomass C increased from base conditions to 2075 in all scenarios, but the absolute amount of increase was slight for GRSM and the two alpine sites (Tables 4.2, 4.4). There was a dramatic increase in belowground C (belowground live and dead plant material and plant residue) at CWT in response to HIGH N compared with LOW N, but the influence of HIGH N was less than 10% at all other sites (Figure 4.1). WARM scenarios stimulated 29% greater belowground C accumulation at NWT, but the difference in belowground C accrual between WARM and NO WARM was not large at other sites, with slightly greater accumulation from warming at some, and slightly less overall accumulation at both young and old HJA sites. As with aboveground biomass C production, belowground biomass C was stimulated by HIGH N WARM, at those forest sites with the lowest mean annual temperatures and also at the two alpine sites. Belowground biomass C was stimulated by 9% and 6% at ANDCK and NWT, respectively, by the HIGH CO_2 scenarios, but there was negligible response to CO_2 at any other site (Figure 4.1).

4.4.3 Soil Organic Matter C Responses to Individual and Cumulative Drivers

Soil organic matter C either increased slightly, decreased slightly, or did not change from base conditions over the simulations (Tables 4.2, 4.4), and most sites showed little response to the drivers (Figure 4.1). HIGH N scenarios stimulated SOM C at all forested sites except GRSM. WARM scenarios decreased SOM C at all sites. There was very little response in SOM C to the HIGH CO_2 scenario. The greatest enhancement of SOM over baseline conditions occurred with HIGH N NO WARM at all sites. HJA (young) had a net loss SOM C for all scenarios because the clearcut in 1975 left a large amount of litter which subsequently decomposed.

4.4.4 Trends in Net Ecosystem Production

Net ecosystem production fluctuated with precipitation and air temperature over the simulation period, but there was significant change in NEP either over time or with treatments at only half of the sites (Figure 4.2, Table 4.5). Most sites showed modest gains in NEP under some scenarios by 2075, but the alpine sites had slightly negative NEP for some scenarios. Positive responses in NPP or Rh to N, warming, and CO_2, while often statistically significant, appeared to cancel each other out (Table 4.5). HIGH N scenarios showed the greatest gain (0.86 – 1.02 g C m^{-2} yr^{-1}) in NEP, particularly at CWT, HJA (young) and HJA (old) compared with the LOW N scenarios (0.41-0.43 g C m^{-2} yr^{-1}). NEP at GRSM responded to WARM scenarios. Only two forests, ACAD and MORA, showed greater NEP specifically in response to HIGH N WARM. There were no significant changes in NEP with any scenario for HBR, ANDCK, or NWT. The NEP responses to HIGH CO_2 scenarios were not much different than NEP responses to their MEDIUM CO_2 counterparts.

4.4.5 Nitrogen Use Efficiency

For most sites, NUE values were higher with warming than with no warming (Figure 4.3). However, this was not the case for HBR and the two alpine sites. The alpine sites did not respond to increases in N. Among forests, NUE values were lowest for the sites with initially high N deposition (HBR, ACAD, GRSM) and were highest at both Young and Old HJA sites, where N deposition was initially lowest.

4.4.6 Nitrogen mineralization rates

HIGH N increased N mineralization at some, but not all, forested sites. GRSM and the two HJA sites were the least responsive to HIGH N (Figure 4.1). Nitrogen mineralization rates increased strongly under WARM scenarios in the alpine and less so at most forested

sites (Table 4.6). HIGH CO_2 had little effect on N mineralization. As with above- and belowground biomass C production, increased mineralization in response to HIGH N WARM was observed at HBR, ACAD, and MORA, the forested sites with low mean annual temperatures. At any given site, the magnitude of change in rates of mineralization and soil organic matter decomposition (indicated by modeled Rh) were similar in response to warming and N deposition.

4.4.7 N_2O, NO_x, and N_2 emissions

Total N gas ($N_2O + NO_x + N_2$) emissions from soils ranged from a low of 0.03 g N m^{-2} yr^{-1} at HBR and MORA to a high of 0.70 g N m^{-2} yr^{-1} at GRSM (Table 4.6). Sites fell into two categories in terms of which driving variable caused the greatest response: (1) western sites where the largest cumulative change in N_2O emissions was due to warming and (2) eastern sites where increases in N_2O emissions were greatest in scenarios with high N deposition, often in combination with warming (Figure 4.4). For four of the western sites (HJA (young), HJA (old), ANDCK, and NWT) N_2O emissions were greater with both HIGH N WARM than with either HIGH N or WARM alone. Both HIGH N and WARM individually stimulated N_2O production at all sites. The influence of HIGH CO_2 was slight at most sites. HIGH CO_2 depressed N_2O production compared with MEDIUM CO_2 slightly at HJA (young), HJA (old), ANDCK, and NWT (Figure 4.4), and depressed total N-gas flux by 20% at HJA (young) and 50% at ANDCK (Figure 4.1). The CO_2-C equivalents from cumulative direct plus indirect N_2O flux, which were all positive fluxes to the atmosphere, ranged from 121 to 864 g CO_2-Ce m^{-2}. These were of roughly the same magnitude as the change in SOM C (which ranged from -720 to +858 g CO_2-C m^{-2}) over the simulation period (Figure 4.4). MORA, the site with the lowest N_2O flux, was the only watershed with greater soil C storage than N_2O emissions for all scenarios.

4.4.8 Stream Nitrate Trends

Stream NO_3^- fluxes were positively related to HIGH N at all sites, and increased with the WARM scenarios only at HJA(young) and HJA (old) (Table 4.6, Figure 4.1). At CWT there was a 100% decline in stream NO_3^- flux under the WARM scenario compared with NO WARM, while other sites had a more modest response. HIGH CO_2 was associated with decreased stream NO_3^- flux at HJA(young), HJA (old), NWT, and ANDCK. For most sites, stream NO_3^- fluxes were low and the absolute change in stream NO_3^- flux with scenarios was slight, but the 138% increase under HIGH N at GRSM translated to a stream NO_3^- flux of 2.6 g N m^{-2} yr^{-1} in 2075 (Table 4.6). With HIGH N, fluxes of stream NO_3^- at ACAD and NWT also increased by more than 50% over baseline conditions and reached 0.3 g N m^{-2} yr^{-1} or greater (Table 4.6). Cumulative indirect N_2O emissions from 1980-2075 from N leaching and runoff were proportional to stream NO_3^- leaching and ranged from a high of 27 – 29% of direct soil N_2O emissions (186 – 193 g CO_2-C m^{-2}) under HIGH N at GRSM and a low of about 2 – 3% of direct soil N_2O emissions (6 – 9 g CO_2-C m^{-2}) at the two HJA sites for all scenarios.

4.4.9 Net Ecosystem Greenhouse Gas Flux

Net GHG flux ranged from 13,372 g CO_2-Ce m^{-2} (HJA Young, a terrestrial sink) to -1,223 g CO_2-Ce m^{-2} at ANDCK, a GHG source (Figure 4.5). Both GRSM and ANDCRK were a source of GHGs for nearly all scenarios. In general, net ecosystem GHG sequestration was enhanced by HIGH N. For ACAD, HBR, MORA, and NWT, the net ecosystem GHG sequestration was greatest with HIGH N WARM HIGH CO_2; these sites were the three coldest forests and the colder of the two alpine sites. For other sites, CWT, GRSM, both HJA sites, and ANDCRK, the net GHG sink was greatest with HIGH N NO WARM; these sites were the warmest forests and the warmer of the two alpine sites. The least net ecosystem

GHG sequestration occurred with LOW N NO WARM for the three coldest forest sites, ACAD, HBR, and MORA. The least ecosystem GHG sequestration or greatest GHG source occurred with LOW N WARM for the two alpine sites and the warmest forest sites (ANDCRK, NWT, CWT, GRSM, and both HJA sites). Among the LOW N deposition scenarios, net GHG sequestration was greatest with the WARM, HIGH CO_2 scenario, except for NWT and the two HJA sites that had greatest sequestration with NO WARM.

The rank of net carbon sequestration by site (g CO_2-Ce m^{-2}), from greatest to lowest based on the average of the net balance of six scenarios was HJA (Young), HBR, HJA (Old), MORA, CWT, and ACAD. GRSM, ANDCK, and NWT lost C to the atmosphere. Adding up net GHG sequestration for all sites by scenario, the model suggested (in the absence of any ecologically negative effects of HIGH N on production) that net ecosystem GHG sequestration would be 49% greater with HIGH N NO WARM than with LOW N WARM. When other factors are equal, net GHG sequestration is 7% greater with NO WARM than with WARM, 39% greater with HIGH N compared to LOW N, and 4–6% greater with HIGH CO_2 concentrations vs. MEDIUM CO_2 concentrations.

The simulations showed all forests except GRSM were net sinks for GHGs under all scenarios, including LOW N NO WARM. The response ratios for forests ranged from 0.98 to 1.63 with median values that ranged from 1.14 to 1.21 and were greatest when there was HIGH N (Figure 4.6). In contrast, the alpine sites released a slight amount of GHGs with WARM and were unresponsive to HIGH N or CO_2 (Figure 4.6). Response ratios for the alpine sites ranged from 0.86 to 1.04. A response ratio greater than 1.0 indicates that the system was a net sink for GHGs over the 75 years, whereas a response ratio less than 1.0 indicates a net source of GHGs.

4.5 Discussion

There was no universal response to N deposition, warming, or their combinations among the forested and alpine watersheds. Sites responded individually according to their vegetation type, climate, and N status. An overarching result, however, is that initial conditions with respect to N availability and mean annual temperature exert strong controls on the responses of the sites to N deposition and warming scenarios. Where initial N deposition was low, HIGH N scenarios stimulated NEP and GHG sequestration. At sites with high initial N deposition HIGH N scenarios increased stream NO_3^- fluxes. Warming stimulated ecosystem processes at those sites with the lowest mean initial annual temperatures. Warming and N deposition acted synergistically to stimulate NEP, N mineralization, and net GHG sequestration only at the colder forested sites, which were also stimulated to a lesser extent by either warming or N deposition alone.

In contrast to the marked ecosystem responses to N deposition and warming, increased CO_2 by itself was rarely an important driver of ecosystem responses based on DayCent-Chem. This is consistent with other work that suggests that the CO_2 effect is constrained due to N and soil moisture limitation in forests and grasslands (Saleska et al. 1999, Norby et al. 2010, Melillo et al. 2011, Pinder et al. 2012). Although Earth System Models suggest a strong CO_2 fertilization effect when N is not limiting (Bonan and Levis 2010), we found limited CO_2 response even in the presence of high N deposition. The only possible exceptions to this were in the alpine sites where belowground C biomass increased and stream NO_3^- fluxes decreased in the HIGH CO_2 scenarios (Figure 4.1). The generally limited response to CO_2 in this study may be because endpoints of our two CO_2 scenarios (MEDIUM: 600 ppm; HIGH: 760 ppm), although realistic, were not that different from each other. Zaehle et al. (2010) suggest a decreasing C gain with increasing CO_2 and a small C gain with warming.

Our model output for specific processes and locations was consistent with the results of other research. For instance, HIGH N scenarios increased aboveground C storage by 9 – 20% in all forests, as noted also by (LeBauer and Treseder 2008, Thomas et al. 2010, Butterbach-Bahl et al. 2011). The mechanism is likely to be high C:N in wood, and N-derived stimulation of wood production that promotes C sequestration (Nadelhoffer et al. 1999). In contrast, grasslands and foliar biomass in forests have much lower C:N ratios and thus a more limited capacity for C storage stimulated by N deposition. Liu and Greaver (2009) also found that in general N addition to grasslands does not increase C storage whereas N stimulates more C storage in forests. Warming stimulated aboveground C storage by an extra 4 – 19% only in our focal forests with the lowest initial mean annual temperatures, HBR, ACAD, and MORA, and had no or a negative effect on warmer forests or the alpine (Figure 4.1). Alpine sites lost aboveground C with warming. Boisvenue and Running (2006) found that warming increased forest biomass when water was not limiting, and this is a plausible explanation of our model results. Moisture stress in regions with warm, dry summers might limit aboveground C accumulation at sites such as HJA and the two alpine sites that rely on snowmelt for soil moisture.

Belowground biomass C accrued more with both HIGH N and WARM than with LOW N and NO WARM at all sites except HJA (young and old). The HJA sites responded negatively to warming. Like aboveground biomass C, belowground biomass C increased in response to HIGH N scenarios. However, when comparing the LOW N to HIGH N scenarios, the increase in aboveground C was usually greater than the increase in belowground C; CWT and HJA (young) were exceptions (Figure 4.1). Our model results are in partial agreement with experimental and theoretical studies that suggest fine root production and root respiration decline as the plant investment for nutrient acquisition declines (Aerts and Chapin 2000, Janssens et al. 2010). Belowground biomass response to

warming varied among sites. Experimental studies have also shown both a strong reduction in fine root biomass with warming, consistent with the idea that warming increases N mineralization rates and plants allocate less C to root biomass if there is greater soil nutrient availability (Melillo et al. 2011).

The greatest accumulation of SOM C at all sites occurred with HIGH N and NO WARM scenarios; warming either slowed SOM C accumulation or caused SOM C to decline (Table 4.4, Figure 4.4). Warming increases heterotrophic respiration, which can lead to a loss of SOM C (Melillo et al. 2011), a result highly consistent with the significant increase in Rh that occurred at all sites in WARM scenarios (Table 4.5). The model showed that HIGH N stimulated plant litterfall and coarse woody debris which led to high levels of SOM C. The rates of Rh were greater for HIGH N than for LOW N (Table 4.5) as C and N inputs to the soil increased and C:N ratios of plant litter decreased, but the enhanced decomposition rates did not compensate for increased litter inputs. Some studies have linked litter quality to a decline in SOM C in response to N addition, with measurable SOM C losses where the litter was readily decomposed, and SOM C gains with low-quality or high-lignin litter inputs (Dijkstra et al. 2004, Waldrop et al. 2004).

Published rates of NUE range 20 – 177 (Pinder et al. 2012) and our NUE values fell within this range except for the two HJA forests which were substantially above it. While these two stands, with NUE above 240 g C g N^{-1}, appear to be outliers, we believe these values are appropriate. Recent published literature for Europe and North America NUE suggests values this high should be subject to suspicion (Sutton et al. 2008), but several papers for Douglas-fir forests in the Pacific Northwest that receive >1500 mm annual precipitation describe NUE values of this magnitude (Binkley et al. 1992, Perakis and Sinkhorn 2011). Furthermore, it is not surprising that the NUE was greatest at sites that began with the lowest measured N deposition (Figure 4.3). With the exception of HBR and the two

alpine sites, warming enhanced NUE . NUE can rise with increased NEP or decreased N–gas and stream N losses; NEP increased more with warming than no warming for ACAD, CWT, GRSM, and MORA (Figure 4.2, Table 4.5) while N losses decreased with warming for the CWT (Figure 4.1), but these hypotheses do not explain increased NUE with warming for the two HJA sites.

4.5.1 Net Greenhouse Gas Sequestration

Nitrous oxide emissions that increased with warming and HIGH N dampened, and at four sites negated, the soil C sequestration ability caused by N fertilization (Figure 4.4). For four of the sites (HBR, ACAD, CWT, and HJA (old)) N_2O emissions were greater than the increase in soil C storage for all warming scenarios. Nitrous oxide emissions from GRSM and NWT cancelled out long-term soil C storage for NO WARM scenarios, and N_2O emissions equaled the loss of SOM C for ANDCRK and HJA (young).

Despite the increase in N_2O emissions that came with HIGH N relative to LOW N scenarios at all but ANDCK, the greatest gains in net GHG sequestration and NEP came from the addition of N to the forested sites where increases in biomass complemented soil C changes to lead to net GHG sequestration at most sites (Figure 4.5). Our simulation results are in keeping with the findings of field, modeling and meta-analysis results of experimental N additions. LeBauer and Treseder (2008) found that most ecosystems, including temperate forests and temperate grasslands, averaged 29% growth response to N additions, which can come from N deposition (Thomas et al. 2010) or from warming-induced acceleration of the nitrogen cycle (Melillo et al. 2011). Other studies show variation in the stimulation provided by N depending on the degree of initial N limitation and on other confounding factors such as degree of soil acidification or adverse effects from ozone (Bedison and McNeil 2009, Thomas et al. 2010).

Even though cumulative net GHG sequestration from HIGH N was 40% greater than net GHG sequestration from LOW N, the response of ecosystem C content to N additions was modest. The median forest response ratios, a measure of the change in ecosystem C content from the beginning to end of the simulations, ranged from 1.14 to 1.21 and were 5 - 7% greater for HIGH N compared to LOW N in our forest simulations (Figure 4.6). Liu and Greaver (2009), in their meta-analysis of U.S. forest N-fertilization results also found on average that N addition increased ecosystem carbon content of forests by 6%. There was no effect on net GHG sequestration in response to warming, N, or CO_2 at the alpine sites.

DayCent-Chem model output reinforces the growing consensus that there will be a limited ability for continued forest or alpine GHG mitigation stimulated by N deposition or warming, and any ability may be further limited by disturbance—a factor not considered in this research except at HJA (young). Harvest or an increased amount of decomposition from fire or insect-caused mortality, can have stand-level effects on carbon uptake and storage (Hyvonen et al. 2007). Furthermore, while our simulation of HJA (young) demonstrated that forest regrowth can result in a strong GHG sink, we did not account for the fate of the harvested wood. Even disturbance and regrowth will not alter the conclusion, however, that in the long run forests and alpine will provide limited capability for reduction of atmospheric CO_2 (Melillo et al. 2011).

4.5.2 Nitrogen mineralization and stream nitrate

Climate change and N deposition have ramifications beyond terrestrial C cycling. Our ecosystem model was developed in large part to understand how changes in terrestrial C and N processes propagate downstream to aquatic ecosystems. Nitrate in upland waters contributes to nutrient enrichment and surface water acidification, and both these drive changes to aquatic ecosystem biodiversity, productivity, and water quality (Aber et al. 2003,

Baron et al. 2011). Stream NO_3^- will reflect the combined plant and soil system response to N deposition, warming, and CO_2. The residual N from above- and belowground N uptake, and microbial N cycling, particularly mineralization, immobilization, and N-gas emissions (N_2O, NO_x, and N_2), determine what gets flushed to surface waters (Aber et al. 1998). A synthesis of a data sets from the northeastern U.S. (including HBR and ACAD), found the strongest relation of stream water NO_3^- was with N deposition alone, since heterogeneity across sites from climate variability, vegetation type, and disturbance history obscured other global drivers (Aber et al. 2003). Likewise here we observed that although the magnitude of the effect of N deposition differed across sites, stream NO_3^- was higher at all sites in the HIGH N relative to LOW N simulations (Figure 4.1). In contrast, warming and CO_2 effects on stream NO_3^- were more variable across sites underscoring the importance of N deposition as a primary driver of downstream water quality under scenarios of global change.

Watersheds with a history of high atmospheric N deposition relative to their terrestrial cycles showed strong increases in stream NO_3^- fluxes with the HIGH N scenarios. Both the greatest rate and greatest absolute increase in stream N flux occurred at GRSM, which has been N-saturated for many years (Van Miegroet et al. 2001). Stream NO_3^- at ACAD also increased with the HIGH N scenarios, reflecting the lower ability of N to be taken up in old growth spruce-fir forests on shallow soils (Hartman et al. 2009). ANDCK and NWT have received elevated N deposition and also displayed symptoms of N saturation for decades (Baron et al. 2011). With a snowmelt-dominated hydrograph, shallow soils, short growing season, and low overall plant biomass the alpine is expected to be responsive to increased N deposition. These patterns make sense since we would expect the sites with the greatest biologic stores of N to be prone to leakage of additional N inputs.

4.6 Summary and Conclusions

Both GHG sequestration potential and stream water quality responses to atmospheric N deposition, climate change, and increasing atmospheric CO_2 are of interest both to scientists and to regulatory and land management agencies. We, like others, believe that models can be excellent heuristic tools that can reveal what we do, and do not, understand about how ecosystems function. DayCent-Chem simulations for diverse forest and alpine sites revealed the importance of individual site antecedent conditions in their response to global change. While DayCent-Chem results showed limited response to CO_2, responses to N deposition and temperature were similar to those reported from increasing numbers of empirical studies. Our results suggest N deposition could modestly strengthen the terrestrial net GHG sink primarily by increasing C stored in wood biomass of montane forests. This is countered by CO_2 emissions from accelerated soil organic carbon decomposition due to warming and increased N_2O emissions due to warming and high N deposition, reducing the overall strength of GHG storage. High N deposition did not enhance net GHG sequestration for the alpine sites or for an N-saturated forest. Warming scenarios increased net GHG sequestration only at the three coldest forested sites, and the combined effects of N deposition and warming further increased net GHG sequestration in these cold forests. However, high rates of N deposition increased NO_3^- output at all sites, particularly those that have historically received high N deposition as well as those with low productivity. However, in scenarios with low N deposition, stream NO_3^- fluxes declined below measured values in some systems illustrating that water quality improvements could occur in the face of climate change if N deposition decreases below current amounts.

4.7 Acknowledgments

Funding was provided by the EPA Clean Air Markets Division, the National Park Service Air Resources Division, and the U.S. Geological Survey. We thank Amanda Elliot Lindsey for the graphics, and Lois St. Brice for her help with the Acadia simulations. This is a product of the USGS Western Mountain Initiative.

.

Table 4.1. Site characteristics including years of measured data, catchment name, vegetation type and stand age, measured mean annual temperature, measured mean annual temperature precipitation, measured mean annual N deposition, and simulated N deposition for years 2001, 2075 (LOW N), and 20075 (HIGH N).

Site Name (abbreviation)	Years of Measured Data	Catchment	Vegetation Type (stand age)	Mean (std dev) Annual Temperature (°C)	Mean (std dev) Annual Precipitation (cm)	Mean Annual N deposition (kg N ha^{-1})	Simulated 2001 N deposition (kg N ha^{-1})	Simulated 2075 LOW N deposition (kg N ha^{-1})	Simulated 2075 HIGH N deposition (kg N ha^{-1})
Hubbard Brook LTER, NH (HBR)	1979-2004	Watershed 6	Northern mixed hardwood (~100 yrs)	4.4 (0.8)	142 (20)	7.0	5.5	3.9	9.6
Acadia NP, ME (ACAD)	1983-2005	Hadlock Brook	Spruce-fir (>300 yrs)	7.6 (0.7)	152 (32)	10.0	6.5	4.0	11.3
Coweeta LTER, NC (CWT)	1985-1995	Watershed 2	Mixed mesophytic hardwood (>100 yrs)	13.5 (0.7)	177 (41)	6.9	7.6	6.0	13.3
Great Smoky Mountains NP, NC (GRSM)	1981-1999	Noland Divide	Spruce-fir (>300 yrs)	8.6 (0.6)	232 (39)	30.6	30.0	22.1	52.4
HJ Andrews LTER, OR (HJA young)	1981-2004	Watershed 10	Douglas fir (35 yrs)	10.2 (0.8)	219 (44)	1.5	2.4	2.0	4.1
HJ Andrews LTER, OR (HJA old)	1981-2004		Douglas fir (>500 yrs)	10.2 (0.8)	219 (44)	1.5	2.4	2.0	4.1
Mount Rainier NP, WA (MORA)	1990-2007	Lake Louise	Coniferous (>300 yrs)	4.5 (0.5)	298 (61)	2.8	4.1	3.7	7.2
Rocky Mountain NP, CO (ANDCK)	1984-2006	Andrews Creek	Alpine (10,000 yrs)	-1.1 (0.5)	106 (18)	3.5	3.0	2.8	5.3
Niwot Ridge LTER, CO (NWT)	1990-2006	Green Lakes Valley	Alpine (10,000 yrs)	-3.1 (0.5)	124 (16)	5.9	7.2	6.9	12.7

Table 4.2. Mean (and standard deviation) of base ecological characteristics for each site: net primary production (NPP), heterotrophic respiration (Rh), AG-C (above ground live and dead plant material and surface plant residue), BG-C (below ground live and dead plant material and plant residue), SOM-C (below ground plant residue and partially decomposed soil organic matter), N-gas (NO_x, N_2O, N_2) flux (N-gas), net N mineralization rate (Nmin), and stream NO_3^- flux (strmNO_3^- The years for which there are measured values are shown in parentheses in the first column.

Site	NPP (g C m^{-2} yr^{-1})	Rh (g C m^{-2} yr^{-1})	NEP (g C m^{-2} yr^{-1})	AG-C (g C m^{-2})	BG-C (g C m^{-2})	SOM-C (g C m^{-2})	Nmin (g N m^{-2} yr^{-1})	N-gas (g N m^{-2} yr^{-1})	strmNO_3^- (g N m^{-2} yr^{-1})
HBR (1979-2004)	414 (58)	290 (15)	124 (52)	11203 (594)	3432 (278)	4133 (85)	5.5 (0.5)	0.03 (0003)	0.70 (0.06)
ACAD (1983-2005)	567 (55)	417 (17)	150 (37)	20817 (340)	5265 (99)	7701 (66)	5.6 (0.3)	0.04 (0.01)	0.22 (0.08)
CWT (1985-1995)	589 (84)	538 (37)	51 (82)	11210 (70)	3156 (38)	5363 (22)	7.6 (0.6)	0.16 (0.06)	0.01 (0.01)
GRSM (1981-1999)	747 (39)	621 (32)	120 (81)	27008 (71)	3523 (87)	11689 (130)	9.4 (1.1)	0.13 (0.02)	1.09 (0.34)
HJA (young) (1981-2004)	402 (35)	289 (16)	114 (33)	5579 (719)	11395 (69)	4940 (82)	4.2 (0.3)	0.05 (0.02)	0.03 (0.02)
HJA (old) (1981-2004)	482 (45)	357 (16)	124 (43)	35748 (377)	12631 (156)	5209 (21)	5.2 (0.3)	0.07 (0.02)	0.04 (0.02)
MORA (1990-2007)	255 (63)	199 (329)	56 (48)	16718 (96)	7582 (109)	7229 (29)	3.0 (0.5)	0.03 (0.01)	0.07 (0.06)
ANDCK (1984-2006)	142 (27)	149 (41)	-6 (21)	893 (18)	1168 (15)	7472 (30)	3.0 (0.8)	0.17 (0.04)	0.21 (0.07)
NWT (1990-2006)	109 (23)	113 (27)	-4 (9)	900 (16)	1228 (20)	7451 (23)	2.2 (0.6)	0.16 (0.02)	0.36 (0.07)

Table 4.3. The six scenarios of N deposition, climate, and atmospheric CO_2 concentrations. N deposition and climate were site-specific. Observed N deposition, weather, and CO_2 concentrations were used to drive the model prior to 2001. Low N deposition (LOW N) after 2001 was based on expected deposition with implementation of the Clean Air Interstate Rule (CAIR). High N deposition (HIGH N) scenarios added 1% of the site's 2001 N deposition amount each year. MM5 is the Penn State/NCAR Mesoscale Model downscaled climate predictions for 2001 – 2075. Atmospheric CO_2 concentrations were increased from the measured value in 2001 to medium concentrations (MED CO_2) based on the IPCC IS92a business-as-usual projections (IPCC 1996) or high concentrations (HIGH CO_2) based on CO_2 scenarios from A1F1, the highest SRES CO_2 emissions scenario (Nakicenovic 2000).

	LOW N WARM MED CO_2	LOW N NO WARM MED CO_2	LOW N WARM HIGH CO_2	HIGH N WARM MED CO_2	HIGH N NO WARM MED CO_2	HIGH N WARM HIGH CO_2
N deposition 2001 – 2075	CAIR to 2020, then constant	CAIR to 2020, then constant	CAIR to 2020, then constant	increased 1% annually	increased 1% annually	increased 1% annually
Climate 2001 – 2075	MM5, 2–3°C warming	historic, randomized years, no temperature trend	MM5, 2–3°C warming	MM5, 2–3°C warming	historic, randomized years, no temperature trend	MM5, 2–3°C warming
CO_2 concentration year 2075 (ppm)	600	600	760	600	600	760

Table 4.4. Carbon pools. Above ground C (AG-C), below ground C (BG-C, and total soil organic matter C (SOM-C) (g C m^{-2}) in 2075 for the six scenarios (% difference from base values from Table 4.2). ABOVEGROUND C includes above ground live and dead plant material and surface plant residue. BELOWGROUND C includes below ground live and dead plant material and plant residue. SOM C includes below ground plant residue and partially decomposed soil organic matter.

	LOW N NO WARM MED CO_2	LOW N WARM MED CO_2	HIGH N NO WARM MED CO_2	HIGH N WARM MED CO_2	LOW N WARM HIGH CO_2	HIGH N WARM HIGH CO_2
HBR						
AG-C	14,602 (30)	16,737 (49)	16,830 (50)	18,215 (63)	16,959 (51)	18,515 (65)
BG-C	4,823 (41)	4,972 (45)	4,799 (40)	5,167 (51)	4,975 (45)	5,250 (53)
SOM -C	4,294 (4)	4,398 (6)	4,775 (16)	4,512 (9)	4,423 (7)	4,505 (9)
ACAD						
AG-C	22,013 (6)	22,902 (10)	23,716 (14)	24,724 (19)	22,989 (10)	24,798 (19)
BG-C	5,559 (6)	5,837 (11)	5,962 (13)	6,291 (20)	5,866 (11)	6,316 (20)
SOM -C	8,030 (4)	7,542 (-2)	8,246 (7)	7,823 (2)	7,543 (-2)	7,810 (1)
CWT						
AG-C	13,512 (21)	13,575 (21)	15,373 (37)	15,405 (37)	13,608 (21)	15,431 (38)
BG-C	4,031 (28)	4,012 (27)	4,935 (56)	4,903 (55)	4,018 (27)	4,908 (56)
SOM -C	5,704 (6)	5,539 (3)	6,094 (14)	5,891 (10)	5,519 (3)	5,877 (10)
GRSM						
AG-C	27,344 (1)	27,274 (1)	27,781 (3)	27,708 (3)	27,375 (1)	27,810 (3)
BG-C	3,555 (1)	3,623 (3)	3,601 (2)	3,667 (4)	3,638 (3)	3,681 (4)
SOM -C	11,958 (2)	11,476 (-2)	12,002 (3)	11,518 (-2)	11,454 (-2)	11,498 (-2)
HJA (young)						
AG-C	15,783 (183)	14,769 (165)	16,790 (201)	15,603 (180)	14,998 (169)	15,846 (184)
BG-C	12,346 (8)	11,608 (2)	13,015 (14)	12,157 (7)	11,748 (3)	12,304 (8)
SOM -C	4,877 (-1)	4,638 (-6)	4,992 (1)	4,728 (-4)	4,661 (-5)	4,753 (-3)
HJA (old)						
AG-C	41,048 (15)	39,763 (11)	42,055 (18)	40,606 (14)	40,000 (12)	40,878 (14)
BG-C	14,579 (15)	13,755 (9)	15,247 (21)	14,306 (13)	13,898 (10)	14,476 (15)
SOM -C	5,532 (6)	5,265 (1)	5,644 (8)	5,354 (3)	5,288 (2)	5,380 (3)
MORA						
AG-C	18,507 (11)	19,407 (16)	19,578 (17)	20,449 (22)	19,506 (17)	20,550 (23)
BG-C	9,025 (19)	9,495 (25)	9,355 (23)	9,817 (30)	9,536 (26)	9,859 (30)
SOM -C	7,776 (8)	7,534 (4)	8,091 (12)	7,825 (8)	7,537 (4)	7,828 (8)
ANDCK						
AG-C	945 (6)	844 (-5)	1,013 (13)	882 (-1)	850 (-5)	893 (0)
BG-C	1,288 (10)	1,334 (14)	1,322 (13)	1,364 (17)	1,444 (24)	1,468 (26)
SOM -C	7,459 (0)	6,795 (-9)	7,525 (1)	6,853 (-9)	6,943 (-7)	7,010 (-6)
NWT						
AG-C	1,261 (40)	1,148 (28)	1,338 (49)	1,224 (36)	1,134 (26)	1,214 (35)
BG-C	1,342 (9)	1,647 (34)	1,373 (12)	1,687 (37)	1,722 (40)	1,764 (44)
SOM -C	7,603 (2)	7,280 (-2)	7,644 (3)	7,356 (-1)	7,344 (-1)	7,424 (0)

Table 4.5. Slopes (average increase per year) of net primary production (NPP), heterotrophic respiration (Rh), and net ecosystem production (NEP) (g C m^{-2} yr^{-1} yr^{-1}) for each site and scenario from 2001 to 2075. Significant trends ($p \leq 0.01$) are noted with *. The alpine sites are shaded.

	LOW N NO WARM MED CO_2			LOW N WARM MED CO_2			HIGH N NO WARM MED CO_2			HIGH N WARM MED CO_2			LOW N WARM HIGH CO_2			HIGH N WARM HIGH CO_2		
SITE	NPP	Rh	NEP	NPP	Rh	NEP	NPP	Rh	NEP	NPP	Rh	NEP	NPP	Rh	NEP	NPP	Rh	NEP
HBR	0.36	0.46*	-0.1	0.84*	0.81*	0.03	1.48*	1.06*	0.42	1.05*	0.97*	0.09	0.94*	0.86*	0.07	1.00*	0.96*	0.03
ACAD	-0.02*	0.22*	-0.24	0.31*	0.41*	-0.10	0.55*	0.45*	0.10	1.20*	0.80*	0.40	0.37*	0.45*	-0.08	1.22*	0.81*	0.40
CWT	0.71*	0.51*	0.19	1.03*	0.80*	0.23	2.43*	1.34*	1.09*	2.79*	1.61*	1.18*	0.96*	0.77*	0.19	2.73*	1.59*	1.14*
GRSM	0.15	-0.03	0.18	1.79*	0.56*	1.23	0.31	0.00	0.31	1.97*	0.59*	1.37*	1.94*	0.67*	1.27	2.12*	0.71*	1.41*
HJA (young)	0.78*	0.35*	0.43*	0.69*	0.28*	0.41*	1.58*	0.55*	1.02*	1.31*	0.45*	0.86*	0.74*	0.31*	0.43*	1.37*	0.48*	0.89*
HJA (old)	0.62*	0.39*	0.23	0.51	0.34*	0.18	1.40*	0.58*	0.82*	1.13*	0.50*	0.63	0.54	0.36*	0.19	1.20*	0.52*	0.68
MORA	0.19	0.27*	-0.08	0.53*	0.55*	-0.02*	0.97*	0.49*	0.47*	1.33*	0.79*	0.53*	0.60*	0.61*	-0.01	1.40v	0.85*	0.55*
ANDCRK	-0.12	-0.10	-0.01	0.92*	0.99*	-0.07	0.00*	-0.04	0.05	1.06*	1.09*	-0.03	1.10*	1.16*	-0.06	1.23*	1.25v	-0.02
NWT	0.07	0.01	0.06	1.40*	1.42*	-0.02	0.18*	0.05	0.13*	1.59*	1.53*	0.05	1.47*	1.49*	-0.02	1.67*	1.61*	0.06

Table 4.6. Nitrogen fluxes. The mean (and standard deviation) N-gas (NO_x, N_2O, N_2) flux (N-gas, g N m^{-2} yr^{-1}), net N mineralization rate (Nmin, g N m^{-2} yr^{-1}), stream NO_3^- flux ($strmNO_3^-$, g N m^{-2} yr^{-1}), and the percent difference from base conditions from Table 4.2 (% diff) for the last ten years of simulations (2065-2075) for all six scenarios.

	LOW N NO WARM MED CO_2		LOW N WARM MED CO_2		HIGH N NO WARM MED CO_2		HIGH N WARM MED CO_2		LOW N WARM HIGH CO_2		HIGH N WARM HIGH CO_2	
	mean (sd)	% diff	mean (sd)	% diff	mean (sd)	% diff	mean (sd)	% diff	mean (sd)	% diff	mean (sd)	% diff
HBR												
N-gas	0.03 (0.0)	0	0.04 (0.0)	33.3	0.05 (0.0)	66.7	0.07 (0.0)	133.3	0.04 (0.0)	33.3	0.07 (0.0)	133.3
Nmin	5.1 (0.3)	-6.5	5.9 (0.3)	7.8	6.1 (0.3)	11.1	6.4(0.3)	16.5	5.8 (0.3)	6.2	6.23(0.3)	13.3
$strmNO_3^-$	0.1 (0.1)	-35	0.1 (0.0)	-60	0.2 (0.1)	20	0.2 (0.1)	-10	0.1 (0.0)	-60	0.2 (0.1)	-10
ACAD												
N-gas	0.05 (0.0)	25	0.07 (0.0)	75	0.12 (0.0)	200	0.12 (0.0)	200	0.08 (0.0)	100	0.12 (0.1)	200
Nmin	5.6 (0.3)	0.4	6.3 (0.3)	13.2	6.0 (0.3)	7.3	6.8 (0.4)	20.5	6.3 (0.3)	13.2	6.8 (0.0)	20.5
$strmNO_3^-$	0.2 (0.1)	-27.3	0.2 (0.1)	-27.3	0.4 (0.1)	59.1	0.4 (0.1)	59.1	0.2 (0.1)	-27.3	0.4 (0.1)	63.6
CWT												
N-gas	0.22 (0.1)	37.5	0.15 (0.0)	-6.3	0.29 (0.0)	81.2	0.25 (0.0)	56.3	0.15 (0.0)	-6.3	0.25 (0.0)	56.2
Nmin	7.6 (0.3)	0	7.5 (0.4)	-1.3	8.4 (0.3)	10	8.2 (0.5)	8.4	7.2 (0.4)	-4.6	8.0 (0.4)	5
$strmNO_3^-$	< 0.1(0.0)	100	< 0.1(0.0)	0	< 0.1(0.0)	200	< 0.1(0.0)	100	< 0.1(0.0)	0	< 0.1(0.0)	100
GRSM												
N-gas	0.15 (0.0)	15.4	0.17 (0.0)	30.8	0.17 (0.0)	30.8	0.20 (0.0)	53.8	0.18 (0.0)	38.5	0.20 (0.0)	53.8
Nmin	10.7 (0.7)	14	12.1 (1.0)	28.7	10.5 (0.2)	11.9	12.0 (0.2)	27.8	12.1 (1.0)	28.7	12.0 (1.0)	27.7
$strmNO_3^-$	1.1 (0.1)	2.8	1.1 (0.1)	-1.8	2.6 (0.3)	138.5	2.6 (0.3)	137	1.1 (0.1)	0	2.6 (0.2)	139.4
HJA (young)												
N-gas	0.06 (0.0)	20	0.12 (0.0)	140	0.07 (0.0)	40	0.14 (0.0)	180	0.11 (0.0)	120	0.13 (0.0)	160
Nmin	4.8 (0.3)	15	4. (0.4)	16.4	5.0 (0.3)	18.8	5.1 (0.4)	20.5	4.8 (0.4)	13.8	4.9 (0.4)	17.1
$strmNO_3^-$	< 0.1(0.0)	-33.3	0.1 (0.0)	66.7	< 0.1(0.0)	0	0.1 (0.0)	133.3	0.1 (0.0)	66.7	0.1 (0.0)	100
HJA (old)												
N-gas	0.07 (0.0)	0	0.13 (0.0)	85.7	0.08 (0.0)	14.3	0.16 (0.0)	128.6	0.13 (0.0)	85.7	0.16 (0.0)	128.6
Nmin	5.1 (0.3)	-1.3	5.2 (0.4)	0.2	5.3 (0.4)	2.1	5.4 (0.4)	3.1	5.1 (0.4)	-2.1	5.2 (0.4)	0.6
$strmNO_3^-$	< 0.1(0.0)	-25	0.1 (0.0)	50	< 0.1(0.0)	-25	0.1 (0.0)	75	0.1 (0.0)	50	0.1 (0.0)	50
MORA												
N-gas	0.03 (0.0)	0	0.04 (0.0)	33.3	0.04 (0.0)	33.3	0.04 (0.0)	33.3	0.04 (0.0)	33.3	0.05 (0.0)	66.7
Nmin	3.3 (0.4)	9	3.8 (0.6)	26.3	3.6 (0.4)	18.7	4.1 (0.6)	36.3	3.8 (0.6)	26.7	4.1 (0.61)	36.3
$strmNO_3^-$	0.1 (0.1)	14.3	0.1 (0.1)	0	0.1 (0.1)	42.9	0.1 (0.1)	42.9	0.1 (0.1)	0	0.1 (0.1)	42.9

	LOW N NO WARM MED CO_2		LOW N WARM MED CO_2		HIGH N NO WARM MED CO_2		HIGH N WARM MED CO_2		LOW N WARM HIGH CO_2		HIGH N WARM HIGH CO_2	
	mean (sd)	% diff	mean (sd)	% diff	mean (sd)	% diff	mean (sd)	% diff	mean (sd)	% diff	mean (sd)	% diff
ANDCK												
N-gas	0.15 (0.0)	-11.8	0.42 (0.2)	147.1	0.17 (0.0)	0	0.46 (0.2)	170.6	0.34 (0.1)	100	0.37 (0.1)	117.6
Nmin	2.8 (0.8)	-6.3	5.5 (0.7)	84.7	2.9 (0.8)	-4	5.7 (0.7)	88.3	5.5 (0.8)	82	5.5 (0.8)	83.7
strmNO_3^-	0.1 (0.0)	-33.3	0.1 (0.1)	-33.3	0.3 (0.0)	28.6	0.3 (0.1)	23.8	0.1 (0.0)	-38.1	0.2 (0.1)	14.3
NWT												
N-gas	0.17 (0.0)	6.3	0.30 (0.0)	87.5	0.22 (0.0)	37.5	0.35 (0.0)	118.7	0.28 (0.0)	75	0.33 (0.0)	106.3
Nmin	2.3 (0.5)	4.1	4.9 (0.8)	121	2.3 (0.6)	5.9	5.0 (0.8)	125.5	4.8 (0.8)	117.7	4.9 (0.9)	122.3
strmNO_3^-	0.3 (0.1)	-8.3	0.3 (0.1)	-16.7	0.7 (0.1)	91.7	0.6 (0.1)	69.4	0.3 (0.1)	-19.4	0.6 (0.1)	66.7

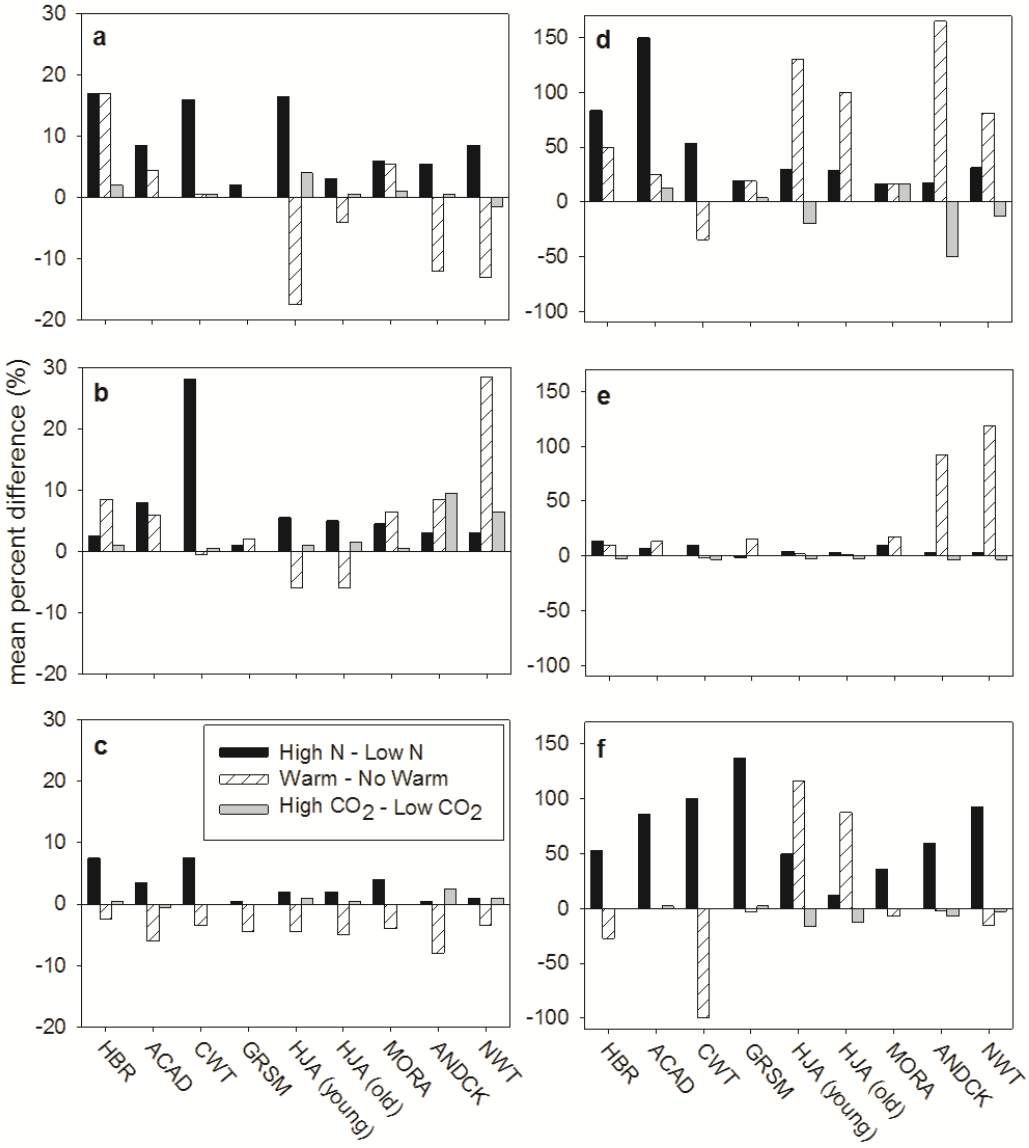

Figure 4.1. The mean difference in percent change from base conditions for the last ten years of simulations (2065-2075) between HIGH N and LOW N, WARM and NO WARM, and HIGH CO_2 and MED CO_2 scenarios. a) above ground carbon; b) below ground carbon; c) soil organic matter carbon; d) Total N-gas (N_2O + NO_x + N_2) emissions; e) net N mineralization; f) stream nitrate fluxes. A negative value indicates a flux to the atmosphere or a loss from the ecosystem; a positive value indicates sequestration.

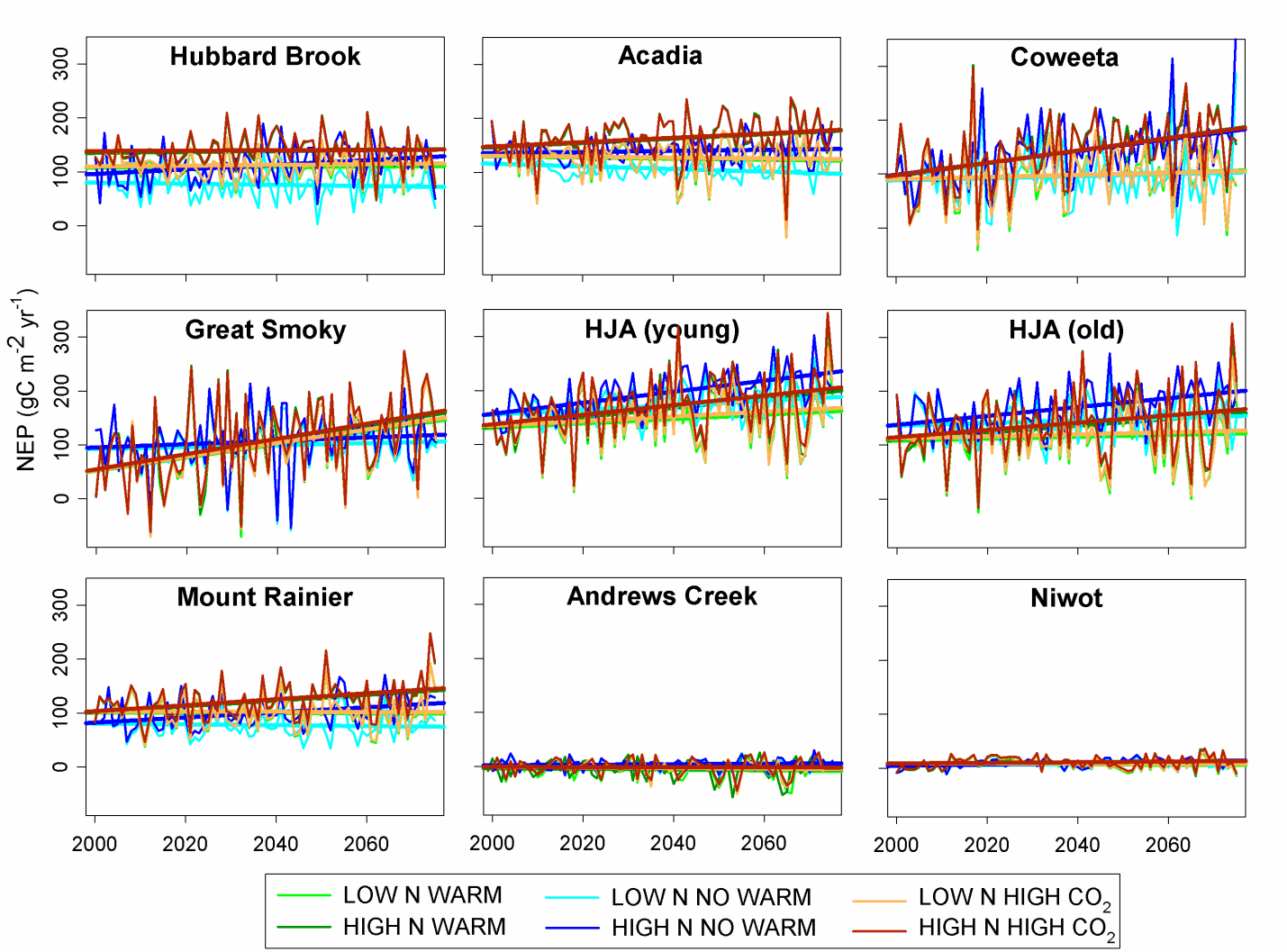

Figure 4.2. Simulated annual Net Ecosystem Production (NEP) and trends from 2000 – 2075 for all sites and all scenarios (g C m^{-2} yr^{-1}).

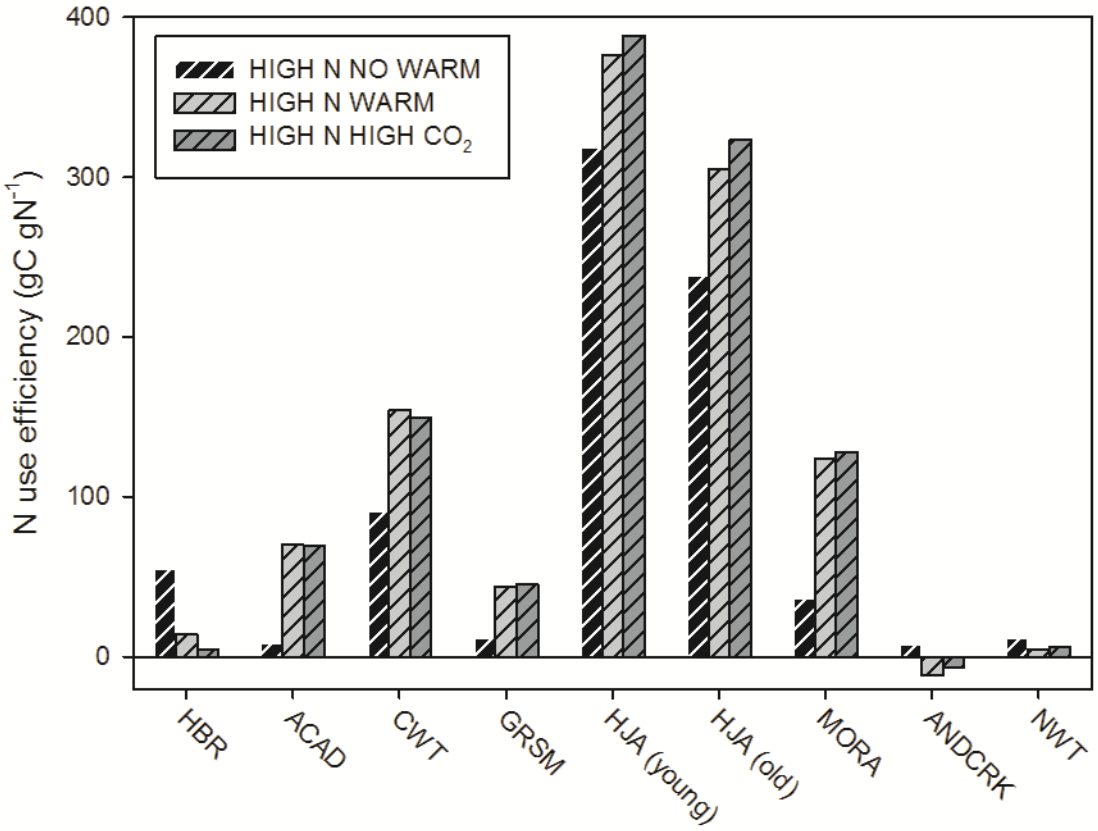

Figure 4.3. Nitrogen use efficiency (NUE, g C g N^{-1}), the increase in NEP (g C) for every 1 g increase in N deposition, for High N deposition scenarios. NUE was calculated as the slope of regression line when NEP was plotted against N deposition.

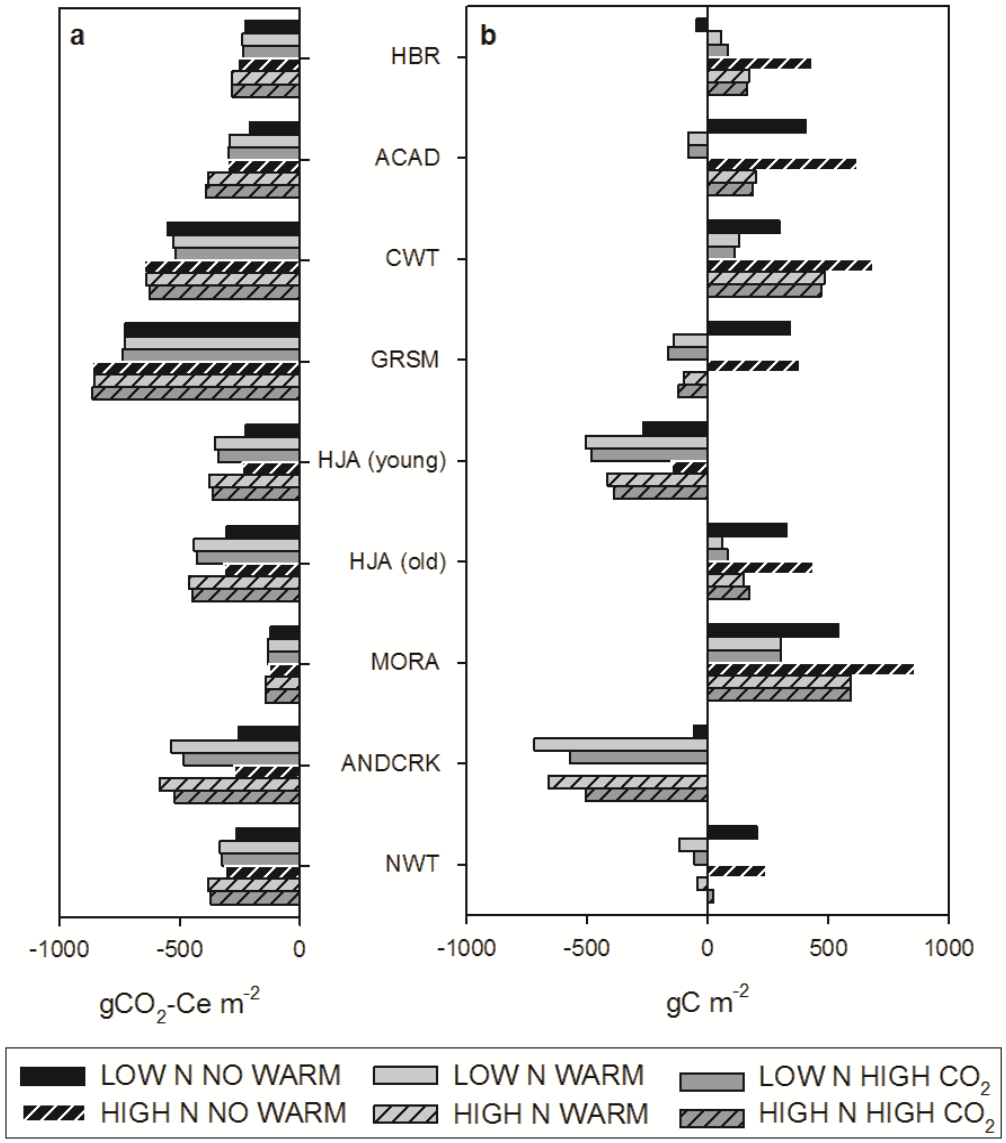

Figure 4.4. Cumulative soil N_2O and carbon fluxes: a) Cumulative N_2O emissions for 1980 – 2075, expressed as g CO_2-C equivalents, from direct soil N_2O and indirect N_2O from N leaching/runoff for all sites and all scenarios; b) Change in total soil organic matter carbon from 1980 to 2075 in g C m^{-2}. A negative value indicates a flux to the atmosphere or a loss from the ecosystem; a positive value indicates sequestration.

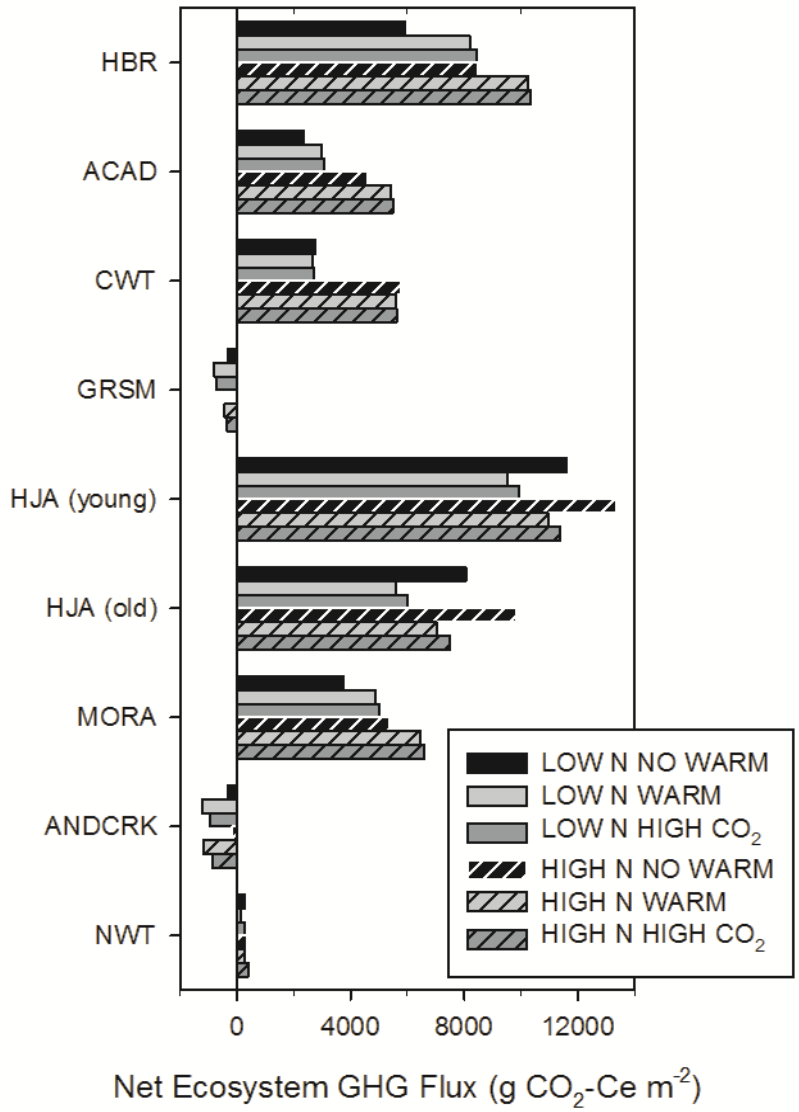

Figure 4.5. The gain in ecosystem carbon from 1980 – 2075 minus cumulative direct and indirect N_2O emissions from the same time period, expressed as g CO_2-C equivalents. A negative value indicates a flux to the atmosphere or a loss from the ecosystem; a positive value indicates sequestration.

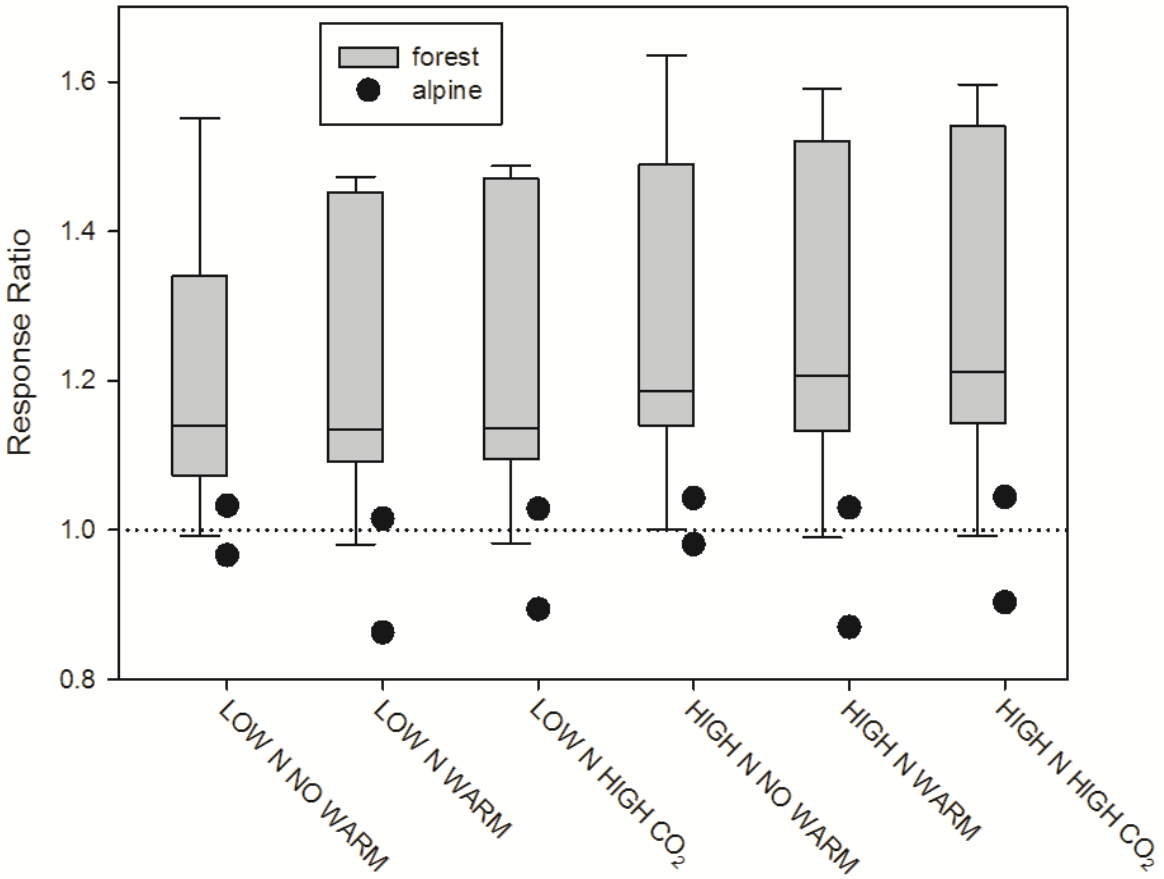

Figure 4.6. The range of response ratios for forest (box plots) and alpine sites (black dots) for all scenarios. Response ratios were determined by dividing the total above- and below-ground C and soil organic matter C in 2075 (less the CO_2-C equivalent lost as direct and indirect N_2O emissions from 1980 – 2075) by the above-and below-ground C and soil organic matter C at base conditions (year 1980). For the box plots, the line represents the median and then the ends of the boxes are the 25th and 75th percentiles and the whiskers show the 10th and 90th percentiles.

5 CONCLUSION

5.1 Overview of Results

The DayCent-Chem model is appropriate for simulating terrestrial and fresh water response of small watersheds to global change. The model adequately recreated multiple lines of evidence, including ecosystem variables, stream discharge, and stream chemistry, for eight unique sites across the U.S. For some sites the model's ability to reproduce geochemistry was constrained by gaps in empirical data, including dry plus fog deposition, soil mineral composition and mineral dissolution rates, soil cation exchange capacity, and sulfate absorption. These discrepancies between DayCent-Chem model output and empirical data can guide future data collection efforts. DayCent-Chem also revealed the importance of individual site antecedent conditions, including climate, soils, plant types, disturbance history, and history of N deposition, in their response to global change (Chapter 4).

Because alpine watersheds are characterized by shallow, poorly developed soils, low biomass, and short growing seasons with limited moisture, there is limited capacity for the sparse vegetation and soils to take up and store N. Simulated alpine tundra production and soil organic matter turnover increased only slightly with N deposition (Chapters 3 and 4). Both the MAGIC model (Sullivan et al. 2005) and DayCent-Chem (Chapter 3) suggest episodic acidification will occur with only a slight increase in N deposition amounts, from current values of 2.0–4.5 to 6.6–8.0 kg N $ha^{-1}yr^{-1}$, and that chronic acidification will occur at 14–15 kg N ha^{-1} yr^{-1}. DayCent-Chem's estimate of the episodic acidification critical load for ANDCRK is in the range determined by recent field experiments and empirical studies. Fertilization experiments showed that N deposition loads under 10 kg $ha^{-1}yr^{-1}$ are needed to prevent future acidification of soils and

surface waters in alpine communities in Rocky Mountain National Park (Bowman et al. 2012). Baron et al. (2011) determined an episodic acidification critical load of 4.0 kg $ha^{-1}yr^{-1}$ for high-elevation western lakes. In our worst case scenario, where N deposition increased at a rate of 5% yr^{-1} after 2004, the model predicted that episodic acidification will begin around 2020. Fortunately, since 2006, both dry and wet N deposition annual rates in Rocky Mountain National Park have generally been declining (CASTNET 2013, NADP/NTN 2013).

In comparing the individual and combined effects of N deposition, warming, and atmospheric CO_2 concentration to net GHG sequestration and stream NO_3^- concentrations, DayCent-Chem showed that N deposition was the main driver of change to ecosystems, followed by warming and CO_2 fertilization (Chapter 4). While DayCent-Chem results showed limited difference in response to two CO_2 scenarios, responses to N deposition and temperature were similar to those reported from increasing numbers of empirical studies. Our results suggest increased N deposition could modestly strengthen the terrestrial net GHG sink primarily by increasing C stored in wood biomass of montane forests. This is countered by CO_2 emissions from accelerated soil organic C decomposition due to warming and increased N_2O emissions due to warming and high N deposition, reducing the overall strength of GHG storage. High N deposition did not enhance net GHG sequestration for the alpine sites or for an N-saturated forest. Warming scenarios increased net GHG sequestration only at the three coldest forested sites, and together high N deposition and warming additively increased net GHG sequestration in these cold forests. However, high rates of N deposition increased stream NO_3^- concentrations at all sites, particularly those that have historically received high N deposition as well as those with low productivity. In scenarios with low N deposition, stream NO_3^- fluxes declined below measured values in some systems illustrating that water quality improvements could occur in the

face of climate change if N deposition decreases below current amounts. The bottom line is that increasing N deposition is not the remedy for sequestering more carbon as levels of atmospheric CO_2 increase in the future.

5.2 Unexpected Results

Models can be excellent heuristic tools which can reveal what we do, and do not, understand about how ecosystems function. The ability of DayCent-Chem to recreate observed ecosystem variables and stream chemistry for six forested montane watersheds and two alpine watersheds attests that there is much we do understand about how these ecosystems function. In the process of parameterizing and running DayCent-Chem, the model exposed peculiar processes happening at four watersheds. These unexpected results emphasize that models cannot truly replicate all ecosystem processes, particularly when there is much to be learned about how watersheds work. Global change, and recovery from acid deposition and disturbance will introduce new processes that influence hydrology and stream chemistry. These site-specific processes once again point out the importance of antecedent conditions, disturbance history, and history of acid deposition in understanding observed watershed biogeochemistry: the thawing of glacial ice and permafrost in alpine watersheds, the history of forest logging and acid deposition in northeastern U.S. forests, and heavy sea salt deposition at ACAD.

5.2.1 Permafrost thaw or glacial ablation at Andrews Creek and Niwot Ridge

For ANDCRK the model captured total annual flow best through 1997, and after 1997 the model underpredicted annual totals (Figure 2.4a). This underestimate of annual total discharge was reflected in the daily hydrographs on the falling limb of years 1998 and 2000–

2003 when simulated flow was less than measured flow (Figure 2.3a). For the nearby alpine watershed, NWT, the model correctly matched the timing of melt but underestimated flow in August and September some years (Figure 7.5 in Hartman et al. 2009). The model also underestimated stream Ca and SO_4^{2-} concentrations year round, particularly in the autumn months (Figures 7.5 and 7.7 in Hartman et al. 2009). From 1990–2006, total discharge averaged 73% of precipitation, but was 84%, 92%, and 103% of precipitation for water years 2001, 2003, and 2005, respectively (Figures 7.8 in Hartman et al. 2009); the discrepancy between simulated and measured discharge was largest for these years (2001, 2003, 2005). This all suggests an additional source of water, Ca, and SO_4^{2-} to the stream that was not included in the model.

The discrepancies between model output and measurements for ANDCRK and NWT may be due to thawing permafrost or surface ice/rock glacier ablation in these alpine watersheds (Clow et al. 2003, Baron et al. 2009, Caine 2010). Baron et al. (2009) concluded that recent changes in observed stream chemistry in the Loch Vale watershed (LVWS) (that encompasses ANDCRK) are the result of warmer summer and autumn mean temperatures that are melting surface ice and rock glaciers. Mean annual stream NO_3^- concentrations and mean annual N export at LVWS since 2000 are higher by 50% and 40% higher, respectively, than during an earlier monitoring period of 1991–1999, even though mean wet atmospheric N deposition from 1991 to 2006 did not increase. The concentrations of weathering products Ca and SO_4^{2-} were higher for the period 2000–2006 in rock glacier meltwater at the top of the watershed above the influence of alpine and subalpine vegetation and soils. Similarly, hydrologic and hydrochemical studies that have been conducted in Green Lakes Valley, above 3550m since 1982 show an increasing trend in flows in September and October of 2.6±0.7 mm yr^{-1} which is not seen at higher elevations and cannot be accounted for by increased autumn precipitation and the melting

of surface ice (Caine 2010). Increased autumn concentrations of base cations and silica, and particularly in Ca and SO_4^{2-} were also observed in the stream discharge starting in 2000. The evidence presented by Caine (2010) suggests the degradation of ice-rich permafrost on the north-facing slopes of the valley below 3700 m, where it has been detected at 3m depth by geophysical surveys. The thawing of permafrost may be explained by an increase in air temperatures and positive degree-days which have occurred over the last few decades and have been measured at the nearby the D-1 weather station (3740m elevation), the thawing occurred in autumn after the ground had warmed sufficiently.

5.2.2 Declining stream nitrate concentrations at Hubbard Brook

For Hubbard Brook, the model did well in predicting the timing and magnitude of stream NO_3^- concentrations from about 1979 through 1991, but it did not capture the overall decline in stream NO_3^- concentrations that have been observed since the early 1990s. Another ecosystem model (PnET) computed climate-driven variation in N cycling and was able to reproduce much of the interannual variability in stream NO_3^- concentrations for the 1980s, but like DayCent-Chem it was not able to predict the extremely low values in the 1990s (Aber and Driscoll 1997, Aber et al. 2002). There has been a decline in stream NO_3^- concentrations and export at HBR and other long-term monitoring watersheds in New England, including old growth and successional watersheds, over the past few decades which cannot be explained by changes in atmospheric deposition or biomass assimilation (Goodale et al. 2003, Bernhardt et al. 2005). There are many probable causes for the declining trend in stream NO_3^- concentrations. Reduced stream NO_3^- has been partially explained by changes in instream NO_3^- uptake (Bernhardt et al. 2005) and increased N immobilization and/ or denitrification driven by increased availability of terrestrial

dissolved organic carbon (DOC) (Goodale et al. 2005). The DOC increase is thought to be the result of recovery from acid deposition as DOC becomes more soluble in soils with higher pH and lower aluminum solubility (Monteith et al. 2007). Bernal et al. (2012) suggest that the reduced stream NO_3^- concentrations in Northeastern forests are due to a shift in snowmelt hydrology due to climate change resulting in reduced water flow through soils when they are the most concentrated in NO_3^- providing more opportunity for N uptake; they also suggest the these forests are recovering from the long-lasting effect of forest cutting.

5.2.3 Unexplained sources of sulfate at Acadia National Park

There are unexplained sources of Ca and SO_4^{2-} to Hadlock Brook in Acadia National Park. DayCent-Chem underestimated annual volume-weighted mean (VWM) SO_4^{2-} concentrations by 22–42 μeq L^{-1} or by 23–46% (Table 2.7 in Hartman et al. 2009). We set SO_4^{2-} deposition as high as we could justify given measures of SO_4^{2-} deposition at Acadia National Park (Weathers et al. 2006). Additionally, simulated S-mineralization was greater than simulated S-uptake, thus allowing for net loss of S from organic material in the soil. Nevertheless, the model still underestimated SO_4^{2-} export into stream water. I speculate that there is a source of SO_4^{2-} to Hadlock Brook that comes from mineralization of organic matter and/or desorption of SO_4^{2-} due to the watershed's legacy high S deposition. The unexplained source of Ca could be from mineral dissolution or release from the exchange complex. Biotic cycling of base cations may not be in equilibrium. The sources of acid cation and anion inputs to the stream, and the relative importance of different buffering systems at Hadlock Brook warrant further investigation.

5.3 The Future of DayCent-Chem

In the coming years the model will still be useful for the purposes it was originally developed: for investigating such problems as episodic or chronic acidification, for determining critical loads on ecosystems, for understanding biological controls on stream chemistry, and for examining ecosystem responses to atmospheric deposition, elevated atmospheric CO_2 concentrations, and climate change. The model can be applied to any ecosystem that DayCent has been applied to in the past, including agro-ecosystems.

Model enhancements will create opportunities for additional applications. For example, if the model included biological uptake and nutrient cycling of Ca, Mg, K, and Na, it could be used to evaluate total soil nutrient availability (rather than just N availability) in non-equilibrium conditions due to natural and anthropogenic disturbances. Furthermore, with the ever increasing amount of reactive N in the environment, scientists are turning their attention to the role of phosphorous (P) limitation to plant productivity and C sequestration. DayCent-Chem is set up to simulate the biological cycling of P, but it needs more evaluation against empirical data for P cycling.

The model could be used to address a variety of questions and hypotheses. Some of these questions have already been addressed in the chapters in this dissertation. With sufficient data to drive and test the model it can be applied to other sites.

1) When will acidification occur under a set of plausible N deposition scenarios? How much N deposition causes episodic and chronic acidification?
2) What is the role of biology in mitigating the harmful effects of atmospheric deposition?
3) What is the individual response of plants and soils to increased N deposition? Climate change? Increasing CO_2 concentrations? Any combination of these drivers?

4) Will rising atmospheric CO_2 concentrations increase net ecosystem productivity? If so, can this response be sustained? What resources (water, N, or other nutrients) could down regulate the response?
5) Once a forest has been decimated by bark beetle kill, what are the relative impacts of clearing dead trees vs. leaving them in place to decompose? What will be the short- and long-term impacts on stream water quantity and quality?
6) What processes are governing biogeochemical outputs as ecosystems recover from long term N and S deposition?

The limitation of applying DayCent to a wider range of ecosystems is not only the model's data needs, but also the number of hours it takes to calibrate the model to predict multiple observations simultaneously. Modelers using DayCent-Chem would benefit greatly from an automated way of parameterizing the model (within realistic values of the parameters). Also, it is becoming increasingly important, if not mandatory, to report model uncertainty on model parameters and model results. These two worthy goals could be accomplished using optimization software, Monte Carlo simulations, Bayesian statistics, and lots of CPU time, and they become more feasible with ever-increasing computer power and advanced numerical techniques.

Ecosystem models are useful for understanding processes that interact in complex ways, for investigating the response of ecosystems to environmental change when the responses go beyond the time frame and spatial extent of experiments and observation, and for performing experiments that would be too harmful to actual ecosystems. Blending modeling with empirical studies and long-term observation is a powerful method of testing scientific hypotheses and assuring that we can predict long-term response of ecosystems to global environmental change.

REFERENCES

Aber, J., W. McDowell, K. Nadelhoffer, A. Magill, G. Berntson, M. Kamakea, S. McNulty, W. Currie, L. Rustad, and I. Fernandez. 1998. Nitrogen saturation in temperate forest ecosystems - Hypotheses revisited. Bioscience **48**:921-934.

Aber, J. D., E. S. Bernhardt, F. A. Dijkstra, R. H. Gardner, K. H. Macneale, W. J. Parton, S. T. A. Pickett, D. L. Urban, and K. C. Weathers. 2003. Standards of practice for review and publication of models: Summary of discussion.

Aber, J. D. and C. T. Driscoll. 1997. Effects of land use, climate variation, and N deposition on N cycling and C storage in northern hardwood forests. Global Biogeochemical Cycles **11**:639-648.

Aber, J. D., S. V. Ollinger, C. T. Driscoll, G. E. Likens, R. T. Holmes, R. J. Freuder, and C. L. Goodale. 2002. Inorganic nitrogen losses from a forested ecosystem in response to physical, chemical, biotic, and climatic perturbations. Ecosystems **5**:648-658.

Aerts, R. and F. S. Chapin. 2000. The mineral nutrition of wild plants revisited: A re-evaluation of processes and patterns. Pages 1-67 *in* A. H. Fitter and D. G. Raffaelli, editors. Advances in Ecological Research, Vol 30.

Appelo, C. A. J. and D. Postma. 1993. Geochemistry, Groundwater and Pollution. A.A. Balkema, Rotterdam, Netherlands.

Arthur, M. A. 1990. The Effects of Vegetation on Watershed Biogeochemistry at Loch Vale Watershed, Rocky Mountain National Park, Colorado. Ph.D. Dissertation. Cornell University, Ithaca, NY.

Arthur, M. A. 1992. Vegetation. Pages 76–92 *in* J. Baron, editor. Biogeochemistry of a Subalpine Ecosystem: Loch Vale Watershed. Ecol. Studies, vol. 90. . Springer-Verlag, New York.

Arthur, M. A. and T. J. Fahey. 1992. Biomass and nutrients in an Englemann spruce—subalpine fir forest in north central Colorado: pools, annual production, and internal cycling. Can. J. For. Res. **22**:315–325.

Baker, J. P., D. P. Bernard, S. W. Christensen, and M. J. Sale. 1990. Biological Effects of Changes in Surface Water Acid-Base Chemistry. National Acid Precipitation Assessment Program, Washington, D.C.

Bales, R. C. 1992. Snowmelt and the ionic pulse. Pages 199-207 The Encyclopedia of Earth Science Volume 1. Academic Press, Orlando, FL.

Baron, J. and A. S. Denning. 1992. Hydrologic budget estimates. Pages 28-47 *in* J. Baron, editor. Biogeochemistry of a Subalpine Ecosystem: Loch Vale Watershed. Ecol. Studies, vol. 90. Springer-Verlag, New York.

Baron, J., A. S. Denning, and P. McLaughlin. 1992a. Deposition. Pages 48-75 *in* J. Baron, editor. Biogeochemistry of a Subalpine Ecosystem: Loch Vale Watershed. Ecol. Studies, vol. 90. Springer-Verlag, New York.

Baron, J., D. S. Ojima, E. A. Holland, and W. J. Parton. 1994. Nitrogen consumption in high elevation Rocky Mountain tundra and forest and implications for aquatic systems. Biogeochemistry **27**:61-82.

Baron, J., P. M. Walthall, M. A. Mast, and M. A. Arthur. 1992b. Soils. Pages 108–141 *in* J. Baron, editor. Biogeochemistry of a Subalpine Ecosystem: Loch Vale Watershed. Ecol. Studies, vol. 90. Springer-Verlag, New York.

Baron, J. S. 2002. Rocky Mountain Futures: An Ecological Perspective. Island Press, Washington.

Baron, J. S. 2006. Hindcasting nitrogen deposition to determine an ecological critical load. Ecological Applications **16**:433-439.

Baron, J. S., S. Del Grosso, D. S. Ojima, D. M. Theobald, and W. J. Parton. 2004. Nitrogen Emissions Along the Colorado Front Range: Response to Population Growth, Land and Water Use Change, and Agriculture. Ecosystems and Land Use Change. Pages 117-127 Geophysical Monograph Series 153. American Geophysical Union.

Baron, J. S., C. T. Driscoll, J. L. Stoddard, and E. E. Richer. 2011. Empirical Critical Loads of Atmospheric Nitrogen Deposition for Nutrient Enrichment and Acidification of Sensitive US Lakes. Bioscience **61**:602-613.

Baron, J. S., M. D. Hartman, L. E. Band, and R. B. Lammers. 2000. Sensitivity of a high-elevation Rocky Mountain watershed to altered climate and CO2. Water Resources Research **36**:89-99.

Baron, J. S., T. M. Schmidt, and M. D. Hartman. 2009. Climate-induced changes in high elevation stream nitrate dynamics. Global Change Biology **15**:1777-1789.

Bedison, J. E. and B. E. McNeil. 2009. Is the growth of temperate forest trees enhanced along an ambient nitrogen deposition gradient? Ecology **90**:1736-1742.

Bernal, S., L. O. Hedin, G. E. Likens, S. Gerber, and D. C. Buso. 2012. Complex response of the forest nitrogen cycle to climate change. Proceedings of the National Academy of Sciences of the United States of America **109**:3406-3411.

Bernhardt, E. S., G. E. Likens, R. O. Hall, D. C. Buso, S. G. Fisher, T. M. Burton, J. L. Meyer, M. H. McDowell, M. S. Mayer, W. B. Bowden, S. E. G. Findlay, K. H. Macneale, R. S.

Stelzer, and W. H. Lowe. 2005. Can't see the forest for the stream? - In-stream processing and terrestrial nitrogen exports. Bioscience **55**:219-230.

Binkley, D., P. Sollins, R. Bell, D. Sachs, and D. Myrold. 1992. Biogeochemistry of adjacent conifer and alder-conifer stands. Ecology **73**:2022-2033.

Boisvenue, C. and S. W. Running. 2006. Impacts of climate change on natural forest productivity - evidence since the middle of the 20th century. Global Change Biology **12**:862-882.

Boisvenue, C. and S. W. Running. 2010. Simulations show decreasing carbon stocks and potential for carbon emissions in Rocky Mountain forests over the next century. Ecological Applications **20**:1302-1319.

Bonan, G., M. Hartman, W. Parton, and W. Wieder. 2013. Evaluating litter decomposition in earth system models with long-term litterbag experiments: an example using the Community Land Model version 4 (CLM4). Global Change Biology **19**:957-974.

Bonan, G. B. 2008. Forests and climate change: Forcings, feedbacks, and the climate benefits of forests. Science **320**:1444-1449.

Bonan, G. B. and S. Levis. 2010. Quantifying carbon-nitrogen feedbacks in the Community Land Model (CLM4). Geophysical Research Letters **37**:1-6.

Bowman, W. D. 1992. Inputs and storage of nitrogen in winter snowpack in an alpine ecosystem. Arctic Alpine Res. **24**:211–215.

Bowman, W. D. and M. C. Fisk. 2001. Primary production. Pages 177–197 *in* W. D. Bowman and T. R. Seastedt, editors. Structure and Function of an Alpine Ecosystem: Niwot Ridge, Colorado. Oxford University Press, New York, NY.

Bowman, W. D., J. R. Gartner, K. Holland, and M. Wiedermann. 2006. Nitrogen critical loads for alpine vegetation and terrestrial ecosystem response: Are we there yet? Ecological Applications **16**:1183-1193.

Bowman, W. D., J. Murgel, T. Blett, and E. Porter. 2012. Nitrogen critical loads for alpine vegetation and soils in Rocky Mountain National Park. Journal of Environmental Management **103**:165-171.

Bulger, A. J., B. J. Cosby, and J. R. Webb. 2000. Current, reconstructed past and projected future status of brook trout (Salvelinus fontinalis) streams in Virginia. Canadian Journal of Fisheries and Aquatic Sciences **57**:1515-1523.

Butterbach-Bahl, K., P. Gundersen, P. Ambus, J. Augustin, C. Beier, P. Boeckx, M. Dannenmann, B. S. Gimeno, A. Ibrom, R. Kiese, B. Kitzler, R. M. Rees , K. Smith, C. Stevens, T. Vesala, and S. Zechmeister-Boltenstern. 2011. Nitrogen processes in terrestrial ecosystems. Pages 99-125 *in* M. Sutton, C. Howard, J. Erisman, G. Billen, A. Bleeker, P. Grennfelt, H. v. Grinsven, and B. Grizzetti, editors. The European nitrogen assessment : sources, effects and policy perspectives. Cambridge University Press, Cambridge, UK.

Caine, N. 2010. Recent hydrologic change in a Colorado alpine basin: an indicator of permafrost thaw? Annals of Glaciology **51**:130-134.

Campbell, D. H., J. S. Baron, K. A. Tonnessen, P. D. Brooks, and P. F. Schuster. 2000. Controls on nitrogen flux in alpine/subalpine watersheds of Colorado. Water Resources Research **36**:37-47.

Campbell, D. H., D. W. Clow, G. P. Ingersoll, M. A. Mast, N. E. Spahr, and J. T. Turk. 1995. Processes Controlling the Chemistry of 2 Snowmelt-Dominated Streams in the Rocky-Mountains. Water Resources Research **31**:2811-2821.

Campbell, J. L., L. E. Rustad, E. W. Boyer, S. F. Christopher, C. T. Driscoll, I. J. Fernandez, P. M. Groffman, D. Houle, J. Kiekbusch, A. H. Magill, M. J. Mitchell, and S. V. Ollinger. 2009. Consequences of climate change for biogeochemical cycling in forests of northeastern North America. Canadian Journal of Forest Research-Revue Canadienne De Recherche Forestiere **39**:264-284.

Canadell, J. G., C. Le Quere, M. R. Raupach, C. B. Field, E. T. Buitenhuis, P. Ciais, T. J. Conway, N. P. Gillett, R. A. Houghton, and G. Marland. 2007. Contributions to accelerating atmospheric CO2 growth from economic activity, carbon intensity, and efficiency of natural sinks. Proceedings of the National Academy of Sciences of the United States of America **104**:18866-18870.

Canadell, J. G. and M. R. Raupach. 2008. Managing forests for climate change mitigation. Science **320**:1456-1457.

Canham, C. D., J. J. Cole, and W. K. Lauenroth. 2003a. Models in ecosystem science.

Canham, C. D., J. J. Cole, and W. K. W. K. Lauenroth. 2003b. The Role of Modeling in Ecosystem Science. Pages 1-12 *in* C. D. Canham, J. S. Cole, and W. K. W. K. Lauenroth, editors. Models in Ecosystem Science. Princeton University Press, Princeton, New Jersey.

CASTNET. 2004. Clean Air Status and Trends Network, U.S. Environmental Protection Agency, http://www.epa.gov/castnet/. Washington D.C., United States.

CASTNET. 2013. Clean Air Status and Trends Network, U.S. Environmental Protection Agency, http://www.epa.gov/castnet/. Washington D.C., United States.

CDLA. 2012. Colorado Department of Local Affairs. State Demography Office, Population Totals. http://dola.colorado.gov/demog/PopulationTotals.cfm.

CENTURY5. 2006. CENTURY Soil Organic Matter Model Version 5. Hilinski, T.E. http://www.nrel.colostate.edu/projects/century5/. Fort Collins, CO, United States.

Chapin, F. S., J. T. Randerson, A. D. McGuire, J. A. Foley, and C. B. Field. 2008. Changing feedbacks in the climate-biosphere system. Frontiers in Ecology and the Environment **6**:313-320.

Chen, B. Z., N. C. Coops, T. A. Black, R. S. Jassal, J. M. Chen, and M. Johnson. 2011. Modeling to discern nitrogen fertilization impacts on carbon sequestration in a Pacific Northwest Douglas-fir forest in the first-postfertilization year. Global Change Biology **17**:1442-1460.

Clow, D. W. 1992. Weathering Rates from Field and Laboratory Experiments on Naturally Weathered Soils. Ph.D. Dissertation. University of Wyoming, Larmie.

Clow, D. W. and M. A. Mast. 1995. Composition of precipitation, bulk deposition, and runoff at a granitic bedrock catchment in the Loch Vale Watershed, Colorado, USA, . Pages 235-242 *in* K. A. Tonnessen, M. W. Williams, and M. Tranter, editors. Biogeochemistry of seasonally snow-covered catchments International Association of Hydrological Sciences, Boulder, Colorado

Clow, D. W., M. A. Mast, T. D. Bullen, and J. T. Turk. 1997. Strontium 87 strontium 86 as a tracer of mineral weathering reactions and calcium sources in an alpine/subalpine watershed, Loch Vale, Colorado. Water Resources Research **33**:1335-1351.

Clow, D. W., L. Schrott, R. Webb, D. H. Campbell, A. Torizzo, and M. Dornblaser. 2003. Ground Water Occurrence and Contributions to Streamflow in an Alpine Catchment, Colorado Front Range. Ground Water **41**:937–950.

Clow, D. W. and J. K. Sueker. 2000. Relations between basin characteristics and stream water chemistry in alpine/subalpine basins in Rocky Mountain National Park, Colorado. Water Resources Research **36**:49-61.

CMAQ. 2005. U.S. EPA Community Multiscale Air Quality (CMAQ v4.5) Modeling System. http://www.cmaq-model.org/

Cole, J. J., N. F. Caraco, G. W. Kling, and T. K. Kratz. 1994. Carbon Dioxide Supersaturation in Surface Waters of Lakes. Science **265**:1568-1570.

Conley, A. H., E. A. Holland, T. R. Seastedt, and W. J. Parton. 2000. Simulation of carbon and nitrogen cycling in on alpine tundra. Arctic Antarctic and Alpine Research **32**:147-154.

Cosby, B. J., R. C. Ferrier, A. Jenkins, and R. F. Wright. 2001. Modelling the effects of acid deposition: refinements, adjustments and inclusion of nitrogen dynamics in the MAGIC model. Hydrology and Earth System Sciences **5**:499-517.

Cosby, B. J., G. M. Hornberger, J. N. Galloway, and B. F. Wright. 1985. Modeling the effects of acid deposition: assessment of a lumped parameter model of soil water and streamwater chemistry. Water Resources Research **21**:51-63.

Daly, C., W. P. Gibson, G. H. Taylor, G. L. Johnson, and P. Pasteris. 2002. A knowledge-based approach to the statistical mapping of climate. Climate Research **22**:99-113.

de Vries, W., S. Solberg, M. Dobbertin, H. Sterba, D. Laubhann, M. van Oijen, C. Evans, P. Gundersen, J. Kros, G. W. W. Wamelink, G. J. Reinds, and M. A. Sutton. 2009. The

impact of nitrogen deposition on carbon sequestration by European forests and heathlands. Forest Ecology and Management **258**:1814-1823.

DeAngelis, D., W. Mooij, and W. K. W. K. Lauenroth. 2003. In Praise of Mechanistically Rich Models. Pages 63-?? *in* C. D. Canham, J. S. Cole, and W. K. W. K. Lauenroth, editors. Models in Ecosystem Science. Princeton University Press, Princeton, New Jersey.

Del Grosso, S. J., D. S. Ojima, W. J. Parton, E. Stehfest, M. Heistermann, B. DeAngelo, and S. Rose. 2009. Global scale DAYCENT model analysis of greenhouse gas emissions and mitigation strategies for cropped soils. Global and Planetary Change **67**:44-50.

Del Grosso, S. J., W. J. Parton, A. R. Mosier, M. D. Hartman, J. Brenner, D. S. Ojima, and D. S. Schimel. 2001. Simulated interaction of carbon dynamics and nitrogen trace gas fluxes using the DAYCENT model. Pages 303-332 *in* M. J. Shaffer, L. Ma, and S. Hansen, editors. Modeling Carbon and Nitrogen Dynamics for Soil Management. Lewis Publishers, Boca Raton, Florida,.

Del Grosso, S. J., W. J. Parton, A. R. Mosier, D. S. Ojima, A. E. Kulmala, and S. Phongpan. 2000a. General model for N2O and N-2 gas emissions from soils due to dentrification. Global Biogeochemical Cycles **14**:1045-1060.

Del Grosso, S. J., W. J. Parton, A. R. Mosier, D. S. Ojima, C. S. Potter, W. Borken, R. Brumme, K. Butterbach-Bahl, P. M. Crill, K. Dobbie, and K. A. Smith. 2000b. General CH4 oxidation model and comparisons of CH4 oxidation in natural and managed systems. Global Biogeochemical Cycles **14**:999-1019.

Del Grosso, S. J., W. J. Parton, A. R. Mosier, M. K. Walsh, D. S. Ojima, and P. E. Thornton. 2006. DAYCENT national-scale simulations of nitrous oxide emissions from cropped soils in the United States. Journal of Environmental Quality **35**:1451-1460.

Dijkstra, F. A., S. E. Hobbie, J. M. H. Knops, and P. B. Reich. 2004. Nitrogen deposition and plant species interact to influence soil carbon stabilization. Ecology Letters **7**:1192-1198.

Drever, J. I. 1982. The Geochemistry of Natural Waters. Prentice-Hall, Inc, Englewood Cliffs, NJ.

Driscoll, C. T., M. D. Lehtinen, and T. J. Sullivan. 1994. Modeling the Acid-Base Chemistry of Organic Solutes in Adirondack, New-York, Lakes. Water Resources Research **30**:297-306.

Eastaugh, C. S., E. Potzelsberger, and H. Hasenauer. 2011. Assessing the impacts of climate change and nitrogen deposition on Norway spruce (Picea abies L. Karst) growth in Austria with BIOME-BGC. Tree Physiology **31**:262-274.

Eitzinger, J., W. J. Parton, and M. Hartman. 2000. Improvement and validation of a daily soil temperature submodel for freezing/thawing periods. Soil Science **165**:525-534.

Emmett, B. A., D. Boxman, M. Bredemeier, P. Gundersen, O. J. Kjonaas, F. Moldan, P. Schleppi, A. Tietema, and R. F. Wright. 1998. Predicting the effects of atmospheric nitrogen deposition in conifer stands: Evidence from the NITREX ecosystem-scale experiments. Ecosystems **1**:352-360.

Galloway, J. N., W. C. Keene, and G. E. Likens. 1996. Processes controlling the composition of precipitation at a remote southern hemispheric location: Torres del Paine National Park, Chile. Journal of Geophysical Research-Atmospheres **101**:6883-6897.

Galloway, J. N., A. R. Townsend, J. W. Erisman, M. Bekunda, Z. C. Cai, J. R. Freney, L. A. Martinelli, S. P. Seitzinger, and M. A. Sutton. 2008. Transformation of the nitrogen cycle: Recent trends, questions, and potential solutions. Science **320**:889-892.

Gbondo-Tugbawa, S. S., C. T. Driscoll, J. D. Aber, and G. E. Likens. 2001. Evaluation of an integrated biogeochemical model (PnET-BGC) at a northern hardwood forest ecosystem. Water Resources Research **37**:1057-1070.

Goodale, C. L., J. D. Aber, and P. M. Vitousek. 2003. An unexpected nitrate decline in New Hampshire streams. Ecosystems **6**:75-86.

Goodale, C. L., J. D. Aber, P. M. Vitousek, and W. H. McDowell. 2005. Long-term decreases in stream nitrate: Successional causes unlikely; Possible links to DOC? Ecosystems **8**:334-337.

Hartman, M. D., J. S. Baron, D. W. Clow, I. F. Creed, C. T. Driscoll, H. A. Ewing, B. D. Haines, J. Knoepp, K. Lajtha, D. S. Ojima, W. J. Parton, J. Renfro, R. B. Robinson, H. Van Miegroet, K. C. Weathers, and M. W. Williams. 2009. DayCent-Chem simulations of ecological and biogeochemical processes of eight mountain ecosystems in the United States. U.S. Geological Survey Scientific Investigations Report 2009-5150, 174 p.

Hartman, M. D., J. S. Baron, R. B. Lammers, D. W. Cline, L. E. Band, G. E. Liston, and C. Tague. 1999. Simulations of snow distribution and hydrology in a mountain basin. Water Resources Research **35**:1587-1603.

Hartman, M. D., J. S. Baron, and D. S. Ojima. 2007. Application of a coupled ecosystem-chemical equilibrium model, DayCent-Chem, to stream and soil chemistry in a Rocky Mountain watershed. Ecological Modelling **200**:493-510.

Hartman, M. D., E. R. Merchant, W. J. Parton, M. P. Gutmann, S. M. Lutz, and S. A. Williams. 2011. Impact of historical land-use changes on greenhouse gas exchange in the US Great Plains, 1883-2003. Ecological Applications **21**:1105-1119.

Holland, E. A., F. J. Dentener, B. H. Braswell, and J. M. Sulzman. 1999. Contemporary and pre-industrial global reactive nitrogen budgets. Biogeochemistry **46**:7-43.

Hyvonen, R., G. I. Agren, S. Linder, T. Persson, M. F. Cotrufo, A. Ekblad, M. Freeman, A. Grelle, I. A. Janssens, P. G. Jarvis, S. Kellomaki, A. Lindroth, D. Loustau, T. Lundmark, R. J. Norby, R. Oren, K. Pilegaard, M. G. Ryan, B. D. Sigurdsson, M. Stromgren, M. van Oijen, and G. Wallin. 2007. The likely impact of elevated [CO2], nitrogen deposition, increased temperature and management on carbon sequestration in temperate and boreal forest ecosystems: a literature review. New Phytologist **173**:463-480.

IPCC. 1996. Technical summary. Pages 9-50 *in* J. T. Houghton, L. G. Meira Filho, B. A. Callander, N. Harris, A. Kattenberg, and K. Maskell, editors. Climate change 1995 - the science of climate change: Contribution of Working Group I to the second assessment report of the Intergovernmental Panel on Climate Change. Cambridge University Press, Cambridge, UK.

IPCC. 2007. Climate Change 2007: Synthesis Report. Contribution of Working Groups I, II and III to the Fourth Assessment Report of the Intergovernmental Panel on Climate Change IPCC, Geneva, Switzerland.

IPCC/WMO/UNEP. 2000. Good practice guidance and uncertainty management in national greenhouse gas inventories. Intergovernmental Panel on Climate.

Janssen, P. H. M. and P. S. C. Heuberger. 1995. Calibration of process-oriented models. Ecological Modelling **83**:55-66.

Janssens, I. A., W. Dieleman, S. Luyssaert, J. A. Subke, M. Reichstein, R. Ceulemans, P. Ciais, A. J. Dolman, J. Grace, G. Matteucci, D. Papale, S. L. Piao, E. D. Schulze, J. Tang, and

B. E. Law. 2010. Reduction of forest soil respiration in response to nitrogen deposition. Nature Geoscience **3**:315-322.

Janssens, I. A. and S. Luyssaert. 2009. Nitrogen's carbon bonus. Nature Geoscience **2**:318-319.

Johnson, D. W., W. T. Swank, and J. M. Vose. 1993. Simulated effects of atmospheric sulfur deposition on nutrient cycling in a mixed deciduous forest. Biogeochemistry **23**:169-196.

Kelly, R. H., W. J. Parton, M. D. Hartman, L. K. Stretch, D. S. Ojima, and D. S. Schimel. 2000. Intra-annual and interannual variability of ecosystem processes in shortgrass steppe. Journal of Geophysical Research-Atmospheres **105**:20093-20100.

Kickert, R. N., G. Tonella, A. Simonov, and S. V. Krupa. 1999. Predictive modeling of effects under global change. Environmental Pollution **100**:87-132.

Lamarque, J. F., J. T. Kiehl, G. P. Brasseur, T. Butler, P. Cameron-Smith, W. D. Collins, W. J. Collins, C. Granier, D. Hauglustaine, P. G. Hess, E. A. Holland, L. Horowitz, M. G. Lawrence, D. McKenna, P. Merilees, M. J. Prather, P. J. Rasch, D. Rotman, D. Shindell, and P. Thornton. 2005. Assessing future nitrogen deposition and carbon cycle feedback using a multimodel approach: Analysis of nitrogen deposition. Journal of Geophysical Research-Atmospheres **110**.

Le Quéré, C., M. R. Raupach, J. G. Canadell, G. Marland, L. Bopp, P. Ciais, T. J. Conway, S. C. Doney, R. A. Feely, P. Foster, P. Friedlingstein, K. Gurney, R. A. Houghton, J. I. House, C. Huntingford, P. E. Levy, M. R. Lomas, J. Majkut, N. Metzl, J. P. Ometto, G. P. Peters, I. C. Prentice, J. T. Randerson, S. W. Running, J. L. Sarmiento, U. Schuster, S. Sitch, T. Takahashi, N. Viovy, G. R. van der Werf, and F. I. Woodward. 2009. Trends in the sources and sinks of carbon dioxide. Nature Geoscience **2**:831-836.

LeBauer, D. S. and K. K. Treseder. 2008. Nitrogen limitation of net primary productivity in terrestrial ecosystems is globally distributed. Ecology **89**:371-379.

Leung, L. R. and Y. Qian. 2005. Hydrological response to climate variability, climate change, and climate extreme in the USA: climate model evaluation and projections *in* Regional Hydrological Impacts of Climatic Variability and Change—Impact Assessment and Decision Making (Proceedings of symposium S6 held during the Seventh IAHS Scientific Assembly). IAHS Publ., Foz do Iguaçu, Brazil

Leung, L. R., Y. Qian, X. D. Bian, and A. Hunt. 2003. Hydroclimate of the western United States based on observations and regional climate simulation of 1981-2000. part II: Mesoscale ENSO anomalies. Journal of Climate **16**:1912-1928.

Lindsay, W. L. 2001. Chemical Equilibria in Soils. The Blackburn Press, Caldwell, NJ.

Litaor, M. I. 1988. Soil solution chemistry in an alpine watershed, Front Range, Colorado, U.S.A. Arctic and Alpine Research **20**:485-491.

Liu, L. L. and T. L. Greaver. 2009. A review of nitrogen enrichment effects on three biogenic GHGs: the CO2 sink may be largely offset by stimulated N2O and CH4 emission. Ecology Letters **12**:1103-1117.

Liu, L. L. and T. L. Greaver. 2010. A global perspective on belowground carbon dynamics under nitrogen enrichment. Ecology Letters **13**:819-828.

Lu, L. X., R. A. Pielke, G. E. Liston, W. J. Parton, D. Ojima, and M. Hartman. 2001. Implementation of a two-way interactive atmospheric and ecological model and its application to the central United States. Journal of Climate **14**:900-919.

LVWS. 2004. Loch Vale Watershed, Long-term Ecological Research & Monitoring Program. http://www.nrel.colostate.edu/projects/lvws/data.html. Fort Collins, CO, United States.

Magnani, F., M. Mencuccini, M. Borghetti, P. Berbigier, F. Berninger, S. Delzon, A. Grelle, P. Hari, P. G. Jarvis, P. Kolari, A. S. Kowalski, H. Lankreijer, B. E. Law, A. Lindroth, D. Loustau, G. Manca, J. B. Moncrieff, M. Rayment, V. Tedeschi, R. Valentini, and J. Grace. 2007. The human footprint in the carbon cycle of temperate and boreal forests. Nature **447**:848-850.

Mast, M. A. 1992. Geochemical characteristics. Pages 93–107 *in* J. Baron, editor. Biogeochemistry of a Subalpine Ecosystem: Loch Vale Watershed. Ecol. Studies, vol. 90 Springer-Verlag, New York.

Mast, M. A., J. I. Drever, and J. Baron. 1990. Chemical-Weathering in the Loch Vale Watershed, Rocky-Mountain-National-Park, Colorado. Water Resources Research **26**:2971-2978.

Matson, P., K. A. Lohse, and S. J. Hall. 2002. The globalization of nitrogen deposition: Consequences for terrestrial ecosystems. Ambio **31**:113-119.

McMahon, S. M., G. G. Parker, and D. R. Miller. 2010. Evidence for a recent increase in forest growth. Proceedings of the National Academy of Sciences of the United States of America **107**:3611-3615.

Meixner, T., R. C. Bales, M. W. Williams, D. H. Campbell, and J. S. Baron. 2000. Stream chemistry modeling of two watersheds in the Front Range, Colorado. Water Resources Research **36**:77-87.

Melillo, J. M., S. Butler, J. Johnson, J. Mohan, P. Steudler, H. Lux, E. Burrows, F. Bowles, R. Smith, L. Scott, C. Vario, T. Hill, A. Burton, Y. M. Zhou, and J. Tang. 2011. Soil warming, carbon-nitrogen interactions, and forest carbon budgets. Proceedings of the National Academy of Sciences of the United States of America **108**:9508-9512.

Mohren, G. M. J. and J. R. van de Veen. 1995. Forest growth in relation to site conditions: Application of the model FORGRO to the Solling spruce site. Ecological Modelling **83**:173-183.

Monteith, D. T., J. L. Stoddard, C. D. Evans, H. A. de Wit, M. Forsius, T. Hogasen, A. Wilander, B. L. Skjelkvale, D. S. Jeffries, J. Vuorenmaa, B. Keller, J. Kopacek, and J. Vesely. 2007. Dissolved organic carbon trends resulting from changes in atmospheric deposition chemistry. Nature **450**:537-U539.

Musselman, R. C. and W. L. Slauson. 2004. Water chemistry of high elevation Colorado wilderness lakes. Biogeochemistry **71**:387-414.

Nadelhoffer, K. J., B. A. Emmett, P. Gundersen, O. J. Kjonaas, C. J. Koopmans, P. Schleppi, A. Tietema, and R. F. Wright. 1999. Nitrogen deposition makes a minor contribution to carbon sequestration in temperate forests. Nature **398**:145-148.

NADP/NTN. 2004. National Atmospheric Deposition Program/National Trends Network. http://nadp.sws.uiuc.edu/. Illinois State Water Survey, Urbana, IL.

NADP/NTN. 2013. National Atmospheric Deposition Program/National Trends Network. http://nadp.sws.uiuc.edu/. Illinois State Water Survey, Urbana, IL.

Nakicenovic, N., et al. 2000. Special Report on Emissions Scenarios: Intergovernmental Panel on Climate Change. Cambridge University Press, New York.

Nash, J. E. and J. V. Sutcliffe. 1970. River flow forecasting through conceptual models, I, A discussion of principles. Journal of Hydrology **10**:282-290.

NOAA. 2012a. Global Analysis - Annual 2012. National Oceanic and Atmospheric Administration. Asheville. http://www.ncdc.noaa.gov/sotc/global/2012/13. Asheville, NC, United States.

NOAA. 2012b. National Overview - Annual 2012. National Oceanic and Atmospheric Administration. Asheville. http://www.ncdc.noaa.gov/sotc/global/2012/13. Asheville, NC, United States.

Norby, R. J., J. M. Warren, C. M. Iversen, B. E. Medlyn, and R. E. McMurtrie. 2010. CO(2) enhancement of forest productivity constrained by limited nitrogen availability. Proceedings of the National Academy of Sciences of the United States of America **107**:19368-19373.

Pan, Y. D., J. M. Melillo, A. D. McGuire, D. W. Kicklighter, L. F. Pitelka, K. Hibbard, L. L. Pierce, S. W. Running, D. S. Ojima, W. J. Parton, D. S. Schimel, and V. Members. 1998. Modeled responses of terrestrial ecosystems to elevated atmospheric CO(2): a comparison of simulations by the biogeochemistry models of the Vegetation/Ecosystem Modeling and Analysis Project (VEMAP). Oecologia **114**:389-404.

Parkhurst, D. L. and C. A. J. Appelo. 1999. User's Guide to PHREEQC (Version 2)—A Computer Program for Speciation, Batch-Reaction, One-Dimensional Transport, and Inverse Geochemical Calculations., Denver, CO.

Parton, W. and W. L. Silver. 2007. Global-scale similarities in nitrogen release patterns during long-term decomposition (vol 315, pg 361, 2007). Science **315**:940-940.

Parton, W. J., M. P. Gutmann, S. A. Williams, M. Easter, and D. Ojima. 2005. Ecological impact of historical land-use patterns in the great plains: A methodological assessment. Ecological Applications **15**:1915-1928.

Parton, W. J., M. Hartman, D. Ojima, and D. Schimel. 1998. DAYCENT and its land surface submodel: description and testing. Global and Planetary Change **19**:35-48.

Parton, W. J., E. A. Holland, S. J. Del Grosso, M. D. Hartman, R. E. Martin, A. R. Mosier, D. S. Ojima, and D. S. Schimel. 2001. Generalized model for NOx and N2O emissions from soils. Journal of Geophysical Research-Atmospheres **106**:17403-17419.

Parton, W. J., A. R. Mosier, D. S. Ojima, D. W. Valentine, D. S. Schimel, K. Weier, and A. E. Kulmala. 1996. Generalized model for N-2 and N2O production from nitrification and denitrification. Global Biogeochemical Cycles **10**:401-412.

Parton, W. J., D. S. Schimel, C. V. Cole, and D. S. Ojima. 1987. Analysis of Factors Controlling Soil Organic-Matter Levels in Great-Plains Grasslands. Soil Science Society of America Journal **51**:1173-1179.

Parton, W. J., D. S. Schimel, D. S. Ojima, and C. V. Cole. 1994. A general model for soil organic matter dynamics: Sensitivity to litter chemistry, texture and management. Pages 147-167 *in* R. B. B. a. R. W. Arnold, editor. Quantitative Modeling of Soil Forming Processes. Soil Science Society of America, Madison, WI.

Parton, W. J., J. M. O. Scurlock, D. S. Ojima, T. G. Gilmanov, R. J. Scholes, D. S. Schimel, T. Kirchner, J. C. Menaut, T. Seastedt, E. G. Moya, A. Kamnalrut, and J. I. Kinyamario. 1993. Observations and Modeling of Biomass and Soil Organic-Matter Dynamics for the Grassland Biome Worldwide. Global Biogeochemical Cycles **7**:785-809.

Parton, W. J., J. W. B. Stewart, and C. V. Cole. 1988. Dynamics of C, N, P and S in Grassland Soils - a Model. Biogeochemistry **5**:109-131.

Perakis, S. S. and E. R. Sinkhorn. 2011. Biogeochemistry of a temperate forest nitrogen gradient. Ecology **92**:1481-1491.

Pinder, R. W., N. D. Bettez, G. B. Bonan, T. L. Greaver, W. R. Wieder, W. H. Schlesinger, and E. A. Davidson. 2012. Impacts of human alteration of the nitrogen cycle in the US on radiative forcing. Biogeochemistry **10.1007/s10533-012-9787-z**.

Ramaswamy, V. 2001. Radiative Forcing of Climate Change.*in* J. T. Houghton, editor. Climate Change 2001: The Scientific Basis. Cambridge Univ. Press,, Cambridge.

Robinson, D., D. Brown, N. French, and B. Reed. 2013. Linking Land Use and the Carbon Cycle. Pages 3-22 *in* D. Brown, D. Robinson, N. French, and B. Reed, editors. Land Use and the Carbon Cycle: Advances in Integrated Science, Management, and Policy. Cambridge University Press, New York, NY.

Rueth, H. M., J. S. Baron, and E. J. Allstott. 2003. Responses of Engelmann spruce forests to nitrogen fertilization in the Colorado Rocky Mountains. Ecological Applications **13**:664-673.

Saleska, S. R., J. Harte, and M. S. Torn. 1999. The effect of experimental ecosystem warming on CO2 fluxes in a montane meadow. Global Change Biology **5**:125-141.

Schlesinger, W. H. 2009. On the fate of anthropogenic nitrogen. Proceedings of the National Academy of Sciences of the United States of America **106**:203-208.

Seastedt, T. R. 2001. Soils. Pages 157-173 *in* W. D. Bowman and T. R. Seastedt, editors. Structure and function of an alpine ecosystem: Niwot Ridge, Colorado. Oxford University Press, New York, NY.

Sickman, J. O., A. Leydecker, C. C. Y. Chang, C. Kendall, J. M. Melack, D. M. Lucero, and J. P. Schimel. 2003. Mechanisms underlying export of N from high elevation catchments during seasonal transitions. Biogeochemistry **64**:1–24.

Sullivan, T. J., B. J. Cosby, K. A. Tonnessen, and D. W. Clow. 2005. Surface water acidification responses and critical loads of sulfur and nitrogen deposition in Loch Vale watershed, Colorado. Water Resources Research **41**:15.

Sutton, M. A., O. Oenema, J. W. Erisman, A. Leip, H. van Grinsven, and W. Winiwarter. 2011. Too much of a good thing. Nature **472**:159-161.

Sutton, M. A., D. Simpson, P. E. Levy, R. I. Smith, S. Reis, M. van Oijen, and W. de Vries. 2008. Uncertainties in the relationship between atmospheric nitrogen deposition and forest carbon sequestration. Global Change Biology **14**:2057-2063.

Thomas, R. Q., C. D. Canham, K. C. Weathers, and C. L. Goodale. 2010. Increased tree carbon storage in response to nitrogen deposition in the US. Nature Geoscience **3**:13-17.

Tiktak, A. and H. J. M. van Grinsven. 1995. Review of sixteen forest-soil-atmosphere models. Ecological Modelling **83**:35-53.

van Heerden, K., H. J. M. van Grinsven, and A. Tiktak. 1995. Simulation of forest stress for the Solling spruce site with SOILVEG. Ecological Modelling:185-195.

Van Miegroet, H., I. F. Creed, N. S. Nicholas, D. G. Tarboton, K. L. Webster, J. Shubzda, B. Robinson, J. Smoot, D. W. Johnson, S. E. Lindberg, G. Lovett, S. Nodvin, and S. Moore. 2001. Is there synchronicity in N input and output fluxes at the Noland Divide Watershed, a small N-saturated forested catchment in the Southern Appalachians? Pages 480-492 The Scientific World.

Vitousek, P. M. and R. W. Howarth. 1991. Nitrogen Limitation on Land and in the Sea - How Can It Occur. Biogeochemistry **13**:87-115.

Waldrop, M. P., D. R. Zak, and R. L. Sinsabaugh. 2004. Microbial community response to nitrogen deposition in northern forest ecosystems. Soil Biology & Biochemistry **36**:1443-1451.

Walthall, P. M. 1985. Walthall, P.M., 1985. Acidic Deposition and the Soil Environment of Loch Vale Watershed in Rocky Mountain National Park. Ph.D. Dissertation Colorado State University, Fort Collins, CO.

Weathers, K. C., S. M. Simkin, G. M. Lovett, and S. E. Lindberg. 2006. Empirical modeling of atmospheric deposition in mountainous landscapes. Ecological Applications **16**:1590-1607.

Williams, M. W. and N. Caine. 2001. Hydrology and Hydrochemistry. Pages 75-96 *in* W. D. Bowman and T. R. Seastedt, editors. Structure and function of an alpine ecosystem: Niwot Ridge, Colorado. Oxford University Press, New York, NY.

Williams, M. W., E. Hood, and N. Caine. 2001. Role of organic nitrogen in the nitrogen cycle of a high-elevation catchment, Colorado Front Range. Water Resources Research **37**:2569-2581.

Williams, M. W. and J. M. Melack. 1991. Solute chemistry of snowmelt and runoff in an alpine basin, Sierra Nevada. Water Resources Research **27**:1575-1588.

Williams, M. W. and K. A. Tonnessen. 2000. Critical loads for inorganic nitrogen deposition in the Colorado Front Range, USA. Ecological Applications **10**:1648-1665.

Wolford, R. A., R. C. Bales, and S. Sorooshian. 1996. Development of a hydrochemical model for seasonally snow-covered alpine watersheds: Application to Emerald Lake Watershed, Sierra Nevada, California. Water Resources Research **25**:829-837.

Woodward, D. F., A. M. Farag, M. E. Mueller, L. E.E., and F. A. Vertucci. 1989. Sensitivity of endemic Snake River cutthroat trout to acidity and elevated aluminum. Transactions of the American Fisheries Society **118**:630-643.

Zaehle, S., P. Friedlingstein, and A. D. Friend. 2010. Terrestrial nitrogen feedbacks may accelerate future climate change. Geophysical Research Letters **37**.